Volume 73 • Issue 4 • October-December 2024

Journal of The Anatomical Society of India • Volume 73 • Issue 4 • October-December 2024 • Pages 297-382

ISSN : 0003-2778

Scopus
Indexed

JASI

JOURNAL OF THE ANATOMICAL SOCIETY OF INDIA

An International Journal

An Official Publication of Anatomical Society of India

Full text online at **https://journals.lww.com/joai**
Submit articles online at **https://review.jow.medknow.com/jasi**

Editor-in-Chief
Dr. Vishram Singh

Wolters Kluwer

Medknow

Journal of the Anatomical Society of India

Print ISSN: 0003-2778

GENERAL INFORMATION

About the Journal

Journal of the Anatomical Society of India (ISSN: Print 0003-2778) is peer-reviewed journal. The journal is owned and run by Anatomical Society of India. The journal publishes research articles related to all aspects of Anatomy and allied medical/surgical sciences. Pre-Publication Peer Review and Post-Publication Peer Review Online Manuscript Submission System Selection of articles on the basis of MRS system Eminent academicians across the globe as the Editorial board members Electronic Table of Contents alerts Available in both online and print form. The journal is published quarterly in the months of January, April, July and October.

Scope of the Journal

The aim of the *Journal of the Anatomical Society of India* is to enhance and upgrade the research work in the field of anatomy and allied clinical subjects. It provides an integrative forum for anatomists across the globe to exchange their knowledge and views. It also helps to promote communication among fellow academicians and researchers worldwide. The Journal is devoted to publish recent original research work and recent advances in the field of Anatomical Sciences and allied clinical subjects. It provides an opportunity to academicians to disseminate their knowledge that is directly relevant to all domains of health sciences.

The Editorial Board comprises of academicians across the globe.

JASI is indexed in Scopus, available in Science Direct.

Abstracting and Indexing Information

The journal is registered with the following abstracting partners:

Baidu Scholar, CNKI (China National Knowledge Infrastructure), EBSCO Publishing's Electronic Databases, Ex Libris – Primo Central, Google Scholar, Hinari, Infotrieve, Netherlands ISSN center, ProQuest, TdNet, Wanfang Data

The journal is indexed with, or included in, the following:

SCOPUS, Science Citation Index Expanded, IndMed, MedInd, Scimago Journal Ranking, Emerging Sources Citation Index.

Impact Factor® as reported in the 2023 Journal Citation Reports® (Clarivate Analytics, 2024): 0.2

Information for Authors

Article processing and publication charges will be communicated by the editorial office. All manuscripts must be submitted online at https://review.jow.medknow.com/jasi.

Subscription Information

A subscription to JASI comprises 4 issues. Prices include postage. Annual Subscription Rate for non-members-		
Rates of Membership (with effect from 1.1.2022)		
	India	**International**
Ordinary membership	INR 1500	US $ 100
Couple membership	INR 2250	
Life membership	INR 8000	US $ 900
Subscription Rates (till 31st August)		
Individual	INR 6000	US $ 650
Library/Institutional Trade discount of 10% for agencies only	INR 12000	US $ 1000
Subscription Rates (after 31st August)		
Individual	INR 6500	US $ 700
Library/Institutional	INR 12500	US $ 1050
The Journal of Anatomical Society of India (ISSN: 0003-2778) is published quarterly **Subscriptions** are accepted on a prepaid basis only and are entered on a calendar year basis. Issues are sent by standard mail Priority rates are available upon request.		

Information to Members/Subscribers

All members and existing subscribers of the Anatomical Society of India are requested to send their membership/existing subscription fee for the current year to the Treasurer of the Society on the following address: Prof (Dr.) Punit Manik, Treasurer, ASI, Department of Anatomy, KGMU, Lucknow - 226003. Email: punitamanik@yahoo.co.in. All payments should be made through an account payee bank draft drawn in favor of the **Treasurer, Anatomical Society of India,** payable at **Lucknow** only, preferably for **Allahabad Bank, Medical College Branch, Lucknow.** Outstation cheques/drafts must include INR 70 extra as bank collection charges.

All complaints regarding non-receipt of journal issues should be addressed to the Editor-in-Chief, JASI at editorjasi@gmail.com. The new subscribers may, please contact wkhlrpmedknow_subscriptions@wolterskluwer.com.

Requests of any general information like travel concession forms, venue of next annual conference, etc. should be addressed to the General Secretary of the Anatomical Society of India.

For mode of payment and other details, please visit www.medknow.com/subscribe.asp

Claims for missing issues will be serviced at no charge if received within 60 days of the cover date for domestic subscribers, and 3 months for subscribers outside India. Duplicate copies cannot be sent to replace issues not delivered because of failure to notify publisher of change of address. The journal is published and distributed by Wolters Kluwer India Pvt. Ltd. Copies are sent to subscribers directly from the publisher's address. It is illegal to acquire copies from any other source. If a copy is received for personal use as a member of the association/society, one cannot resale or give-away the copy for commercial or library use.

The copies of the journal to the subscribers are sent by ordinary post. The editorial board, association or publisher will not be responsible for non receipt of copies. If any subscriber wishes to receive the copies by registered post or courier, kindly contact the publisher's office. If a copy returns due to incomplete, incorrect or changed address of a subscriber on two consecutive occasions, the names of such subscribers will be deleted from the mailing list of the journal. Providing complete, correct and up-to-date address is the responsibility of the subscriber.

Nonmembers: Please send change of address information to subscriptions@medknow.com.

Advertising Policies

The journal accepts display and classified advertising. Frequency discounts and special positions are available. Inquiries about advertising should be sent to Wolters Kluwer India Pvt. Ltd, advertise@medknow. com.

The journal reserves the right to reject any advertisement considered unsuitable according to the set policies of the journal.

The appearance of advertising or product information in the various sections in the journal does not constitute an endorsement or approval by the journal and/or its publisher of the quality or value of the said product or of claims made for it by its manufacturer.

Addresses

Editorial Office

Dr. Vishram Singh, Editor-in-Chief, JASI
B5/3 Hahnemann Enclave, Plot No. 40, Sector 6, Dwarka Phase – 2,
New Delhi - 110 075, India.
Email: editorjasi@gmail.com

Published by

Wolters Kluwer India Private Limited,
Survey No. 15, 5th & 6th Floor,
Building E, East Tower, Marisoft III,
Kalyani Nagar, Pune - 411 014,
Maharashtra, India.
Website: www.medknow.com

Printed at

Nikeda Art Printers Pvt. Ltd.,
Building No. C/3 - 14,15,16, Shree Balaji Complex, Vehele Road,
Village Bhatale, Taluka Bhiwandi, District Thane - 421302, India.

Journal of the Anatomical Society of India

Print ISSN: 0003-2778

EDITORIAL BOARD

Journal of the Anatomical Society of India

Volume 73 | Issue 4 | October-December 2024

CONTENTS

EDITORIAL

Neuroanatomical Basis of Depression and Bipolar Disorder: Insights into the Brain's Role in Mood Disorders
Vishram Singh, Rashi Singh, Gaurav Singh 297

ORIGINAL ARTICLES

Ectopic Bronchial Arteries – Incidental Findings on Multi-detector Computed Tomography
C. S. Ramesh Babu, Vinay Sharma, Om Prakash Gupta 300

O-GalNAc Glycosylation - Key Pathway for Hashimoto's Thyroiditis in Patients with Metabolically Unhealthy Obesity
Rui Yang, Jianli Han 307

Estimating Morphological Nose Features for Craniofacial Reconstruction: A Retrospective Study
Nazan Guner Sak, Serdar Babacan, Sefa Işıklar, İlker Mustafa Kafa, Gökhan Gökalp 313

Evaluation of Dural Venous Sinus Variations through Three-dimensional Phase-Contrast Magnetic Resonance Venography
Songül Erdem Özkoç, Mehmet Guli Çetinçakmak, Salih Hattapoğlu 318

The Impact of Tri (2-ethylhexyl) Trimellitate on Renal Functions in Sprague–Dawley Rats
Ayesha Zafar Rajpoot, Humaira Fayyaz Khan, Fatima Iqbal, Rubab Rameez, Tayyaba Anis, Ayesha Shahid, Shazia Ali, Hassan Mumtaz 323

A Clinicoanatomical Study of Perforators of the Posterior Tibial Artery in Distal One-third of the Leg
Saba Anjum, Jyoti Chopra, Sushma Tomar, Rakesh Kumar Diwan, Brijesh Mishra 328

Analysis of the Relationship between the Angular Characteristics of the Femur and the Dimensions of the Intercondylar Fossa
Burhan Yarar, Aysun Nur Yilmaz 333

A Cadaveric Investigation of Human Middle Meningeal Artery Variations and their Clinical Significance
Abhimanu Kumar, Nidhi Puri, V. V. G. Patnaik, Pratibha Gupta 341

Standardization of the Klingler Dissection Technique at 3400 m above Sea Level
Herminia Naveda, Yuri Vargas, Juan Condori, Alexander Montesinos, Franklin Miranda, Carlos Virto, Cristabel Rivas, Lugo Miranda, Yvan Gallegos, Iris Peralta, Hesed Virto-Farfan 347

Gender- and Age-based Measurement of Morphometric Parameters around the Hip Joint: A Radiographic Study
Mohd. Arif Makdoomi, Shaheen Shahdaad, Javeed Ahmad Khan, Ghulam Mohammad Bhat, R Aijaz Ahmad Hakeem 353

Morphometric Study of Bicipital Groove in Dry Adult Human Cadaveric Humerus in Indian Population
Kesar Khanna, Hina Nafees, Dilshad Ahmad Usmani, Sanjeev Kumar Jain, Sonika Sharma 359

continued...

REVIEW ARTICLE

Morphometric and Histological Changes of the Placenta in Hypertensive Disorders of Pregnancy
Jyothi N. Nayak, Hannahsugirthabai Rajilarajendran, B. Sunitha 364

CASE REPORTS

An Atypical Case of Intracardiac Myxoma Fed by Extracardiac Arteries
Zeliha Coşgun, Süleyman Filiz 368

Additional Tendinous Slips of Extensor Carpi Radialis Longus and Brevis of Hand: A Case Study
Sonia Meend, Sunil Kumar Yadav.....371

OBITUARY

Dr. Ajai Kumar Srivastava: A Legacy in Medical Education and Anatomy
R. K. Verma 374

INSTRUCTIONS TO AUTHOR 375

Neuroanatomical Basis of Depression and Bipolar Disorder: Insights into the Brain's Role in Mood Disorders

Depression is a complex mental health condition that affects millions of individuals worldwide, manifesting primarily through persistent feelings of sadness, loss of interest, and disruptions in daily functioning. It is one of the most common psychiatric disorders, with an estimated 45.7 million people affected in India alone, according to the National Mental Health Survey of India (2015–2016).[1]

Depression can present in various forms, including major depressive disorder (clinical depression) and bipolar disorder (mania, and depressive illness), each with its own unique set of symptoms and neuroanatomical correlates.

Types of Depression and Their Symptoms

There are two broad types of depression: unipolar and bipolar. Unipolar depression, more commonly referred to as major depressive disorder or clinical depression, is characterized by persistent low mood and a range of cognitive, emotional, and physical symptoms that interfere with daily life. These symptoms include:

- Sadness or depressed mood
- Loss of interest or pleasure in activities once found enjoyable
- Sleep disturbances (either insomnia or hypersomnia)
- Appetite changes (either weight gain or weight loss)
- Feelings of guilt, worthlessness, or hopelessness
- Fatigue or a lack of energy
- Difficulty in concentrating or making decisions
- Thoughts of death or suicide.

In contrast, bipolar disorder (or manic depression) is marked by episodes of extreme mood swings, alternating between depressive episodes and mania. During manic phases, individuals may experience:

- Elevated mood or excessive euphoria
- Increased energy and activity levels
- Decreased need for sleep
- Racing thoughts or flight of ideas
- Impulsive or reckless behaviors
- Grandiosity or inflated self-esteem
- In severe cases, delusions and hallucinations.

The basic differences between depression and bipolar mental disorders are:

- Depression has only one phase (i.e., depression) while bipolar disorder has two phases (i.e., depression and mania)
- Depression affects more women than men while bipolar disorder affects both men and women equally
- The main cause of depression is stressful life events while the main cause of bipolar disorder is unknown but likely a combination of heriditary etc.
- Depression can occur at any age (i.e., 12–60 years), while bipolar disorder occurs in adolescents or before the age of 40 years.

The neuroanatomical understanding of depression is critical for both diagnosis and treatment, especially given the intricate role the brain plays in regulating mood and cognition.

Neuroanatomical Basis of Depression

The neuroanatomical basis of depression involves complex interactions between multiple brain regions, neurotransmitter systems, and neural circuits. Depression is thought to result from structural and functional abnormalities in various regions of the brain, particularly those involved in regulating mood, cognition, and emotional responses. Key regions implicated include the limbic system, prefrontal cortex (PFC), basal ganglia, and thalamus.

Neurochemical imbalance: The monoamine hypothesis

One of the most widely studied neuroanatomical theories of depression is the monoamine hypothesis, which posits that depression is linked to an imbalance in neurotransmitters, particularly serotonin, dopamine, and norepinephrine. These monoamine neurotransmitters are critical for regulating mood, reward, and cognitive functions, and abnormalities in their functioning have been observed in individuals with depression.

- Serotonin: A key regulator of mood, anxiety, and sleep
- Dopamine: Involved in the brain's reward system and motivation
- Norepinephrine: Plays a role in arousal and alertness.

In addition, glutamate, an excitatory neurotransmitter, has been implicated in depression, especially with regard to neuroplasticity and synaptic functioning. Dysregulation in these neurotransmitter systems affects the activity and connectivity of brain regions responsible for mood regulation, such as the PFC, amygdala, and hippocampus.[2]

Brain regions involved in depression

- Amygdala: The amygdala is a central structure in the brain's emotional processing system. In individuals with depression, the amygdala often shows increased activity, which is thought to contribute to heightened emotional responses (e.g., fear and sadness). This overactivity is often seen alongside reduced activity in the PFC, which is involved in regulating emotions and executive functions[3]
- PFC: The PFC, especially the dorsolateral PFC, plays a critical role in decision-making, emotional

regulation, and cognitive control. Studies have shown decreased gray matter volume in the PFC of individuals with depression, which may contribute to cognitive impairment and difficulty regulating negative emotions[4]

- Hippocampus: The hippocampus is essential for memory formation and emotional regulation. Chronic depression has been associated with reduced hippocampal volume, possibly due to the effects of prolonged stress and elevated levels of cortisol, a stress hormone. This shrinkage may impair emotional regulation and contribute to cognitive difficulties seen in depression[5]
- Basal ganglia: The basal ganglia, including the striatum, are involved in reward processing and motor activity. Dysfunction in this circuit, particularly in the ventral striatum, has been linked to anhedonia (the inability to feel pleasure) and apathy, which are common symptoms of depression.[6]

Other structural and functional abnormalities

Beyond neurotransmitter imbalances, depression is also associated with various structural changes in the brain, including:

- Decreased number of glial cells: Specifically in areas such as the amygdala and pregenual anterior cingulate cortex. Glial cells support neurons and are critical for maintaining brain function
- Decreased myelination: Myelin, the insulating sheath around neurons, is essential for fast and efficient communication between brain regions. In depression, myelination is often reduced in areas such as the dorsolateral PFC and middle temporal gyrus, potentially impairing cognitive and emotional regulation
- White matter lesions: These lesions, particularly in the corpus callosum (which connects the two hemispheres of the brain), are more commonly observed in individuals with chronic depression, especially in older adults.[7]

Imbalanced communication in neuronal networks

Recent research emphasizes that depression involves disrupted communication within neural networks, particularly between the PFC, amygdala, and other regions involved in emotional processing. This dysregulation in communication likely contributes to the persistent negative thoughts, emotional dysregulation, and cognitive impairments that characterize the disorder.[8]

Neuroanatomical Basis of Mania

- It includes: Convergent model of lateralized circuit dysfunction of the brain. It involves hypoactivity of the ventromedial and ventrolateral PFC of the right cerebral hemisphere and hyperactivity of amygdala, basal nuclei, and anterior cingulate gyrus of the left cerebral hemisphere
- Abnormal serotonin chemistry in the brain. Serotonin receptors such as 5-HT1D and 5-HT1A are associated with manic episodes
- Increased excitatory input from the subthalamic nucleus (STN) to dopaminergic nuclei of the brain. These nuclei are involved in emotion-based behaviors such as motivation and reward
  - The STN is a brain structure that is involved in regulating movement
  - Increased excitatory input from the STN to the basal ganglia is associated with manic episodes.

Treatment Options for Depression and Bipolar Disorder

Given the neuroanatomical and neurochemical underpinnings of depression, treatment approaches target both the brain's structure and function. These include:

- Medications: Antidepressants and antipsychotics that modulate the activity of neurotransmitters such as serotonin, norepinephrine, and dopamine (e.g., selective serotonin reuptake inhibitors, serotonin-norepinephrine reuptake inhibitors, and monoamine oxidase inhibitors) are commonly used to address the neurochemical imbalances in depression and panic disorder[9]
- Psychotherapy: Cognitive-behavioral therapy, interpersonal therapy, and problem-solving therapy aim to address maladaptive thinking patterns and improve coping mechanisms, ultimately influencing brain activity and structure.[10]

Conclusion

The neuroanatomical basis of depression is complex, involving both structural and functional changes in key brain regions that regulate mood, cognition, and emotion. Understanding these changes is crucial for developing effective treatments and improving the lives of those affected by these debilitating conditions. With continued research, our ability to intervene and address the underlying causes of depression will only improve, leading to better outcomes for individuals worldwide.

Vishram Singh, Rashi Singh[1], Gaurav Singh[2]

Department of Anatomy, Kasturba Medical College, Mangalore, Manipal Academy of Higher Education, Manipal, Karnataka, [1]Department of Pediatric and Preventive Dentistry, Santosh Dental College and Hospital, NCR Delhi, [2]Clinical Editor, British Medical Journal, NCR Delhi, India

Address for correspondence: *Prof. Vishram Singh, B5/3 Hahnemann Enclave, Plot No. 40, Sector 6, Dwarka Phase – 2, New Delhi - 110 075, India.*
E-mail: drvishramsingh@gmail.com

References

1. Murthy RS. National mental health survey of India 2015-2016. Indian J Psychiatry 2017;59:21-6.
2. Green CE, Gupta T, MacMullin G, *et al.* Neurotransmitter dysregulation in depression: The role of glutamate. J Clin Psychiatry 2020;81:154-62.
3. Clark MA, Douet D, Beare R, *et al.* Amygdala activity in

depression and its link to prefrontal cortical dysfunction. J Neurosci 2022;42:567-78.
4. Singh T, Cho RY, Kaur M, *et al.* Prefrontal cortex and depression: Reduced gray matter volumes and impaired cognitive function. Brain Imaging Behav 2021;15:459-69.
5. Harris A, Wallace M, Lindholm A, *et al.* Cortisol and hippocampal volume in major depressive disorder: Evidence from longitudinal studies. Psychiatry Res 2023;305:113-22.
6. Tyler EA, Evans DR, Jones Y, *et al.* Reduced reward processing in the ventral striatum and its relationship to anhedonia in depression. Biol Psychiatry 2023;79:289-97.
7. Chawla V, Kulkarni S, Mehta R, *et al*. White matter lesions and their impact on brain connectivity in chronic depression. Am J Psychiatry 2020;177:733-41.
8. Simmons WK, Pan L, Blanchard T, *et al.* Connectivity between the prefrontal cortex and amygdala in depression: A neuroimaging study. Biol Psychiatry 2021;90:15-23.
9. Kumar D, Patel J, Shah K, *et al.* Antidepressants and neurotransmitter reuptake mechanisms: A comprehensive review. Psychopharmacology 2020;237:123-34.
10. Vaidya J, Chandran K, Kamat S, *et al.* Cognitive-behavioral therapy in treatment-resistant depression: Evidence and outcomes. J Clin Psychol 2022;78:310-8.

Article Info

Received: 11 December 2024
Accepted: 12 December 2024
Available online: 28 December 2024

Access this article online	
Quick Response Code:	**Website:** https://journals.lww.com/joai
	DOI: 10.4103/jasi.jasi_192_24

How to cite this article: Singh V, Singh R, Singh G. Neuroanatomical basis of depression and bipolar disorder: Insights into the brain's role in mood disorders. J Anat Soc India 2024;73:297-9.

Original Article

Ectopic Bronchial Arteries – Incidental Findings on Multi-detector Computed Tomography

C. S. Ramesh Babu, Vinay Sharma, Om Prakash Gupta[1]

Department of Anatomy, Muzaffarnagar Medical College, Muzaffarnagar, [1]O. P. Gupta Imaging Centre, Meerut, Uttar Pradesh, India

Abstract

Introduction: Orthotopic bronchial arteries (BAs) arise from the descending aorta between T5 and T6 vertebral levels and those emanating from the aortic arch, distal descending aorta, and subclavian arteries are called ectopic and are present in about one-third of cases. **Study Design:** Rare and unreported origin of ectopic BAs incidentally detected while analyzing 710 multi-detector computed tomography (MDCT) scans are presented. **Observations:** Ectopic BAs of subclavian origin supplying ipsilateral lungs are seen in two cases. Ectopic common bronchial trunk arising from the left subclavian and dividing into right and left branches was observed in two cases. Bilateral subclavian origin of both BAs is a rare presentation. Till now, an unreported variant is the common trunk of the left bronchial and left vertebral (bronchovertebral trunk) arising from the left subclavian close to its root from the aortic arch. Another rare variant of right bronchial arising from the left subclavian (Contralateral origin) is also noted. **Discussion and Conclusion:** The number of BAs varies. At least one ectopic BA is present in 36% of cases and in nearly half of these cases, ectopic arteries are the only supply. BAs are embolized to control severe hemoptysis and are used for infusion chemotherapy for lung neoplasms. A prerequisite for successful interventional and surgical procedures on BA is precise anatomical knowledge and preprocedural MDCT can provide accurate anatomical information to prevent complications following BA embolization to control hemoptysis.

Keywords: *Aberrant bronchial artery, bronchovertebral trunk, common bronchial trunk, descending aorta, multi-detector computed tomography, orthotopic bronchial artery*

Introduction

Bronchial arteries (BAs) carry oxygenated blood at a pressure six times that of the pulmonary artery to nourish the conducting portion of the respiratory tree, pulmonary lymph nodes, and visceral pleura, and generally do not participate in gaseous exchange. These arteries are resistant to arteriosclerotic changes and contribute 1% of the blood supply to the lungs.[1,2] BAs are slender vessels measuring 1–1.5 mm in diameter and difficult to visualize, but become dilated and tortuous measuring 2 mm or more in certain congenital and acquired pathologies.[2] Normally, a single right bronchial artery (RBA) arising in common with the right third posterior intercostal artery (as an intercostobronchial trunk [ICBT]) and two left bronchial arteries (LBAs) arising separately from descending thoracic aorta (DA) from the level of the upper-end plate of T5 (D5) to lower end plate of T6 (D6) vertebrae, 1–2 cm above or below the level of carina, supply the lungs. Sometimes, a common bronchial trunk (CBT) from DA bifurcates into RBA and LBA. These BAs are termed as "orthotopic" and the arteries originating from the arch of the aorta and its branches and lower DA distal to T6 (D6) level are termed "Ectopic."[3] Cauldwell (1948) in his classical study on 150 cadavers observed ectopic BAs in 16.7% of cases and classified the pattern of origin and number of RBA and LBAs into nine types, of which four patterns are more common.[4] In these four common patterns, the RBA arose as a branch of ICBT or directly from DA and LBA directly from DA. Type I has one RBA and two LBAs (40.6%), type II has one RBA and one LBA (21.3%), type III has two BAs on each side (one RBA from ICBT and another from DA) (20.6%), and type IV has one LBA and two RBAs (9.7%).[4] Other studies have reported the prevalence of ectopic BAs ranging from 7.4% to 38.3%.[5,6] In their study on 600 patients with hemoptysis, Choi *et al.* observed 87.5% orthotopic and 12.5%

How to cite this article: Babu CS, Sharma V, Gupta OP. Ectopic bronchial arteries – incidental findings on multi-detector computed tomography. J Anat Soc India 2024;73:300-6.

Article Info

Received: 16 August 2024
Revised: 08 November 2024
Accepted: 18 November 2024
Available online: 28 December 2024

Address for correspondence:
Prof. C. S. Ramesh Babu, Department of Anatomy, Muzaffarnagar Medical College, Muzaffarnagar, Uttar Pradesh, India.
E-mail: csrameshb@gmail.com

Access this article online

Website: https://journals.lww.com/joai

DOI: 10.4103/jasi.jasi_123_24

Quick Response Code:

ectopic BAs.[7] Common sites of origin of ectopic BAs include the arch of the aorta, distal DA, and subclavian artery and its branches.[7,8]

BA is the major source of bleeding in nearly 90% of cases of hemoptysis and the treatment of choice is BA embolization (BAE).[9] Because of the complex nature of different patterns of BAs, in terms of site of origin, number of arteries on right and left sides, variant mediastinal course, and variant relationship with trachea and esophagus, precise anatomical knowledge of BAs is most essential for successful catheterization of culprit BA and multi-detector computed tomography (MDCT) angiography is emerging as the preferred modality for pre- and postembolization analysis. Precise knowledge of orthotopic and ectopic BA anatomy becomes of paramount importance because nearly two-thirds of right ectopic BAs and half of left ectopic BAs are the only source of BA supply.[5] This knowledge is also important to prevent complications during esophageal, mediastinal thoracoscopic, oncological, and cardiothoracic surgeries and prevent the rare complications of tracheobronchial, spinal cord, and cerebral infarction.[10,11]

Materials and Methods

The present study is designed as a retrospective analysis of MDCT chest scans of 710 patients (Male 435 and Female 275) retrieved from the archives of a single imaging center. All subjects were referred to undergo CECT chest for suspected mediastinal and lung pathologies. The imaging center routinely obtains informed consent from the patients before administration of the contrast medium. While examining the CECT chest scans for aortic arch branching patterns with a special emphasis on left vertebral artery origin, we incidentally noted the ectopic origin of BAs. Some of the variant origins of BAs noted incidentally is rare and one variant is not reported so far in the literature which prompted the present submission.

Observations

Subclavian artery origin of ectopic BA supplying ipsilateral lung was observed in two male subjects, one right and one left [Figures 1 and 2]. The ectopic LBA originates from the left subclavian artery (LSA) close to its origin from the arch which had two branches only, the brachiocephalicocarotid trunk (BCCT so-called "bovine trunk") and LSA. In this case, an orthotopic LBA from the descending aorta was also observed [Figure 1a]. The ectopic RBA arises from RSA in the root of the neck and in this case, a typical three-branched arch is present [Figure 2a]. These ectopic BAs had a paratracheal and paraesophageal course to reach the hilum and course on the anterior aspect of the main bronchi [Figures 1b and 2b]. A CBT emanating from LSA close to its root and then bifurcating into a larger RBA and a smaller LBA was noted in two males [Figure 3a-d]. Two-branched arch (BCCT and LSA) was noted in one case [Figure 3a] and normal pattern in the second case. A normal three-branched arch

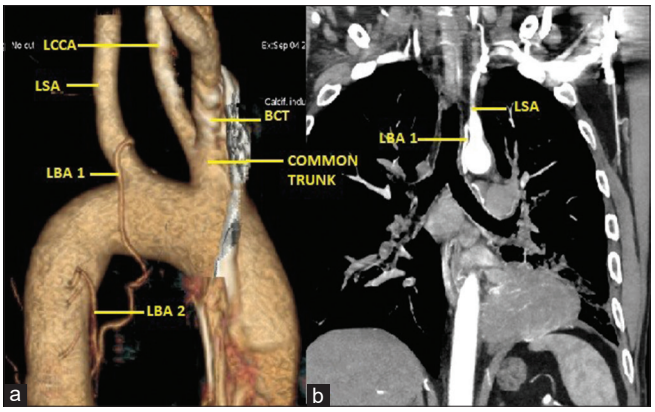

Figure 1: (a) Volume rendered (VR) (posterior view) and (b) Coronal scan showing ectopic left bronchial artery (LBA1) emanating from left subclavian artery (LSA) just above its origin from aortic arch and another orthotopic LBA (LBA2) from descending aorta. Note the presence of common trunk ('bovine trunk') of brachiocephalic (BCT) and left common carotid (LCCA) arteries

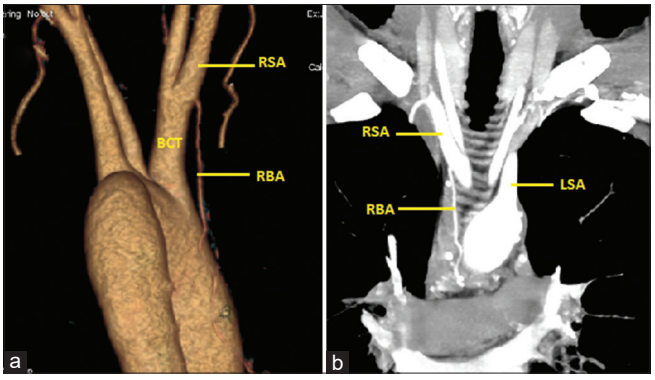

Figure 2: (a) VR image (posterior view) and (b) Coronal scan showing ectopic right bronchial artery (RBA) from right subclavian (RSA) close to its origin from BCT. b-Paratracheal course of RBA is clearly seen

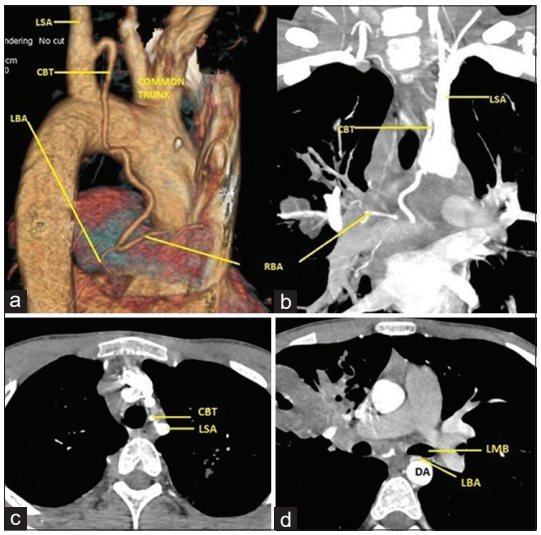

Figure 3: (a) VR image (posterior view) (b) Coronal scan depicting common bronchial trunk (CBT) from left subclavian (LSA) close to its origin from arch. CBT passes posterior to the arch and bifurcates into a larger RBA and a smaller LBA. Note the presence of common trunk ('bovine trunk') in the two branched arch. (c and d) Axial scans showing origin of CBT from LSA and passage of LBA posterior to left main bronchus (LMB)

gives origin to a CBT from its concavity which divides into a larger RBA and a smaller LBA [Figure 4]. In addition, two more LBAs were noted in this case [Figure 4a and b]. Origin of both BAs from the concavity of the aortic arch was observed in a male who also exhibited the presence of a celiacomesenteric trunk (CMT) from the abdominal aorta [Figure 5]. The ectopic origin of an ICBT from the aortic arch giving origin to RBA [Figure 6b] and origin of LBA from the arch were also seen [Figure 6a]. Rarely reported bilateral subclavian origin of ectopic BAs was seen in a female who also had a variant left brachiocephalic vein with subaortic course [Figure 7]. To the best of our knowledge, an unreported pattern of origin of a common "bronchovertebral trunk" from LSA close to its root was found in a male [Figure 8]. This common trunk immediately divided into LBA and LVA which coursed in a caudal and cranial direction along the left margin of the trachea. Ectopic RBA arising from the contralateral subclavian (LSA) was also observed in a male who also had two orthotopic LBAs arising from DA [Figure 9]. Multiple BAs were observed in a male with an ectopic LBA from the aortic arch, two orthotopic LBAs from the DA, and an enlarged tortuous orthotopic RBA from DA [Figure 10]. There is a presence of LVA of aortic arch origin between left common carotid artery and LSA [Figure 10]. It is important to note that ectopic BA arises from LSA close to its arch origin and from RSA in the root of the neck. Ectopic BAs arising from the aortic arch and subclavian arteries descend in the superior mediastinum on either side of the trachea and esophagus (paratracheal/paraesophageal) and generally pass anterior to main bronchi to enter lung hilum.

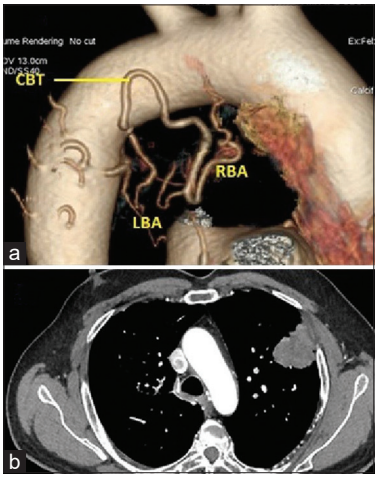

Figure 4: (a) VR image (posterior view) and (b) Axial scan showing origin of common bronchial trunk (CBT) dividing into right and left bronchial arteries and an ectopic left bronchial artery (LBA) from the concavity of the aortic arch. Note origin of an orthotopic LBA from descending aort

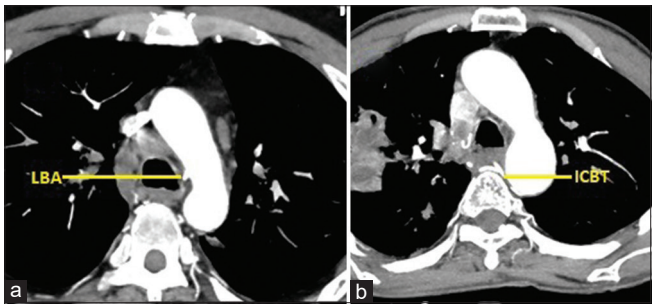

Figure 6: (a and b) Axial scans showing (a) origin of left bronchial (LBA) artery from concavity of aortic arch and (b) arch origin of intercostobronchial trunk (ICBT)

Discussion

Orthotopic bronchial arteries

The anatomy of the BAs is quite variable with respect to their site of origin, course, relationship with the esophagus,

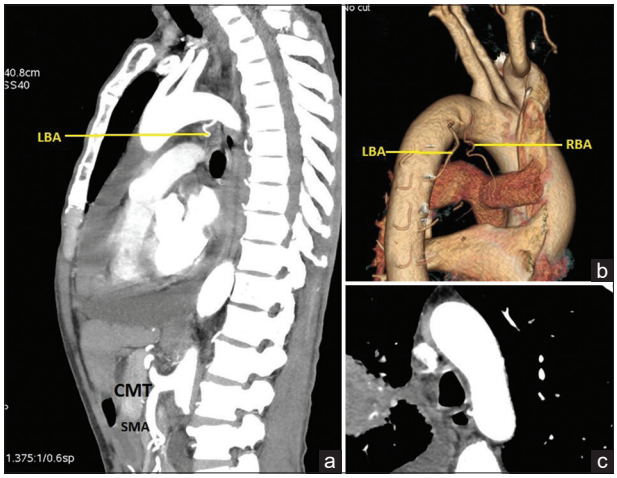

Figure 5: (a) Sagittal scan (b) VR image (posterior view) (c) Axial scan showing origin of ectopic right bronchial (RBA) and left bronchial (LBA) arteries from the concavity of aortic arch. The subject also has Celiacomesenteric trunk (CMT) arising from abdominal aorta bifurcating into superior mesenteric (SMA) artery and celiac trunk

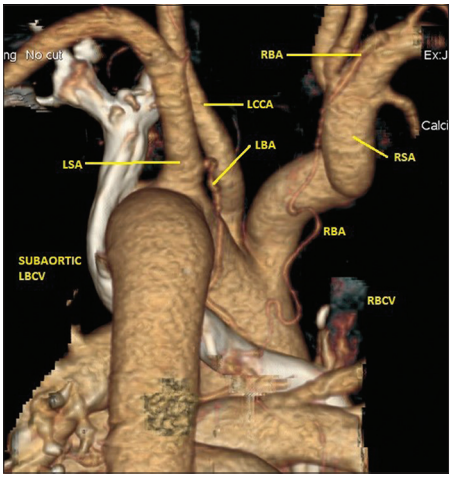

Figure 7: VR image (Posterior view) Bilateral subclavian origin. Left bronchial (LBA) from left subclavian (LSA) close to aortic arch and right bronchial (RBA) from right subclavian (RSA) in root of neck. The patient also exhibited an extremely rare venous anomaly in the form of subaortic left brachiocephalic vein (LBCV) passing under the concavity of aortic arch. RBCV- Right brachiocephalic vein. LCCA- Left common carotid artery

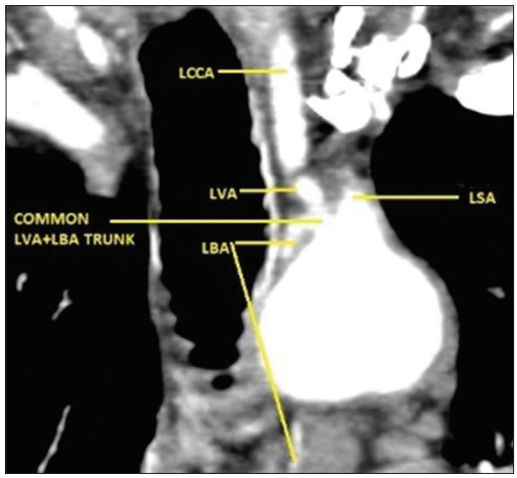

Figure 8: Coronal scan showing an unreported variant - a common trunk from root of left subclavian (LSA) bifurcating into left vertebral (LVA) and left bronchial (LBA) arteries. The common trunk is named as "Broncho-vertebral trunk"

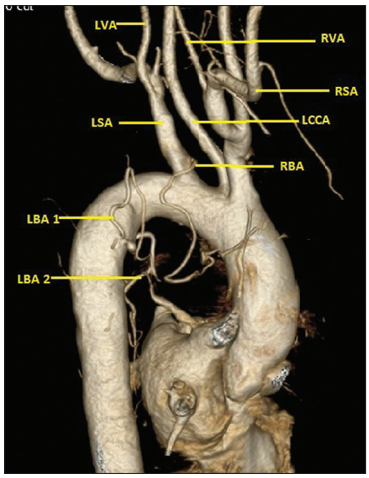

Figure 9: VR Image (posterior view) Ectopic right bronchial (RBA) arise from left subclavian (LSA) just above aortic arch. Also note the origin of two orthotopic left bronchial (LBA) arteries from descending aorta

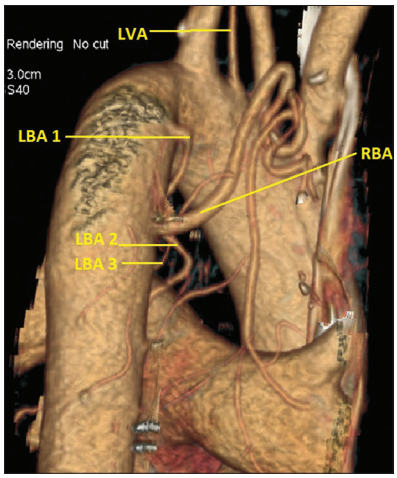

Figure 10: VR image (Posterior view) showing presence of multiple bronchial arteries. Ectopic left bronchial (LBA 1) arise from the aortic arch and two orthotopic left bronchial (LBA 2 and LBA 3) and an orthotopic enlarged tortuous right bronchial (RBA) originate from descending aorta very close to each other. Also note the direct arch origin of left vertebral (LVA) artery

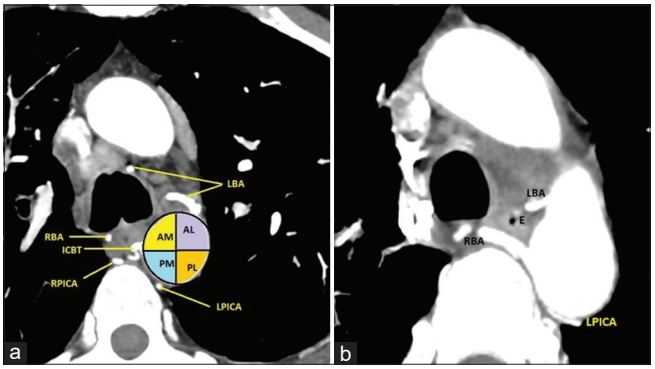

Figure 11: Axial scans (a) Descending aorta is encircled and divided into four quadrants differently colored to indicate normal site of origin of bronchial arteries and intercostobronchial trunk (ICBT). Right and left posterior intercostal arteries (RPICA, LPICA) originate from posterior quadrants whereas, ICBT arise from medial quadrants. (b) Shows course of right and left bronchial arteries dorsal and ventral to esophagus

trachea, main bronchi, and number of branches on each side.[3,7,8,12,13] There are three modes of origin of an orthotopic RBA-from an ICBT, from a CBT, and direct origin from DA, whereas LBA arises directly from DA, as a branch of CBT and very rarely from an ICBT. An orthotopic RBA originates from anteromedial or posteromedial quadrants of DA and LBA arises from anterolateral and anteromedial quadrants and passes anterior or posterior to the esophagus [Figure 11a and b] Normally right third posterior intercostal artery arising from the anteromedial quadrant of DA forms ICBT and courses between the esophagus and spine to reach the right margin of the esophagus and gives off RBA. This RBA makes a characteristic bend parallel and inferior to the arch of the azygos vein to descend along the right margin of the esophagus to reach the hilum posterior to the main bronchus. Extremely rarely present LBA of ICBT origin passes along the left margin of the esophagus to enter the hilum posterior to the main bronchus [Figure 12a]. CBT from anterior quadrants of DA divides into RBA and LBA which always pass along the left margin of the esophagus to enter respective hila either anterior or posterior to main bronchi [Figure 12b]. Direct origin LBA arises from the anterolateral quadrant of DA always run along the left margin of the esophagus to reach the hilum posterior to the main bronchus [Figure 12c]. Direct origin RBA passes along the left margin of the esophagus to reach the hilum passing either posterior or anterior to the main bronchus [Figure 12c]. In essence, only RBAs of ICBT origin run along the right margin of the esophagus and all types of LBAs and RBAs of CBT origin and direct origin pass along the left margin of the esophagus.[6,13-16] It is estimated that RBAs of ICBT origin are present in nearly 70% of cases. RBAs give fine branches to midesophagus, trachea, pericardium, and mediastinal lymph nodes. In 2.5%–18.5% of cases, the CBT forms the sole arterial supply to the bronchial tree.[17]

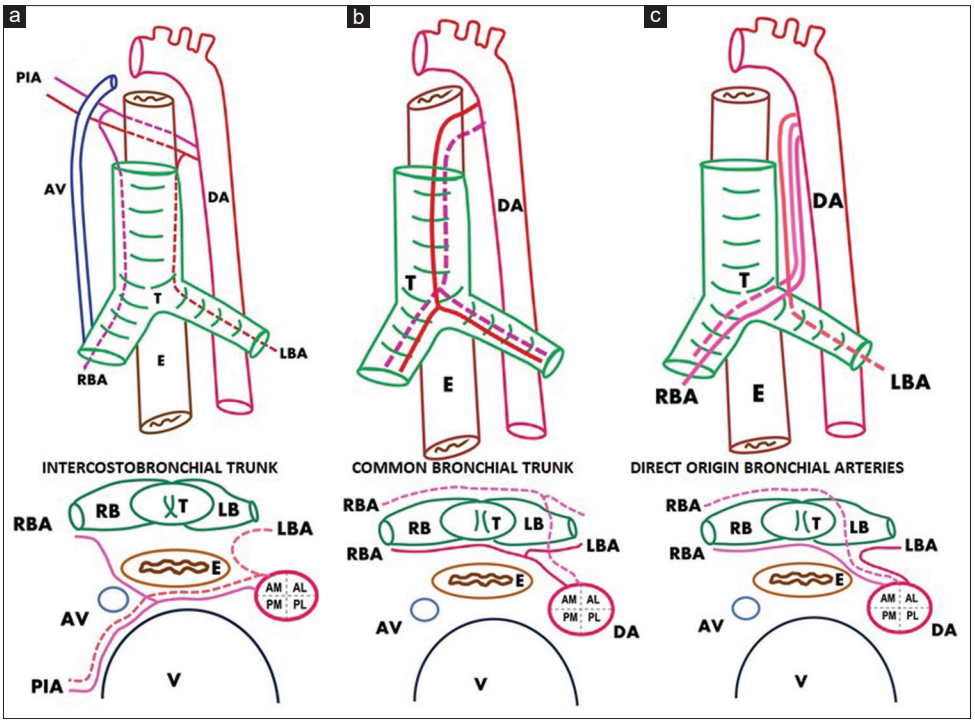

Figure 12: Schematic diagram depicting variable mediastinal course and relationship of orthotopic bronchial arteries arising from intercostobronchial trunk (a), common bronchial trunk (b) and direct origin (c) with esophagus and trachea-bronchus. AV-Azygos vein, E-Esophagus, DA-Descending aorta, LB-Left bronchus, RB-Right bronchus, LBA-Left bronchial artery, PIA- Posterior intercostal artery, RBA- Right bronchial artery, T-Trachea, V-Vertebra

Ectopic bronchial arteries

The so-called "ectopic" (aberrant or anomalous) BAs arise from arch of aorta, subclavian artery and its branches such as internal mammary (IMA), thyrocervical trunk (TCT), and costocervical trunk (CCT), DA distal to T6 level, brachiocephalic trunk, and common carotid artery with a prevalence up to 36%. Gailloud (2022) has proposed distinguishing ectopic BAs as aberrant (replaced) and accessory (supplementary).[18] Based on the number of BAs, their laterality, source of origin, and relations to surrounding structures, different types of classification systems are proposed in the literature.[4,7,9,13,14,19]

Studies describing the anatomy of normal and ectopic BAs are mainly radiological and performed on hemoptysis patients. Cadaveric and radiological studies on the general population are meager. Battal *et al*. examined MDCT scans of 163 subjects and identified a total of 432 BAs of which 26.4% were ectopic. They also noted more number of BAs on the right side and in men.[8] In a CT angiographic study on the Mexican population, the authors noted ectopic BAs in 33.65% of cases and observed 35 different branching patterns.[16] They have described the rare origin of both RBA and LBA from ICBT in two cases.

Aortic arch origin

The most common site of origin of ectopic BAs is the arch of the aorta and it is believed that nearly two-thirds of ectopic BAs arise from the concavity of the arch. Few cases of BAs arising from the convexity of the arch have also been observed.[5] Of the 210 ectopic BAs detected by Choi *et al*. 138 arose from the aortic arch.[7] Hartmann *et al*. noted 92 out of 124 ectopic BAs originating from the arch of the aorta, Yener *et al*. detected 29 out of 78 ectopic BAs, and Battal *et al*. observed 29 ectopic BAs from the arch of the aorta out of 58 ectopic arteries.[5,6,8] We have observed ectopic origin of both RBA and LBA from the concavity of the aortic arch in a patient who had an anomalous CMT arising from the abdominal aorta and origin of ectopic CBT, ICBT, and LBA from the arch of aorta in three other cases.

Ipsilateral subclavian artery origin

It is to be noted that the subclavian artery and its branches constitute the second most common site of origin of ectopic BAs with a reported prevalence ranging from 3.05% to 10.5%.[5,8,13] We have observed two cases of ectopic BAs of subclavian origin, one left and one right and in one case with two-branched arch having the "bovine trunk." Kawate *et al*. observed the origin of LBA from LSA in a cadaver with LVA directly arising from the arch.[20] Battal *et al*. have recorded variations in aortic arch branching pattern in 11 out of 43 cases (25.6%) with ectopic BAs and have also observed the origin of an ectopic RBA from an aberrant RSA.[8] Natsis *et al*. reported a rare origin of RBA in a common stem with right IMA in a cadaver.[21] Origin of ectopic BAs from ipsilateral IMA and TCT was also observed.[5-8]

Contralateral subclavian origin

In the present study, the contralateral subclavian origin of RBA was found in a male. Origin of RBA from the

contralateral subclavian artery and TCT was noted in one case each (0.4%).[8] Yener *et al*. detected the contralateral origin of RBA from LSA (0.68%), LIMA (0.68%), and TCT (0.34%). Contralateral origin of ectopic LBA is very rare and only in one case, the origin of LBA from right IMA (0.41%) was detected.[6] In their MDCT study on 600 patients with hemoptysis, Choi *et al*. found ectopic BAs in 24.7% of cases and only one case of contralateral origin.[7] Ectopic RBA branching off from LSA was also reported.[22,23]

Common bronchial trunk origin

CBTs providing bilateral branches are very rarely associated with unusual sites of origin. We have observed CBT from LSA in two cases and from concavity of arch in one case. Variation in aortic arch branching pattern with "bovine trunk" was noted in one case with CBT. Only four cases of CBTs originating from a subclavian artery have been reported in the literature to the best of our knowledge.[24,25] In all reported cases, including our observation, the variant was located on the left side. Origin of CBT in common with left superior intercostal artery from LSA and from left TCT were also reported.[16,26]

Bilateral subclavian origin

Bilateral subclavian origin of BA is very rare. Jie *et al*. reported a very rare case of bilateral origin of BA from the branches of RSA, RBA from right CCT, and LBA from left TCT.[27] In the present report, BAs originated bilaterally from respective subclavian arteries in a female subject who also exhibited an extremely rare subaortic left brachiocephalic vein. Another observation, to the best of our knowledge not reported so far in the literature, is the origin of LBA from a common trunk with LVA ("bronchovertebral trunk") close to the root of LSA. Amrhein *et al*. and Jiang *et al*. each reported a case of LBA arising from LVA of aortic arch origin.[28,29] In the present report, the LBA and LVA shared a common trunk arising from LSA very close to its origin from the aortic arch.

Embryology

Developmentally, the adult BAs originate due to the involution of the primitive branches, which originate from the dorsal aorta, pharyngeal arch arteries, and intersegmental arteries and initially feed the primitive pulmonary plexus. The persistence of one of these early branches results in an ectopic BA of high origin, originating from the aortic arch, subclavian artery or its branches, brachiocephalic, common carotid, vertebral, and intercostal arteries.[3]

Clinical importance

The BAs constitute nutritive vascular system of the pulmonary tissues, such as bronchial walls and glands, walls of large vessels, and visceral pleura. It is crucial to be aware of the variations of the bronchial arterial system in thoracic surgery, especially in BAE for massive hemoptysis, infusion chemotherapy for treating lung neoplasms, and restoration BA circulation by anastomosing donor BA to recipient BA in lung transplantation.[21] RBA is especially susceptible to injury during esophageal surgeries and inadvertent damage can cause life-threatening tracheobronchial necrosis. Other complications of interventional therapy include chest pain, spinal cord ischemia, dysphagia, subintimal dissection of BA and aorta, bronchial necrosis, nontarget organ embolization, and cerebral posterior circulation infarction including transient cortical blindness.[10,11,18,30] Although the origin of radiculomedullary branches supplying the spinal cord directly arising from the BAs is denied by Befera *et al*., Fei *et al*. observed the origin of radiculomedullary artery from ICBT only after the origin of BA in four cases out of 48 cadavers dissected.[14,31] The anterior spinal artery is very tenuous in midthoracic cord segments (T3-T7) supplemented only by a radiculomedullary artery from an ICBT and any leakage of embolic material into such an artery can lead to spinal cord ischemia.

Limitations of the study

The main limitation of the study is that it was not designed to analyze specifically the normal and variants of the BAs. During the course of analysis of aortic arch variant branching patterns and left vertebral artery variants, the ectopic BAs were detected incidentally. Finding the rarity of some variants and the unreported nature of another variant prompted us to present our observations. Detailed anatomical or radiological study of BAs in Indian subjects is warranted.

Conclusion

As the anatomy of the BAs is quite variable with respect to their site of origin, mediastinal course, relationship with esophagus, trachea, main bronchi and number of branches on each side, a comprehensive study encompassing all these aspects in general population is necessary.

Financial support and sponsorship

Nil.

Conflicts of interest

There are no conflicts of interest.

References

1. Osiro S, Wear C, Hudson R, Ma XX, Zurada A, Michalak M, *et al*. A friend to the airways: A review of the emerging clinical importance of the bronchial arterial circulation. Surg Radiol Anat 2012;34:791-8.
2. Walker CM, Rosado-de-Christenson ML, Martínez-Jiménez S, Kunin JR, Wible BC. Bronchial arteries: Anatomy, function, hypertrophy, and anomalies. Radiographics 2015;35:32-49.
3. Akgun V, Hamcan S, Bozkurt Y, Battal B. Thoracic aorta in Bergman's comprehensive encyclopedia of human anatomic variations. In: Tubbs S, Shoja MM, Loukas M, editors. SMTE Books. New Delhi: Willey Blackwell; 2016.
4. Cauldwell EW, Siekert RG. The bronchial arteries; an

anatomic study of 150 human cadavers. Surg Gynecol Obstet 1948;86:395-412.
5. Hartmann IJ, Remy-Jardin M, Menchini L, Teisseire A, Khalil C, Remy J. Ectopic origin of bronchial arteries: Assessment with multidetector helical CT angiography. Eur Radiol 2007;17:1943-53.
6. Yener Ö, Türkvatan A, Yüce G, Yener AÜ. The normal anatomy and variations of the bronchial arteries: Evaluation with multidetector computed tomography. Can Assoc Radiol J 2015;66:44-52.
7. Choi WS, Kim MU, Kim HC, Yoon CJ, Lee JH. Variations of bronchial artery origin in 600 patients: Systematic analysis with multidetector computed tomography and digital subtraction angiography. Medicine (Baltimore) 2021;100:e26001.
8. Battal B, Akgun V, Karaman B, Bozlar U, Tasar M. Normal anatomical features and variations of bronchial arteries: An analysis with 64-detector-row computed tomographic angiography. J Comput Assist Tomogr 2011;35:253-9.
9. Uflacker R, Kaemmerer A, Picon PD, Rizzon CF, Neves CM, Oliveira ES, *et al*. Bronchial artery embolization in the management of hemoptysis: Technical aspects and long-term results. Radiology 1985;157:637-44.
10. Gao F, Xu Y, Fang S. Cerebral infarct after bronchial artery embolization. BJR Case Rep 2019;5:20180087.
11. Yu L, Li X, Lin F, Wan T, Cao Z. Posterior circulation infarction after bronchial artery embolization. Acta Radiol Open 2023;12:20584601231168968.
12. Almeida J, Leal C, Figueiredo L. Evaluation of the bronchial arteries: Normal findings, hypertrophy and embolization in patients with hemoptysis. Insights Imaging 2020;11:70.
13. Morita Y, Takase K, Ichikawa H, Yamada T, Sato A, Higano S, *et al*. Bronchial artery anatomy: Preoperative 3D simulation with multidetector CT. Radiology 2010;255:934-43.
14. Fei QL, Zhou YY, Yuan YX, Sun SQ. An applied anatomical study of bronchial artery. Surg Radiol Anat 2018;40:55-61.
15. Maeda T, Fujiwara H, Konishi H, Shiozaki A, Kobayashi T, Ohashi T, *et al.* Preoperative 3D-CT evaluation of the bronchial arteries in transmediastinal radical esophagectomy for esophageal cancer. Esophagus 2022;19:77-84.
16. Esparza-Hernández CN, Ramírez-González JM, Cuéllar-Lozano RA, Morales-Avalos R, González-Arocha CS, Martínez-González B, *et al.* Morphological analysis of bronchial arteries and variants with computed tomography angiography. Biomed Res Int 2017;2017:9785896.
17. Riquet M. Bronchial arteries and lymphatics of the lung. Thorac Surg Clin 2007;17:619-38, viii.
18. Gailloud P. Tracheobronchial arterial variants of vertebral artery origin and bronchovertebral arterial anastomoses. Surg Radiol Anat 2022;44:665-72.
19. Liebow AA. Patterns of origin and distribution of the major bronchial arteries in man. Am J Anat 1965;117:19-32.
20. Kawate T, Futamata H, Kitami Y, Takeda S. Rare multiple combined anomaly of the vertebral vessels and bronchial artery. Anat Sci Int 2008;83:267-72.
21. Natsis K, Asouhidou I, Vizas V, Didagelos M. A rare cadaveric finding of ectopic origin of a bronchial artery: Surgical and imaging consequences. Folia Morphol (Warsz) 2013;72:78-81.
22. Fukaya T, Kasai H, Nagata J, Sugiura T. Haemoptysis due to an atypical right bronchial artery branching from the left subclavian artery evaluated by four-dimensional CT and bronchial arteriography. BMJ Case Rep 2021;14:e239754.
23. Ziyawudong J, Kawai N, Sato M, Ikoma A, Sanda H, Takeuchi T, *et al*. Aortic ostia of the bronchial arteries and tracheal bifurcation: MDCT analysis. World J Radiol 2012;4:29-35.
24. Khalil A, Ricolfi F, Debray MP, Djindjian M, Gaston A. A common bronchial arterial trunk arising from a left subclavian artery: A rare anatomic variant. Surg Radiol Anat 1995;17:171-2, 27-8.
25. Albayram S, Gailloud P, Tatli S, Venbrux A, Murphy KJ. Common bronchial artery trunk originating from the left subclavian artery. J Vasc Interv Radiol 2001;12:774-5.
26. O'rahilly R, Debson H, King TS. Subclavian origin of bronchial arteries. Anat Rec 1950;108:227-38.
27. Jie B, Sun XW, Yu D, Jiang S. Bilateral subclavian origin of the bronchial arteries combined with absence of other origins. Surg Radiol Anat 2014;36:607-11.
28. Amrhein TJ, Kim C, Smith TP, Washington L. Bronchial artery arising from the left vertebral artery: Case report and review of the literature. J Clin Imaging Sci 2011;1:62.
29. Jiang S, Sun XW, Jie B, Yu D. Endovascular embolization of an aberrant bronchial artery originating from the vertebral artery in a patient with massive hemoptysis. Cardiovasc Intervent Radiol 2014;37:1099-102.
30. Maramattom BV, Krishna Prasad BP, Padmanabhan S, Baby J. Spinal cord infarction after bronchial artery embolization. Ann Indian Acad Neurol 2016;19:156-7.
31. Befera NT, Ronald J, Kim CY, Smith TP. Spinal arterial blood supply does not arise from the bronchial arteries: A detailed analysis of angiographic studies performed for hemoptysis. J Vasc Interv Radiol 2019;30:1736-42.

Original Article

O-GalNAc Glycosylation - Key Pathway for Hashimoto's Thyroiditis in Patients with Metabolically Unhealthy Obesity

Rui Yang, Jianli Han

Department of General Surgery, Shanxi Bethune Hospital, Taiyuan, Shanxi, China

Abstract

Objective: The incidence of Hashimoto's thyroiditis (HT) in patients with metabolically unhealthy obesity (MUO) is generally higher than that in normal-weight individuals. However, the relationship among obesity, HT, and hypothyroidism remains unclear. **Subjects and Methods:** We searched the National Center for Biotechnology Information database and analyzed the abnormal expression of miRNAs in patients with MUO. The datasets GSE169290 and GSE138198 were selected as the objects of this data analysis. Using the MirPath tool on the DIANA TOOLS website, the KEGG pathway enrichment results were used for further analysis and explored the differential expression of pathways in patients with HT. **Results:** Four KEGG pathways were identified: "prion diseases (hsa05020)," "ECM-receptor interaction (hsa04512)," "mucin-type O-glycan biosynthesis (hsa00512)," and "cell adhesion molecules (hsa04514)." Sixteen differential genes were obtained, among which GALNT15 ranked the first, GALNT12 ranked the eighth, and GALNT8 ranked the 13th. *GALNT15*, *GALNT12*, and *GALNT8* in the "mucin-type O-glycan biosynthesis" pathway are significantly lower in HT patients, which may be a key factor in the pathogenesis of HT. **Conclusions:** Decreased expression of O-GalNAc glycosylation in patients with MUO may increase the incidence of HT, which may become an important mechanism of HT in patients with obesity and is worthy of further exploration in future.

Keywords: *Enrichment analysis, Hashimoto's thyroiditis, metabolically unhealthy, obesity, O-GalNAc glycosylation*

Introduction

Obesity, a complex health issue, is identified as an excessive accumulation of body fat detrimental to overall health. Large-scale studies have consistently shown a significant link between obesity and the prevalence of a multitude of diseases.[1,2] It is a systemic condition impacting various endocrine organs, notably the thyroid.[3,4] While obesity is tightly interwoven with metabolic disruptions, the manifestation of these metabolic abnormalities diverges at the individual level.[5] Roughly 10%–30% of obese individuals do not exhibit the harmful metabolic consequences typically associated with excess body fat.[6-8] Hence, based on individual metabolic profiles and obesity, it is possible to categorize obesity into metabolically healthy obesity (MHO) and metabolically unhealthy obesity (MUO).[9]

Hashimoto's thyroiditis (HT), also referred to as chronic lymphocytic thyroiditis or autoimmune thyroiditis, stands as the primary source of hypothyroidism in patients maintaining adequate iodine intake.[10] Over the last three decades, there has been a surge in the incidence of HT, yet the root cause remains largely undefined. Observations indicate a positive correlation between serum thyroid-stimulating hormone (TSH) levels and obesity.[11,12] Moreover, conditions such as HT, subclinical hypothyroidism (SH), and hypothyroidism are found more frequently in obese patients as opposed to those with normal weight.[13] Still, the interconnections between obesity, HT, and hypothyroidism remain to be fully understood.

Polypeptide-N-acetyl galactosamine transferase 15 (GALNT15), polypeptide-N-acetyl galactosamine transferase 12 (GALNT12), and polypeptide-N-acetyl galactosamine transferase 8 (GALNT8) belong to the N-acetylgalactosaminyltransferase (galNAc-T) family. They reside in transport vesicles and are believed to facilitate polypeptide galNAc-T activity.[14] The human body houses 20 members of the ppGalNAc-T

How to cite this article: Yang R, Han J. O-GalNAc glycosylation - key pathway for Hashimoto's thyroiditis in patients with metabolically unhealthy obesity. J Anat Soc India 2024;73:307-12.

Article Info

Received: 11 March 2024
Accepted: 18 November 2024
Available online: 28 December 2024

Address for correspondence:
Dr. Jianli Han,
Department of General Surgery, Shanxi Bethune Hospital, Taiyuan, Shanxi, China.
E-mail: hanjianli9560@sina.com

Access this article online

Website: https://journals.lww.com/joai

DOI: 10.4103/jasi.jasi_33_24

Quick Response Code:

enzyme family.[15] This enzyme family holds significant relevance to the growth of tissues and organs, as well as the onset and progression of complex diseases such as tumors, familial calcium deposits, coronary heart disease, Alzheimer's disease, and congenital heart disease.[16]

The focal point of this research is to examine the expression of miRNAs in MUO patients through bioinformatics and gene set enrichment analysis. We aim to pinpoint the distinct expression of pathways in HT patients and explore the probable mechanism triggering HT in MUO patients. This could potentially pave the way for the formulation of a viable plan for subsequent treatment.

Subjects and Methods

Subjects

Utilization of the Gene Expression Omnibus (GEO) dataset tool from the National Center for Biotechnology Information (https://www.ncbi.nlm.nih.gov/geo) was integral to our process. Our focus rested on "obesity" and "HT" as primary keywords, with an individualized inspection of each dataset. From this, datasets GSE169290[17] and GSE138198[18] were earmarked for further analysis.

Processing of Gene Expression Omnibus datasets and statistical analysis of differentially expressed genes

Our dataset GSE169290 encompasses a noncoding RNA sequence examination of 20 obesity patients within the 18–70 age range (body mass index >30 kg/m^2). This included a subset of 10 MHO patients and 10 MUO patients. GEO2R tool application allowed us to discern miRNA expression variations between these two groups, resulting in the identification of 127 miRNAs with a significance threshold set at $P < 0.05$. Notably, there was a marked difference in miRNA levels between these groups.

In contrast, GSE138198 incorporated transcriptional sequencing for 33 patients aged 14–67, comprised 13 HT cases and three standard thyroid cases. Differential gene expression was determined between the two groups through the GEO2R tool, yielding 9874 genes with significant variation in expression.

Differential miRNA pathway enrichment

The 127 miRNAs identified with differential expression were classified into groups. The MUO group was subdivided into a high-expression group (MUO-H, 62) and a low-expression group (MUO-L, 65). To trace the overexpressed miRNAs in MUO patients, miRNAs in the MUO-H group were enriched through a specific pathway. Employing the MirPath tool[19] from the DIANA TOOLS website (http://diana.imis.athena-innovation.gr/DianaTools/index.php), miRNAs were submitted for analysis. The ensuing KEGG pathway enrichment results were then leveraged for more detailed investigation.

Results

Related KEGG pathways obtained by miRNA enrichment in metabolically unhealthy obesity-H group

Sixty-two miRNAs in the MUO-H group obtained from the GSE169290 dataset analysis were submitted to the DIANA TOOLS website for MirPath pathway enrichment. The chosen result merging method was "pathways union" and the method of enrichment analysis was "Fisher's exact test." Four KEGG pathways were identified: "prion diseases (hsa05020)," "ECM-receptor interaction (hsa04512)," "mucin-type O-glycan biosynthesis (hsa00512)," and "cell adhesion molecules (hsa04514)" [Figure 1a and b].

Cross-comparison of miRNA pathway enrichment with GSE138198

Four enrichment pathways were identified from 62 miRNAs in the MUO-H group, including 45 related genes. Forty-five differentially expressed genes were successively substituted into the list of 9874 differential genes in GSE138198 to identify any overlap. Finally, 16 differential genes were obtained, among which GALNT15 ranked the first, GALNT12 ranked the eighth, and GALNT8 ranked the 13th [Figure 2]. Therefore, we speculate that the overexpression of related miRNAs in patients with MUO leads to the translational silencing of *GALNT15, GALNT12,* and *GALNT8 in vivo*, thereby increasing the probability of HT

O-GalNAc glycosylation is the key pathway for Hashimoto's thyroiditis in patients with metabolically unhealthy obesity

The polypeptide-N-acetylgalactosamine transferases (ppGalNAc-Ts) such as GALNT15, GALNT12, and GALNT8 are known for their role in catalyzing the initial stage of human O-GalNAc glycosylation. The typical substrate of O-GalNAc glycoprotein is ppGalNAc-T, also recognized as mucin. Over the past decade, with the advancement in sugar biological analysis techniques such as biomass spectroscopy, numerous cell membrane, and secretory proteins have been confirmed as O-GalNAc-modified proteins.[20,21] Concurrently, extensive research on clinical samples and animal models indicates the pivotal role of O-GalNAc-modified proteins in organ development and disease onset and progression.[22-24]

At present, there are at least 20 known types of ppGalNAc-T isozymes; however, the understanding of their specific substrate proteins and functions is still incomplete, posing challenges in sugar biology research.[25,26] O-GalNAc glycosylation, being one of the most prevalent and varied glycosylation modifications, impacts cell membrane and secretory proteins and participates in numerous physiological processes related to cancer development. Irregularities in O-GalNAc glycosylation and ppGalNAc-T expression may serve as potential indicators of tumor

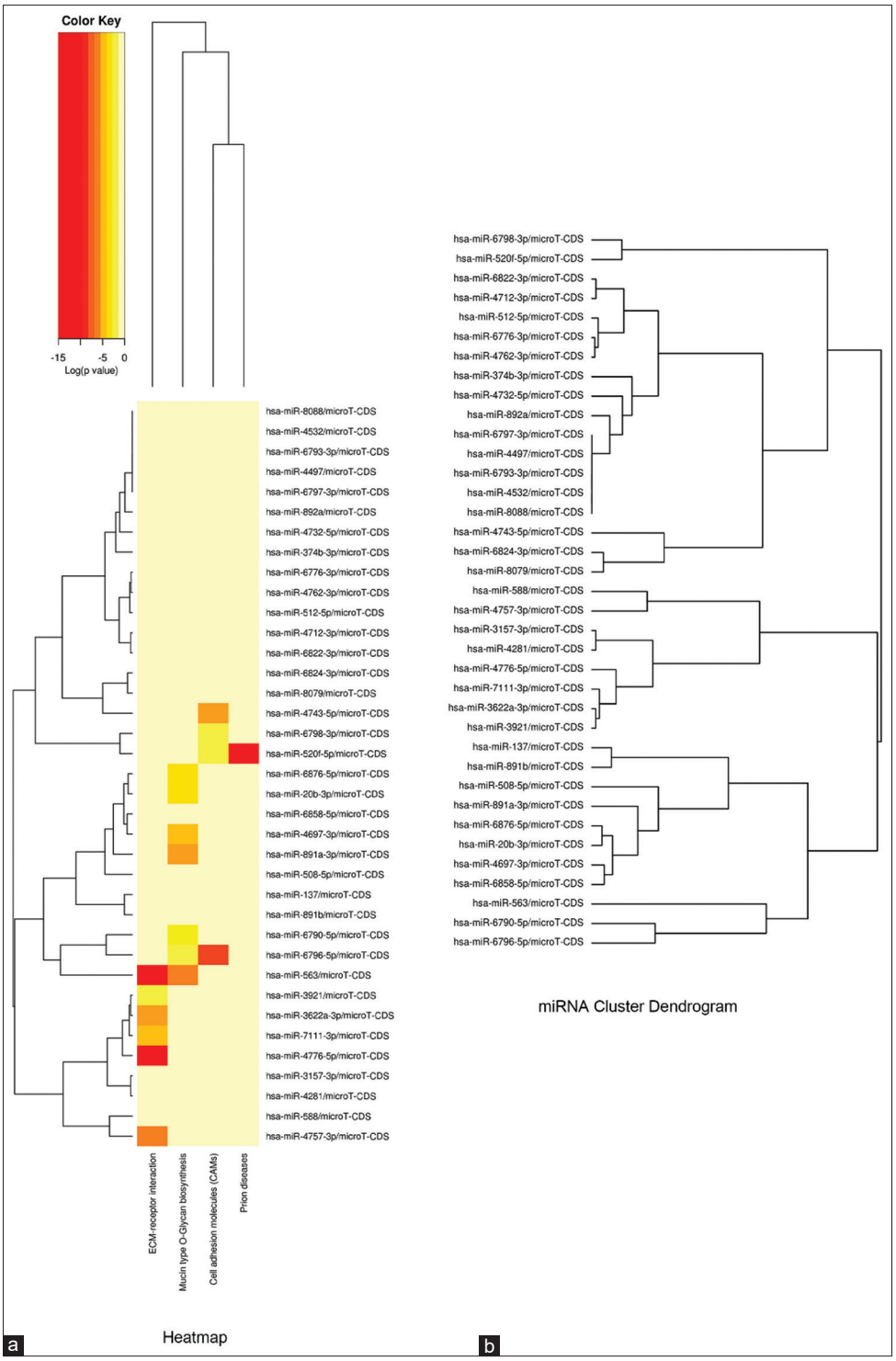

Figure 1: Sixty-two miRNAs in the metabolically unhealthy obesity-H group. (a) Heatmap of the four KEGG pathways (b) MiRNA cluster of the four KEGG pathways

metastasis and prognosis in several types of cancer, including gastric, colon, breast, lung, esophageal, prostate, and endometrial.[27,28] The connection between ppGalNAc-T isozymes and HT, however, remains to be established. Consequently, this study proposes that the diminished expression of O-GalNAc glycosylation in MUO patients may heighten HT prevalence, thereby potentially shedding light on a crucial mechanism of HT in obese patients, worthy of further investigation in future.

Discussion

HT, first identified by Hakaru Hashimoto in 1912,[29] is now recognized as the most prevalent inflammatory lesion impacting thyroid tissue. It is a leading cause of goiter

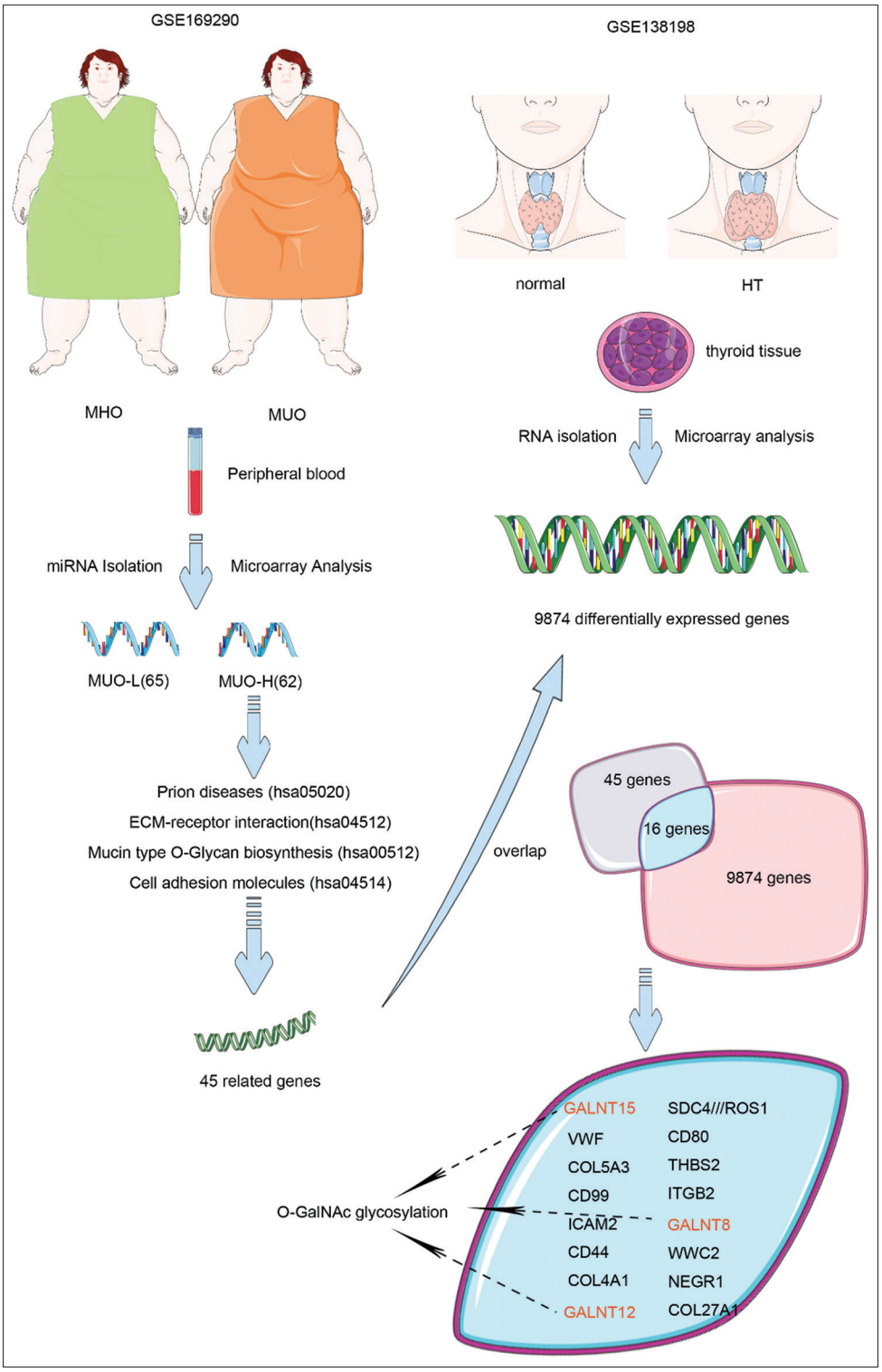

Figure 2: Cross-comparison of miRNA pathway enrichment with GSE138198

in nations with abundant iodine, like the USA and Japan. The worldwide detection rate of HT has seen an upsurge in recent years, thanks to advancements in diagnostic technologies.[30]

Patients with HT usually show two types of clinical features: symptoms related to goiter and symptoms related to hypothyroidism. Hypothyroidism symptoms can be the first symptom in patients with HT. However, when patients complain of hypothyroidism-related symptoms, HT is almost always the cause. Although the above symptoms do not directly threaten the safety of patients, they seriously affect their quality of life.[31]

Currently, the pathogenesis of HT remains unclear. Individuals exhibit autoimmune responses against thyroid-specific antigens through immune cell infiltration under the influence of the environment. This immune response causes apoptosis of the thyroid cells, eventually leading to hypothyroidism.[32] Although HT does not directly threaten the life safety of patients like malignant tumors, it will seriously affect the quality of life of patients because of its high incidence and long course of disease, especially after the symptoms of hypothyroidism. At present, most of the treatment schemes commonly used internationally for many years are thyroid tablet replacement therapy.

Most patients require long-term or lifelong medication, and side effects are inevitable. When a goiter seriously affects the patient's daily life or biopsy cannot rule out a suspected malignant thyroid tumor, HT patients must undergo surgery to remove all or part of the thyroid tissue. Therefore, redefining the traditional definition of HT, finding early subtypes that may cause serious clinical manifestations, proposing practical and effective diagnostic criteria, and introducing new treatment concepts have become revolutionary and challenging tasks for medical workers.

Glycosylation is a post-translational modification that is prevalent in organisms. It primarily takes two forms: N-glycosylation and O-glycosylation. O-GalNAc glycosylation, a widespread form of O-glycosylation, is found in over 80% of cellular membrane proteins and proteins that are secreted.[33] It is implicated in numerous cellular functions such as molecular recognition, activation of signaling pathways, protein transportation and cleavage, and cell adhesion and movement.[34] The initial glycosyltransferase that controls O-GalNAc glycosylation is ppGalNAc-T, which facilitates the covalent attachment of N-acetylgalactosamine (GalNAc) to the side-chain hydroxyl groups of serine or threonine, creating the antigenic Tn sugar chain structure. Our study indicates that reduced expression of GALNT15, GALNT12, and GALNT8 in the MUO population may contribute to HT. Given the role of O-GalNAc glycosylation, we postulate that a decrease in O-glycosylation may trigger a thyroid autoimmune response, a hypothesis that requires further experimental confirmation.

Changes in thyroid function and structure are frequently observed in individuals with obesity.[35] Serum levels of TSH in both children and adults with obesity are often found to be higher than those in normal-weight counterparts (either at the upper limit of the normal range or slightly above).[36-38] Interestingly, these alterations in thyroid function and structure can be significantly ameliorated through weight loss.[36] A comprehensive meta-analysis of 22 studies demonstrated a significant link between obesity and an elevated risk of hypothyroidism, revealing a 70% increase in the risk of SH and more than double the risk of clinical hypothyroidism in individuals with obesity. The primary cause of this hypothyroidism is HT.

In our research, we discovered that O-GalNAc glycosylation might be a critical factor in the occurrence of HT in the MUO population. This finding could be instrumental in reducing the incidence of HT, discovering potential treatments, and managing the metabolically unhealthy state of the MUO population.

Availability of data and materials

Previously reported noncoding RNA sequence data were used to support this study and were available at GSE169290 and GSE138198. These prior studies (and datasets) are cited at relevant places within the text as references.[17,18]

Financial support and sponsorship

Nil.

Conflicts of interest

There are no conflicts of interest.

References

1. González-Muniesa P, Mártinez-González MA, Hu FB, Després JP, Matsuzawa Y, Loos RJ, *et al.* Obesity. Nat Rev Dis Primers 2017;3:17034.
2. Global BMI Mortality Collaboration, Di Angelantonio E, Bhupathiraju SH, Wormser D, Gao P, Kaptoge S, *et al*. Body-mass index and all-cause mortality: Individual-participant-data meta-analysis of 239 prospective studies in four continents. Lancet 2016;388:776-86.
3. Michalaki MA, Vagenakis AG, Leonardou AS, Argentou MN, Habeos IG, Makri MG, *et al*. Thyroid function in humans with morbid obesity. Thyroid 2006;16:73-8.
4. Janković D, Wolf P, Anderwald CH, Winhofer Y, Promintzer-Schifferl M, Hofer A, *et al*. Prevalence of endocrine disorders in morbidly obese patients and the effects of bariatric surgery on endocrine and metabolic parameters. Obes Surg 2012;22:62-9.
5. Stefan N, Häring HU, Hu FB, Schulze MB. Metabolically healthy obesity: Epidemiology, mechanisms, and clinical implications. Lancet Diabetes Endocrinol 2013;1:152-62.
6. van Vliet-Ostaptchouk JV, Nuotio ML, Slagter SN, Doiron D, Fischer K, Foco L, *et al*. The prevalence of metabolic syndrome and metabolically healthy obesity in Europe: A collaborative analysis of ten large cohort studies. BMC Endocr Disord 2014;14:9.
7. Jung CH, Lee WJ, Song KH. Metabolically healthy obesity: A friend or foe? Korean J Intern Med 2017;32:611-21.
8. Geetha L, Deepa M, Anjana RM, Mohan V. Prevalence and clinical profile of metabolic obesity and phenotypic obesity in Asian Indians. J Diabetes Sci Technol 2011;5:439-46.
9. Iacobini C, Pugliese G, Blasetti Fantauzzi C, Federici M, Menini S. Metabolically healthy versus metabolically unhealthy obesity. Metabolism 2019;92:51-60.
10. Ralli M, Angeletti D, Fiore M, D'Aguanno V, Lambiase A, Artico M, *et al*. Hashimoto's thyroiditis: An update on pathogenic mechanisms, diagnostic protocols, therapeutic strategies, and potential malignant transformation. Autoimmun Rev 2020;19:102649.
11. Abu-Ghanem Y, Inbar R, Tyomkin V, Kent I, Berkovich L, Ghinea R, *et al*. Effect of sleeve gastrectomy on thyroid hormone levels. Obes Surg 2015;25:452-6.

12. Lips MA, Pijl H, van Klinken JB, de Groot GH, Janssen IM, Van Ramshorst B, *et al*. Roux-en-Y gastric bypass and calorie restriction induce comparable time-dependent effects on thyroid hormone function tests in obese female subjects. Eur J Endocrinol 2013;169:339-47.
13. Janssen IM, Homan J, Schijns W, Betzel B, Aarts EO, Berends FJ, *et al*. Subclinical hypothyroidism and its relation to obesity in patients before and after Roux-en-Y gastric bypass. Surg Obes Relat Dis 2015;11:1257-63.
14. Cheng L, Tachibana K, Iwasaki H, Kameyama A, Zhang Y, Kubota T, *et al*. Characterization of a novel human UDP-GalNAc transferase, pp-GalNAc-T15. FEBS Lett 2004;566:17-24.
15. Kato K, Hansen L, Clausen H. Polypeptide N-acetylgalactosam inyltransferase-associated phenotypes in mammals. Molecules 2021;26:5504.
16. Garay YC, Cejas RB, Lorenz V, Zlocowski N, Parodi P, Ferrero FA, *et al*. Polypeptide N-acetylgalactosamine transferase 3: A post-translational writer on human health. J Mol Med (Berl) 2022;100:1387-403.
17. Rovira-Llopis S, Díaz-Rúa R, Grau-Del Valle C, Iannantuoni F, Abad-Jimenez Z, Bosch-Sierra N, *et al*. Characterization of differentially expressed circulating miRNAs in metabolically healthy versus unhealthy obesity. Biomedicines 2021;9:321.
18. Subhi O, Schulten HJ, Bagatian N, Al-Dayini R, Karim S, Bakhashab S, *et al*. Genetic relationship between Hashimoto`s thyroiditis and papillary thyroid carcinoma with coexisting Hashimoto`s thyroiditis. PLoS One 2020;15:e0234566.
19. Vlachos IS, Zagganas K, Paraskevopoulou MD, Georgakilas G, Karagkouni D, Vergoulis T, *et al*. DIANA-miRPath v3.0: Deciphering microRNA function with experimental support. Nucleic Acids Res 2015;43:W460-6.
20. Hoffmann M, Marx K, Reichl U, Wuhrer M, Rapp E. Site-specific O-glycosylation analysis of human blood plasma proteins. Mol Cell Proteomics 2016;15:624-41.
21. Zhang Y, Xie X, Zhao X, Tian F, Lv J, Ying W, *et al*. Systems analysis of singly and multiply O-glycosylated peptides in the human serum glycoproteome via EThcD and HCD mass spectrometry. J Proteomics 2018;170:14-27.
22. Miyazaki T, Mori M, Yoshida CA, Ito C, Yamatoya K, Moriishi T, *et al*. Galnt3 deficiency disrupts acrosome formation and leads to oligoasthenoteratozoospermia. Histochem Cell Biol 2013;139:339-54.
23. Duncan AR, Khokha MK. Xenopus as a model organism for birth defects-congenital heart disease and heterotaxy. Semin Cell Dev Biol 2016;51:73-9.
24. Fakhro KA, Choi M, Ware SM, Belmont JW, Towbin JA, Lifton RP, *et al*. Rare copy number variations in congenital heart disease patients identify unique genes in left-right patterning. Proc Natl Acad Sci U S A 2011;108:2915-20.
25. Bennett EP, Mandel U, Clausen H, Gerken TA, Fritz TA, Tabak LA. Control of mucin-type O-glycosylation: A classification of the polypeptide GalNAc-transferase gene family. Glycobiology 2012;22:736-56.
26. Hollingsworth MA, Swanson BJ. Mucins in cancer: Protection and control of the cell surface. Nat Rev Cancer 2004;4:45-60.
27. Gill DJ, Tham KM, Chia J, Wang SC, Steentoft C, Clausen H, *et al*. Initiation of GalNAc-type O-glycosylation in the endoplasmic reticulum promotes cancer cell invasiveness. Proc Natl Acad Sci U S A 2013;110:E3152-61.
28. Springer GF. T and TN, general carcinoma autoantigens. Science 1984;224:1198-206.
29. Sawin CT. The heritage of Dr. Hakaru Hashimoto (1881-1934). Endocr J 2002;49:399-403.
30. Ajjan RA, Weetman AP. The pathogenesis of Hashimoto's thyroiditis: Further developments in our understanding. Horm Metab Res 2015;47:702-10.
31. Mikulska AA, Karaźniewicz-Łada M, Filipowicz D, Ruchała M, Główka FK. Metabolic characteristics of Hashimoto's thyroiditis patients and the role of microelements and diet in the disease management-an overview. Int J Mol Sci 2022;23:6580.
32. Ragusa F, Fallahi P, Elia G, Gonnella D, Paparo SR, Giusti C, *et al*. Hashimotos' thyroiditis: Epidemiology, pathogenesis, clinic and therapy. Best Pract Res Clin Endocrinol Metab 2019;33:101367.
33. Radhakrishnan P, Dabelsteen S, Madsen FB, Francavilla C, Kopp KL, Steentoft C, *et al*. Immature truncated O-glycophenotype of cancer directly induces oncogenic features. Proc Natl Acad Sci U S A 2014;111:E4066-75.
34. Tarp MA, Clausen H. Mucin-type O-glycosylation and its potential use in drug and vaccine development. Biochim Biophys Acta 2008;1780:546-63.
35. Li Q, Liu Z, Guo J, Chen J, Yang P, Tian J, *et al.* Cholesterol overloading leads to hepatic L02 cell damage through activation of the unfolded protein response. Int J Mol Med 2009;24:459-64.
36. Lee H, Herbert RD, McAuley JH. Mediation analysis. JAMA 2019;321:697-8.
37. Baron RM, Kenny DA. The moderator-mediator variable distinction in social psychological research: Conceptual, strategic, and statistical considerations. J Pers Soc Psychol 1986;51:1173-82.
38. Feng B, Yao PM, Li Y, Devlin CM, Zhang D, Harding HP, *et al*. The endoplasmic reticulum is the site of cholesterol-induced cytotoxicity in macrophages. Nat Cell Biol 2003;5:781-92.

Original Article

Estimating Morphological Nose Features for Craniofacial Reconstruction: A Retrospective Study

Nazan Guner Sak, Serdar Babacan[1], Sefa Işıklar[2], İlker Mustafa Kafa, Gökhan Gökalp[3]

Departments of Anatomy and [3]Radiology, Faculty of Medicine, Bursa Uludag University, [2]Medical Imaging Techniques Program, Vocational School of Health Services, Bursa Uludag University, Bursa, [1]Department of Anatomy, Faculty of Medicine, Harran University, Sanliurfa, Turkey

Abstract

Background: Craniofacial reconstruction is one of the techniques used in forensic sciences to rebuild the probable antemortem face of unknown human skulls. Considering the soft-tissue thickness, the skull is covered with clay or similar material. After covering, facial features such as lips, ears, eyes, and nose should be added. The nose has considerable diversity. This variety makes it have substantial importance for facial recognition. **Aims and Objectives:** The current study aimed to determine the morphology of the nose of the Anatolian population and develop regression formulas to estimate the nose shape using the measurements of the skull. **Materials and Methods:** The current study was conducted on three-dimensional computed tomography cranial images. The images belonging to 50 adult patients (25 males, 25 females) were taken from the Radiology Department of Bursa Uludag University Medical Faculty Hospital. Eighteen parameters on bony structure and twenty-four parameters on soft tissue were measured using ImageJ software. SPSS 22.0 was performed for statistical analyses. **Results:** The regression formulas were developed to estimate the nose morphology belonging to the skull using the correlated parameters between the bony structure of the skull and soft tissue. **Conclusion:** Accurate nasal shape prediction means increasing the identification of the unknown skull. We believe that the regression formulas, developed with this idea could be helpful in craniofacial reconstruction.

Keywords: *Craniofacial reconstruction, forensic sciences, nose, nose morphology*

Introduction

Craniofacial reconstruction can be used as a definition for procedures that clearly describe estimating and reconstructing the recognizable state of an individual's face based on the morphology of the skull.[1] Facial reconstruction is widely used in forensic sciences and archeology. In forensic sciences, identifying the person can become difficult, especially as time passes after death. For this reason, facial reconstruction plays a role in determining the dead and sometimes in facilitating the resolution of judicial cases. Besides that, archeology creates three-dimensional (3D) visual images of people from skeletal remains, mummified bodies, or preserved bodies. Thus, it is possible that the definition of what people who lived in the past looked like.[2]

In forensic sciences, identification using DNA and fingerprints is the best option for person recognition. Nevertheless, they may not always be available.[3,4] However, the archeology area has many opportunities to use certain surface features such as hairstyle, facial hair, eye color, skin tone and texture, horizontal forehead lines, eye wrinkles, and under-eye bags that are widely utilized to design the faces of skulls. The use of these structures can also help forensic sciences. Such properties cannot be determined solely from the skeletal material in every situation. Furthermore, their inclusion in judicial cases cannot be scientifically justified without sufficient evidence at the scene; these are obstacles faced in using facial reconstruction in forensic medicine.[1,5]

The basic knowledge of the relationship between the skeleton and soft tissue in the face is crucial to obtaining a reliable and proper depiction of the face in the forensic sciences.[6] This information is the most critical factor determining the accuracy of the individual in facial reconstruction.[7] This accuracy is necessary to make it as good as possible. There have been many studies to determine the relationships

How to cite this article: Sak NG, Babacan S, Işıklar S, Kafa İM, Gökalp G. Estimating morphological nose features for craniofacial reconstruction: A retrospective study. J Anat Soc India 2024;73:313-7.

Article Info

Received: 03 June 2022
Revised: 24 November 2023
Accepted: 25 November 2023
Available online: 09 November 2024

Address for correspondence:
Dr. Nazan Guner Sak, Department of Anatomy, Faculty of Medicine, Uludag University, Gorukle, Nilufer, Bursa 16059, Turkey.
E-mail: nazangunersak@gmail.com

Access this article online

Website: https://journals.lww.com/joai
DOI: 10.4103/jasi.jasi_84_22

Quick Response Code:

between hard and soft tissues on the face.[6,7] Considering these studies, each individual has special facial features, and these structures are closely related to other facial properties found on the face.[8] Many studies examine the use of facial parts such as the mouth, eyes,[9,10] and nose for craniofacial reconstruction.[11]

The nose profile is vital in facial recognition among the facial organs, and usually, the eyes are fixed in the area around the center of the nose for facial recognition.[2,5] Therefore, nasal reconstruction should take precedence in craniofacial reconstruction.[2] Nasal reconstruction techniques use the parameters such as nasal bone, piriform aperture, and anterior or nasal spine to estimate an individual's nasal morphology.[2,4] Although the underlying bones of the nose make up only a small part of the facial skull, in that part the 3D distances between the skeleton and the soft tissue and soft-tissue planes are determinants of nasal morphology much more accurately.[6,7] Most cadaver studies are not considered highly inevitable shrinkage and distortion of soft tissues caused by dehydration after death.[12,13]

Manual or automatic methods such as sculpture, anatomical, or statistical methods are the oldest methods used in craniofacial reconstruction. In contrast, clinical imaging techniques such as laser surface scanning, computed tomography (CT), or magnetic resonance ımaging (MRI) have been used recently. Various methods have started to be used or combined to estimate the face's morphology from the skull in 3D or two-dimensional frontal and profile views.[1,5] While determining the nasal morphology, the primary purpose is to calculate the muscle structure[5] and the average tissue depth according to the local features of the bone.[14] Although, while estimating for reconstruction, the most determinant formation is the nose, it is a structure mainly composed of cartilage rather than bone. The nose is vital in facial reconstruction and hard to predict its morphology. Furthermore, it is still a subject with an immense knowledge gap in the literature.

It was found to accurately predict the soft-tissue anatomy of the nose from the skulls of adults and children. Despite the studies that have been carried out, it is still a very controversial subject. A lack of knowledge is critical, especially for forensic science. In light of this information, our study aims to determine the nasal morphology and develop regression formulas to estimate the soft tissue of the nose shape using complex tissue measurements on the skull.

Materials and Methods

The study was performed on 3D CT images of the head-and-neck regions of 50 individuals (25 females, mean age: 35.40; 25 males, mean age: 34.32). The approval of the Ethics Committee of Clinical Investigations of Bursa Uludag University Faculty of Medicine was taken (number: 2020-22/17).

Cranial CTs taken by Siemens Somatom definition 128-slice multi-detector CT in the Department of Radiology of Bursa Uludag University Medical Faculty were retrospectively evaluated using the centricity RIS 4.2 Plus Picture Archiving and Communication System (PACS). The reformed images were created with AW Suite 2.0 program by using thin-section axial images of 1.5 mm thickness. After the reform, the images were evaluated in the system's bone and soft-tissue windows for optimal examination. Cranium has been rendered in 3D with the choice of volume rendering on the program. 3D cranium images were recorded in the PACS system via AW Suite 2.0. Measurements were taken with the ImageJ program on the photos taken from the PACS system, and the data were recorded 32 parameters were measured either the bone or soft tissue of the nose of total [Figure 1: 1-32 parameters].

Rynn *et al*.[3] (2010) published a method of predicting nose projection from the skull using some parameters, and in this study, some measurements are taken their study and these are used in calculated regression formulae to estimate the nasal dimensions. In our study, these parameters: 8, 9, 12, 13, 14, 15, 16, 17, and 18 were taken from Rynn *et al*. (2010)'s study [Figure 1].

The averages for parameters have been calculated. The data were analyzed at SPSS 22.0 to produces formules (IBM Corp., Armonk, NY). The descriptive statistics of the parameters, the significant differences between males and females, and the correlations between soft and hard tissues were evaluated and the regression formulas were developed to estimate features of the nose using morphometry.

Results

The average values of the measurements are given for males and females (Length measurements are given in cm) [Tables 1 and 2]. A statistically significant ($P < 0.003$) difference was found between males and females in only the nasofrontal angle on the bone (109,59° for males and 127,05° for females) and the length of nose parameter ($P < 0.016$) (5,61 cm. for males and 5,14 cm. Except for that parameter, there was no statistically significant difference in any parameters measured on the right and left sides between the soft tissue and hard tissue. The formulas derived from measurements taken in both hard and soft tissues for men and women have been presented to estimate nasal morphology [Tables 3 and 4].

Discussion

Nose location, size, shape, and proportions provide visual bases for an individual facial character.[1,11] The estimation of external nasal morphology is an important issue that can help individual identification using skulls and could be used to clarify some forensic cases. Over the years, many studies

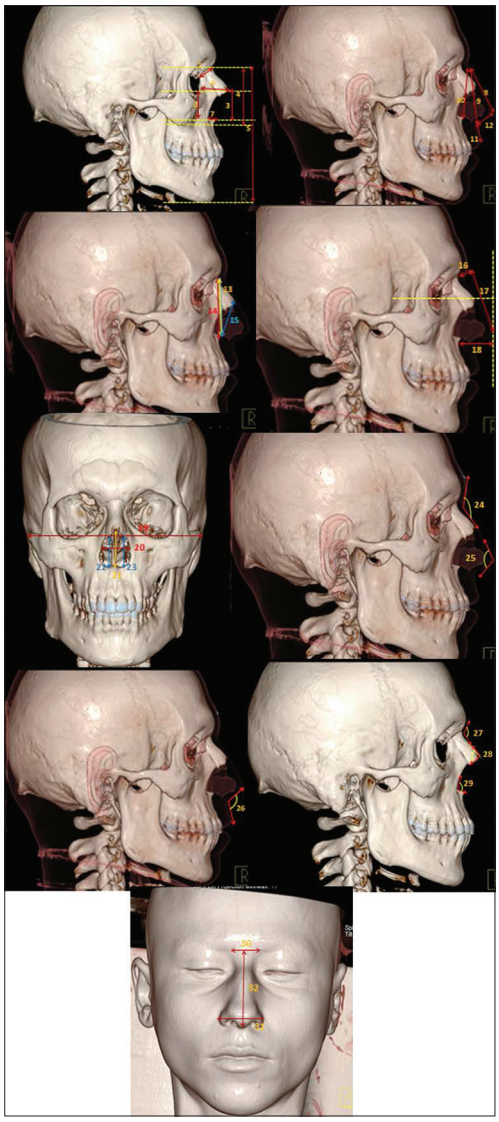

Figure 1: (1) The perpendicular distance between the medial margin of orbit-the nasion (2) the perpendicular distance between the Frankfort horizontal plane passing through the rhinion-the Frankfort horizontal plane passing through the deepest point of the piriform aperture (3) the perpendicular distance between the Frankfort horizontal plane passing through the anterior nasal spine-the Frankfort horizontal plane passing through the rhinion (4) the perpendicular distance between the Frankfort horizontal plane passing through the anterior nasal spine – the Frankfort horizontal plane passing through the nasion (5) the perpendicular distance between the Frankfort horizontal plane passing through the nasion-the Frankfort horizontal plane passing through the inferior margin of the mandibula (6) the perpendicular distance between the medial margin of the orbit – the rhinion (7) the perpendicular distance between the deepest point of the apertura piriformis – the anterior nasal spine (8) the length of nose (9) the height of nose (10) the perpendicular distance between the nasion – the anterior nasal spine (11) the length of philtrum (12) the depth of nose (13) the perpendicular distance between the nasion – the acanthion (14) the perpendicular distance between the nasion – the subspinale (15) the perpendicular distance between the rhinion – the subspinale (16) the anterior projection of pronasale (17) the height of pronasale projection (18) the pronasale projection in the Frankfort horizontal plane (19) the width of bizygomatic (20) the width of piriform aperture (21) the height of piriform aperture (22) the height of right piriform aperture (23) the height of left piriform aperture (24) the nasofrontal angle (25) the angle nose (26) the nasolabial angle (27) the nasofrontal angle on the bone (28) the angle of nose on the bone (29) the deepest angle of the pyriform aperture (30) The proximal width of nose (31) the distal width of nose (32) the length of nose

Table 1: Comparative statistical analysis results of the measurements taken from hard tissue between males and females

Parameters	Males		Females		*P*
	Mean	SD	Mean	SD	
1	1.71	0.31	1.67	0.20	0.646
2	3.79	0.58	3.71	0.43	0.561
3	3.14	0.57	3.06	0.46	0.599
4	6.02	0.84	5.87	0.78	0.523
5	14.02	1.44	13.75	1.36	0.492
6	2.69	0.36	2.54	0.28	0.111
7	1.10	0.22	1.04	0.17	0.28
13	6.07	0.75	5.71	1.10	0.188
14	6.52	0.84	6.49	0.58	0.889
15	4.45	0.87	4.54	0.60	0.665
19	14.33	3.57	14.36	2.87	0.971
20	2.64	0.61	2.51	0.37	0.352
21	3.82	0.51	3.60	0.48	0.133
22	2.83	0.44	2.73	0.37	0.398
23	2.95	0.46	2.79	0.35	0.18
27	109.59	25.34	127.05	12.68	0.003
28	95.29	10.30	95.72	7.77	0.868
29	81.04	10.07	79.22	13.51	0.589

SD: Standard deviation

Table 2: Comparative statistical analysis results of the measurements taken from soft tissue between males and females

Parameters	Males		Females		*P*
	Mean	SD	Mean	SD	
8	5.61	0.74	5.14	0.57	0.016
9	6.05	0.65	5.76	5.76	0.113
10	5.39	0.68	5.16	0.53	0.214
11	1.83	0.33	1.82	0.60	0.907
12	2.84	0.92	2.71	0.30	0.507
16	1.79	0.31	1.60	0.29	0.032
17	6.09	1.01	5.88	0.85	0.451
18	3.94	2.49	3.38	0.29	0.304
24	126.92	13.68	130.25	28.05	0.598
25	103.93	15.24	105.35	26.56	0.311
26	95.92	12.39	93.46	13.62	0.511
30	2.72	0.73	2.97	0.68	0.214
31	4.38	0.62	4.22	0.63	0.369
32	5.86	0.89	6.16	0.89	0.246

SD: Standard deviation

have been conducted evaluating the relationship between soft nasal tissue structures and the bones especially those located surrounding the piriform aperture.[1,11]

Gerasimov revealed in 1955 that information, bone nasal apertura, its maximum width at three-fifths of the total width of the soft nose. Rynn *et al*. confirmed this information with a CT study in 2006, this research also produced formulas to estimate six soft-tissue parameters using three parameters onthe skull. One of the important

Table 3: The regression equations in order to estimate the nose shape of male

Equations	Adjusted R^2	SE	*P*
P8=1.183 + (0.731 × P13)	0.531	0.509	0.000
P9=1.727 + (0.507 × P13) + (0.281 × P15)	0.707	0.352	0.000
P10=0.724 × (0.769 × P13)	0.701	0.376	0.000
P11=0.323 (0.161 × P 3) – (0.588 × P4) + (0.282 × P5) – (0.105 × P6) – (0.526 × P7) – (0.141 × P15) + (0.322 × P14)	0.611	0.208	0.001
P12=1.391 – (0.131 × P19) + (0.597 × P20) + (0.016 × P27)	0.480	0.667	0.001
P16=1.742 – (0.433 × P4) + (0.131 × P5) + (0.394 × P6) + (1.108 × P13) – (0.785 × P14) + (0.103 × P19) – (0.786 × P22) – (0.012 × P28)	0.554	0.212	0.004
P17=−1.481 + (0.358 × P5) – (1.879 × P7) – (0.345 × P13) + (1.054 × P15) + (0.467 × P20) + (0.572 × P21) – (1.546 × P22) + (0.010 × P27) + (0.024 × P29)	0.873	0.360	0.000
P18=1.368 (2.736 × P2) + (0.995 × P3) + (0.572 × P5) + (4.449 × P13) – (4.877 × P14) + (1.146 × P15) + (0.964 × P20) – (1.332 × P22) + (0.025 × P27)	0.944	0.589	0.000
P24=149.713 – (4.917 × P5) – (14.065 × P7) + (5.779 × P14) – (6.508 × P20) + (17.141 × P21) – (12.766 × P23) + (0.122 × P27)	0.790	6.265	0.000
P25=88.676 – (16.596 × P1) - (15.918 × P3) + (26.715 × P21) – (13.762 × P22) + (0.375 × P29)	0.374	12.061	0.014
P26=65.714 – (17.445 × P4) + (16.379 × P6) + (23.175 × P7) + (17.115 × P14) – (9.523 × P15) – (9.679 × P20) + (7.771 × P22)	0.392	9.663	0.023
P30=4.709 – (0.365 × P23) + (0.012 × P27) – (0.028 × P29)	0.169	0.671	0.084
P31=1.284 + (0.408 × P20) + (0.524 × P21)	0.314	0.513	0.007

SE: Standard error

Table 4: The regression equations in order to estimate the nose shape of females

Equations	Adjusted R^2	SE	*P*
P8=1.049 + (0.802 × P14) – (0.459 × P20)	0.704	0.322	0.000
P9=3.741 + (0.652 × P13) – (0.120 × P19)	0.590	0.392	0.000
P10=1.331 + (0.738 × P14) – (0.401 × P20)	0.693	0.302	0.000
P11=3.613 + (0.397 × P15) – (0.028 × P27)	0.685	0.348	0.000
P12=1.605 + (0.390 × P23)	0.150	0.268	0.042
P16=2.516 – (0.555 × P6) + (0.746 × P7) + (0.263 × P15) + (0.042 × P19) – (0.733 × P20) – (0.439 × P22) + (0.823 × P23) – (0.031 × P28) + (0.021 × P29)	0.517	0.206	0.023
P17=0.791 – (0.499 × P13) + (1.536 × P14) – (0.026 × P29)	0.617	0.522	0.000
P18=2.297 + (0.238 × P15)	0.214	0.262	0.018
P24=6.825 + (5.917 × P4) + (20.806 × P7) + (2.928 × P19) – (30.247 × P20) + (0.783 × P27)	0.948	6.547	0.000
P25=289.801 + (14.595 × P4) – (10.752 × P5) – (27.912 × P13) + (9.409 × P19) – (17.380 × P20) – (33.460 × P22) – (1.079 × P27)	0.657	9.178	0.001
P26=73.389 + (8.676 × P14) – (0.450 × P29)	0.330	11.301	0.007
P30=5.795 – (1.121 × P6)	0.165	0.621	0.031
P31=2.830 + (0.397 × P2) – (0.028 × P3) – (.0107 × P6) + (0.104 × P20)	0.141	0.681	0.091
P32=−0.333 + (1.094 × P3) + (1.081 × P14) – (0.042 × P28)	0.496	0.641	0.001

SE: Standard error, P: parameter (Formules shown produced for parameters described that Figure.1)

studies, Krogman (1986) implies the existence of guidelines for estimating nose width, lip width and thickness, and ear size. The estimation of soft-tissue morphology from bone morphology developing with technology over time and have become much useful tecnique.

As a result, studies have shown that the set of regression equations obtained from anthropometric bone measurements can be used to estimate nasal morphology, and this method is becoming increasingly common. Many studies have been carried out on bone and cadavers in the last years, but now they are mainly carried out on MRI and CT images, and the validity of the formulas produced is also increasing. Different studies have been conducted to estimate nasal morphology for craniofacial reconstruction over time in forensic sciences. Various anthropometric analyses can be used.[11,15,16] Each study holds considerable value for fields such as forensic sciences, anthropology, plastic, and reconstructive surgery, all of which may benefit from advancements in complex nasal reconstruction.[17]

In our study, measurements were made in soft and hard tissue, and 32 parameters were evaluated for males and females. Among these parameters, the nasofrontal angle measured only on the bone was found to be significantly different in males (109,59°) and females (127,05°) (P = 0.003). In the study of Moon *et al*. in 2013,[18] the mean nasofrontal angle was 131,14° (range: 112,93°–

146,62°) in the male patients (n = 50) and 140,70° (range: 113,88°–162,80°) in the female patients (n = 50). In 2020, Polat *et al*.[19] found this angle in 118 men, 124,27; in 129 females, they found it to be 133,73°, and a significant difference was found between males and females. That angle plays an important role in rhinoplasty. It can affect the shape of the nose and midfacial length in profile view.[20]

Regression formulas were developed from these 32 measured parameters for use in forensic sciences. Some of the parameters are taken from Rynn *et al*.'s (2010) study, but our formulas that developed are different and original. When we look at the results, the estimation rates of some parameters are different for men and women. The accuracy rates of the formulas are quite different from each other, and this topic is interesting and needs to be studied. It also points to the originality of our study.

Studies related to that subject are very limited. Bulut *et al*. (2019) took the parameters of Rynn *et al*.'s (2010) study and used them in their research to test its accuracy, and we have common some parameters. However, the methodology we developed is different. Rynn *et al*. (2010) produced formulas without gender discrimination, while Bulut *et al*. (2019) have produced different formulas for males and females, which is a unique factor to consider in identification.[21]

Conclusion

It is essential to distinguish the parameters of nasal morphology as females and males; even millimetric changes can cause changes in this regard. Therefore, our study provides morphological information about both male and female nose structures. We foresee that the formulas produced can play a substantial role in facial reconstruction by shedding light on future studies.

Ethics approval

The approval of the Ethics Committee of Clinical Investigations of Bursa Uludag University Faculty of Medicine was taken (number: 2020-22/17).

Financial support and sponsorship

Nil.

Conflicts of interest

There are no conflicts of interest.

References

1. Gerasimov MM. The Reconstruction of the Face from the Basic Structure of the Skull. Translated by Tschernezky. Moscow: Nauka; 1955.
2. Wilkinson C Facial reconstruction – anatomical art or artistic anatomy? J Anat 2010;216:235-50.
3. Rynn C, Wilkinson CM, Peters HL. Prediction of nasal morphology from the skull. Forensic Sci Med Pathol 2010;6:20-34.
4. Wilkinson C. Forensic facial reconstruction. Cambridge: Cambridge University Press; 2004.
5. Gerasimov MM. The face finder. New York: CRC Press; 1971. p. 3.
6. Utsuno H, Kageyama T, Uchida K, Kibayashi K, Sakurada K, Uemura K. Pilot study to establish a nasal tip prediction method from unknown human skeletal remains for facial reconstruction and skull photo superimposition as applied to a Japanese male population. J Forensic Leg Med 2016;38:75-80.
7. Sarilita E, Rynn C, Mossey PA, Black S, Oscandar F. Nose profile morphology and accuracy study of nose profile estimation method in Scottish subadult and Indonesian adult populations. Int J Legal Med 2018;132:923-31.
8. Strapasson RAP, Herrera LM, Melani RFH Forensic facial reconstruction: relationship between the alar cartilage and piriform aperture. J Forensic Sci 2017;62:1460-5.
9. Guyomarc'h Guyomarc'h P, Dutailly B, Charton J, Santos F, Desbarats P, *et al*. Anthropological facial approximation in three dimensions (AFA3D): Computer assisted estimation of the facial morphology using geometric morphometrics. J Forensic Sci 2014;59:1502-16.
10. Stephan CN Facial approximation: An evaluation of mouth-width determination. Ame. J. Phys Anthropol 2003;121:48-57.
11. Stephan CN, Henneberg M, Sampson W. Predicting nose projection and pronasale position in facial approximation: A test of published methods and proposal of new guidelines. Am J Phys Anthropol 2003;122:240-50.
12. Ridel AF, Demeter F, Liebenberg J, L'Abbe EN, Vandermeulen D, Oettle AC Skeletal dimensions as predictors for the shape of the nose in a South African sample: A cone-beam computed tomography (CBCT) study. Forensic Sci Int 2018;289:18-26.
13. Garlie TN, Saunders SR. Midline facial tissue thicknesses of subadults from a longitudinal radiographic study. J Forensic Sci 1999;44:61.
14. Krogman WM Iscan MY. The human skeleton in forensic medicine. Illinois, USA: C.C. Thomas Publishers; 1986. p. 5.
15. Rynn C. Craniofacial approximation and reconstruction: Tissue depth patterning and the prediction of the nose. University of Dundee; 2006. PhD dissertation.
16. Mala PZ. Pronasale position: An appraisal of two recently proposed methods for predicting nasal projection in facial reconstruction. J Forensic Sci 2013;58:957-63.
17. Menick FJ. Nasal reconstruction. Plast Reconstr Surg 2010;125:138e-50e.
18. Moon KM, Cho G, Sung HM, Jung MS, Tak KS, Jung SW, *et al*. Nasal anthropometry on facial computed tomography scans for rhinoplasty in Koreans. Arch Plast Surg 2013;40:610-5.
19. Polat S, Kabakçi AG, Cevik Y, Yücel AH. Facial Angle Profiles in Turkish Healthy Population. J Evol Med Dent Sci 2020;9:1188-119.
20. Yas NK Anthropometric study on the nasofrontal angle in human skulls. Fac Med Baghdad 2012;54:106-9.
21. Bulut O, Yiu C, Liu J, Gurcan S, Hekimoğlu B. Prediction of nasal morphology in facial reconstruction: Validation and recalibration of the Rynn method. Legal Medicine 2019;40:26-31.

Original Article

Evaluation of Dural Venous Sinus Variations through Three-dimensional Phase-Contrast Magnetic Resonance Venography

Songül Erdem Özkoç, Mehmet Guli Çetinçakmak[1], Salih Hattapoğlu[1]

Department of Radiology, Diyarbakir Gazi Yasargil Training and Research Hospital, [1]Department of Radiology, Medical School, Dicle University, Diyarbakir, Turkey

Abstract

Objective: The aim of this study was to evaluate the anatomy of dural venous sinus variations through three-dimensional phase-contrast (3D-PC) magnetic resonance venography (MRV). Awareness of the normal anatomical variations of venous sinuses and apparent MRV flow gaps prevent misdiagnosis of dural venous sinus diseases. **Materials and Methods:** The dural venous sinuses were assessed using nonenhanced 3D PC-MRV. Of these 968 patients, 154 were excluded due to venous thrombosis and mass invasion. A total of 814 patients (186 male and 628 female) were included in the study. **Results:** The most common variation of superior sagittal sinus (SSS) was atresia of anterior one-third SSS 19 (2.3%). Other variations were hypoplasia of the anterior half of SSS 2 (0.2%), atresia of posterior one-third of SSS (7, 0.9%), and combined variation of SSS (13, 1.6%). The left transverse sinus was hypoplastic in 224 (27.5%) and aplastic/atretic in 259 (31.8%) cases. The right transverse sinus was hypoplastic in 76 (9.3%) and aplastic/atretic in 57 (7.0%) patients. The combined variation of bilateral transverse sinuses had 42 (5.2%) cases. The left sigmoid sinus was hypoplastic in 22.2% (181) of cases. The right sigmoid sinus was hypoplastic in 60 (7.4%). Two patients had hypoplastic bilateral sigmoid sinuses (0.2%). The right occipital sinus was identified in 20 (2.5%) patients. Left occipital sinus was noted in 2 (0.2%) patients. Duplication or triplication of the occipital sinus is noted in 5 (0.6%) study populations. Straight sinus continued in 13 (1.6%) cases with the right transverse sinus and in 29 (3.6%) patients with left transverse sinus. **Conclusion:** These anatomical variants can be a potential pitfall in the MRV diagnosis of dural sinus variations, especially when there are no supportive imaging features such as brain infarcts or appropriate clinical background. 3D PC-MRV is a great option for patients with gadolinium allergy/renal insufficiency/pregnant patients. We hope this article can add information and assist in preoperative venous analysis for neurosurgeons and neuroradiologists.

Keywords: *Dural venous sinus, three-dimensional phase-contrast magnetic resonance venography, variation*

Introduction

The anatomy of the dural venous sinuses, variability, and interaction with the surrounding structures are very different. Neurosurgery, otolaryngology, or neurology practice, particularly important, have to obtain a satisfactory knowledge of dural sinus anatomy to avoid complications.[1] Dural venous sinus variations can cause misdiagnosis, such as sinus vein thrombosis and mass invasion.[2]

First described in 1888 by Gowers, the dural venous sinuses are structures that were first mapped out and provided a basis for the understanding of various pathologies.[3] Although digital subtraction angiography is generally used in vascular lesions and is considered relatively invasive compared to other examinations, it is the gold standard method in the evaluation of arterial and venous pathologies.[4] As brain magnetic resonance venography (MRV) is noninvasiveness, lacks radiation exposure, and evaluates brain vascular structures more quickly and sensitively, this cerebral angiography procedure has become more used by clinicians. This technique has a high temporal resolution and successive images are acquired through a volume during the passage of the contrast medium, allowing multiple three-dimensional (3D) datasets to be obtained from the arterial to the venous phase. It is especially preferred in cases where the timing of cerebral venous drainage is of interest, such as the detection of early draining veins in arteriovenous malformations and

How to cite this article: Özkoç SE, Çetinçakmak MG, Hattapoğlu S. Evaluation of dural venous sinus variations through three-dimensional phase-contrast magnetic resonance venography. J Anat Soc India 2024;73:318-22.

Article Info

Received: 03 July 2024
Accepted: 18 November 2024
Available online: 28 December 2024

Address for correspondence:
Dr. Mehmet Guli Çetinçakmak, Department of Radiology, Medical School, Dicle University, Diyarbakır, Türkiye. E-mail: drmehmetguli@gmail.com

Access this article online

Website: https://journals.lww.com/joai

DOI: 10.4103/jasi.jasi_98_24

Quick Response Code:

dural arteriovenous fistulas.[5] Phase-contrast MRV, which uses velocity-induced phase shifts to show flowing blood, is usually used to perform MRV, contrast application is unnecessary.[6]

The most important point in surgical intervention is to knowledge the venous drainage pattern in the preoperative period.[7] In particular, individual variations in venous anatomy can lead to technical difficulties and venous complications in many different surgical operations.[8] It is important to know venous variations for the surgeon during exploration in distinguishing pathological structures from normal anatomy.[7,8]

It is an important advantage to evaluate dural sinuses with MR, which is a noninvasive technique that does not contain radiation and contrast material.

In this article, we report on the angiographic analysis of cranial venous sinus circulation, emphasizing morphological and angiographic characteristics and possible associations, aiming to contribute to current neurosurgical and radiological knowledge.

Materials and Methods

This study included 968 patients who underwent cranial MRV examination with a 3D phase-contrast (3D-PC) sequence with different prediagnosis, without gender and age restrictions, between July 2010 and August 2018 in the Department of Radiology, Faculty of Medicine, Dicle University.

Of these 968 patients, 154 were excluded due to venous thrombosis and mass invasion. A total of 814 patients (186 male and 628 female) were included in the study. Patients' ages ranged between 1 and 92 (mean 35.95 ± 14.979) [Table 1]. Images of patients who underwent an MRI venous examination of archival records in our department's PACS system were examined in terms of dural venous sinus structures. Variations of dural venous sinuses were evaluated in each patient. Before all MRV examinations, informed consent was obtained from all the patients.

Ethical board consent was obtained for this study.

Magnetic resonance technique

All MR venograms were performed at our institute using a Philips 1.5 Tesla Achieva MRI Scanner with standard head coil, Philips workstation, and intellispace software. The MRV protocol consisted of noncontrast 3D PC-MRV in an oblique sagittal plan and employed parallel imaging with the position of the saturation band at the bottom of the block.

In the coronal plane, sections with 0.8 m thickness without gap were taken. Flip angle is 10°, and PC velocity is applied at 15 on average. In 1.5 T MR, TR/TE (ms) 16/62, field of view (FOV) 220 mm, and matrix 244 × 150 were applied in the coronal plane. In 3T MR, TR/TE (ms) 18/63, FOV 230 mm, and matrix 256 × 150 in the coronal plan were applied. In coronal T2 sequences, the flip angle is 90°, FOV: 230 (mm), and slice thickness is 1 mm. In 1.5T MR, the T2 coronal plane was applied as TE: 110 (ms), TR: 5513 (ms), and matrix 384 × 214. In 3T MR, T2 was applied as TE80 (ms), TR3000 (ms), and matrix 400 × 242 in the coronal plane.

Table 1: Numerical distribution of patients according to age ranges and gender

Gender				
Valid	**Frequency**	**Percentage**	**Valid percentage**	**Cumulative percentage**
Female	628	77.1	77.1	77.1
Male	186	22.9	22.9	22.9
Total	814	100.0	100.0	

Evaluation of images

The results were obtained by evaluating the three-dimensional maximum intensity projection and volume rendering images obtained by the 3D PC MRA algorithm and other routine T2A axial brain MRI sequences. Each variation of the dural sinus was studied and the variations were classified without distinction of gender and age. In our study, we classified the dural venous variations according to the study by Goyal *et al*.[9]

Statistical method

Continuous variables are shown as arithmetic mean (Avg) and standard deviation, and categorical variables as number (*n*) and percentage (%).

Calculations were made with statistical software (IBM SPSS Statistics 18, SPSS Inc. an IBM Co, Somers, NY, USA).

Results

The most common variation of Superior sagittal sinüs (SSS) was atresia of anterior one-third SSS 19 (2.3%). Other variations were hypoplasia of the anterior half of SSS 2 (0.2%), atresia of posterior one-third of SSS (7, 0.9%), and combine variation of SSS (13, 1.6%). Six types of variations of SSS were showed at 357 (43.9%) of 814 patients [Table 2]. The left sigmoid sinus was hypoplastic in 22.2% (181) of cases.

The left transverse sinus was hypoplastic in 224 (27.5%) and aplastic/atretic in 259 (31.8%) cases. The right transverse sinus was hypoplastic in 76 (9.3%) and aplastic/atretic in 57 (7.0%) patients. The combined variation of bilateral transverse sinuses had 42 (5.2%) cases [Table 3].

The right sigmoid sinus was hypoplastic in 60 (7.4%). Two patients had hypoplastic bilateral sigmoid sinuses (0.2%) [Table 4].

Table 2: Superior sagittal sinus variations

Superior sagittal sinus				
Valid	**Frequency**	**Percentage**	**Valid percentage**	**Cumulative percentage**
No variation	457	56.1	56.1	56.1
Continuity of SSS with the right transverse sinus	259	31.8	31.8	88.0
Continuity of SSS wth left transverse sınus	57	7.0	7.0	95.0
The front 1/3 sectıon of the SSS is not unified	19	2.3	2.3	97.3
Back 1/3 sectıon of SSS is not united	7	0.9	0.9	98.2
Anterior 1/2 section of SSS is hypoplasic	2	0.2	0.2	98.4
Combined variation of SSS	13	1.6	1.6	1.6
Total	814	100.0	100.0	

SSS: Superior sagittal sinus

Table 3: Transverse sinus variations

Transverse sinus				
Valid	**Frequency**	**Percentage**	**Valid percentage**	**Cumulative percentage**
No variation	472	58.0	58.0	58.0
Hypoplasic left transverse sınus	224	27.5	27.5	85.5
Hypoplasic left transverse sınus	76	9.3	9.3	94.8
Combıned varıatıon of transverse sınus	42	5.2	5.2	5.2
Total	814	100.0	100.0	

Table 4: Sigmoid sinus variations

Sıgmoıd sinus				
Valid	**Frequency**	**Percentage**	**Valid percentage**	**Cumulative percentage**
No variation	571	70.1	70.1	70.1
Hypoplasic left sigmoid sinus	181	22.2	22.2	92.4
Hypoplasic right sigmoid sinus	60	7.4	7.4	99.8
Combıined varıiation of sigmoid sinus	2	0.2	0.2	0.2
Total	814	100.0	100.0	

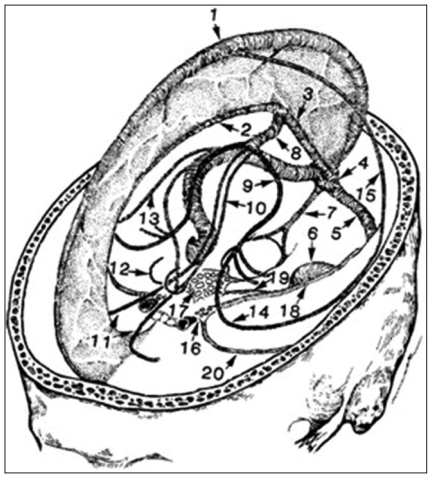

Figure 1: Cerebral Venous System. 1-Superior sagittal sinus (SSS), 2-ISS, 3-SS, 4-Torcular Herophilia (sinus confluens), 5-TS 6-Sigmoid sinus, 7-Occipital sinus, 8-Vein of Galen, 9-Basal Rosenthal vein, 10-Internal cerebral veins, 11-Septal veins, 12-Thalamostriate veins, 13-Labbe vein, 14-Superficial middle cerebral vein, 15-Trolard vein, 16-Cavernous sinus, 17-Clival venous plexus, 18-Superior petrosal sinus, 19-Inferior petrosal sinus, 20-Sphenoparietal sinus[11]

When the sinus rectus was examined, 3 types of variations were seen. 42 (5.2%) of 814 patients showed variation. Continuity of the sinus rectus with the right transverse was present in 13 (1.6%) patients, and continuity of the sinus rectus with the left transverse was present in 29 (3.6%) patients. Sinus rectus superior location was present in 1 patient and was included in the normal group as it did not cause a statistically significant change [Table 5].

The right occipital sinus was identified in 20 (2.5%) patients. Left occipital sinus was noted in 2 (0.2%) patients. Duplication or triplication of the occipital sinus is noted in 5 (0.6%) study population [Table 6].

Discussion

A good understanding of the dural venous sinus neurosurgical anatomy is a crucial prerequisite for optimizing outcomes and limiting the frequency of intra-and postoperative complications [Figure 1].[10]

In our study, we examined the anatomy of dural venous sinus variations through 3D-PC MRV [Figure 2].

MRV is a noninvasive, vulnerable, operator-independent technique for the assessment of venous anatomy and pathologic modifications and is widely used in the clinical

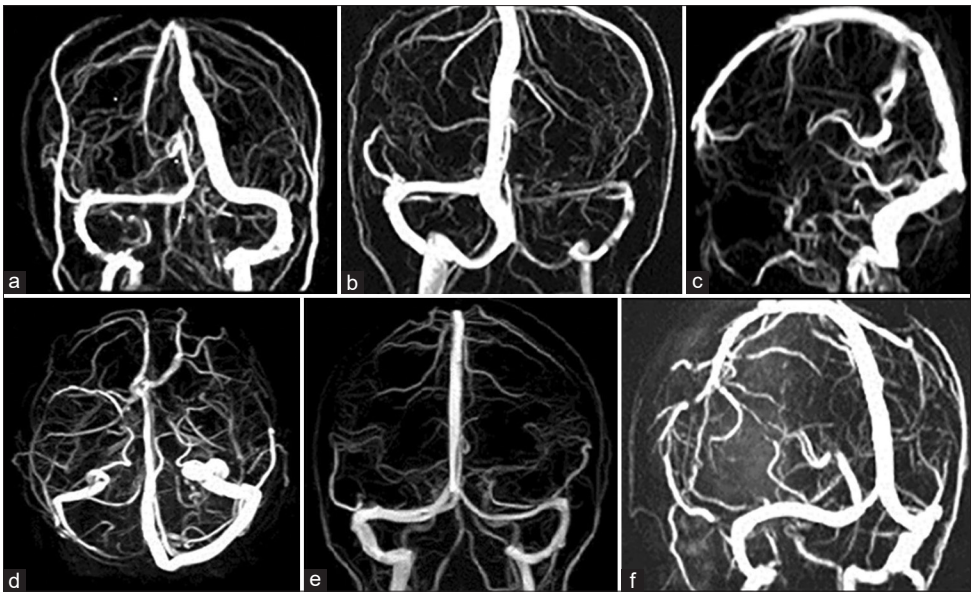

Figure 2: Three-dimensional phase-contrast magnetic resonance venography images. (a) Straight sinus drain the left transverse sinus and Superior sagittal sinus drain the right transverse sinus. (b) Hypoplastic left transverse sinus and paired right occipital sinus. (c) Sinus rectus drains into the superior sagittal sinus superiorly. (d) Hypoplastic right transverse sinus and paired anterior one-third superior sagittal sinus. (e) Hypoplastic left transverse sinus. (f) Sinus rectus drain the right transverse sinus. SSS: Superior sagittal sinus, 3D PC-MRV: Three-dimensional phase-contrast magnetic resonance venography

Table 5: Sinus rectus variations

Rectus sinus				
Valid	**Frequency**	**Percentage**	**Valid percentage**	**Cumulative percentage**
No variation	772	94.8	94.8	94.8
Continuity of sinus rectus with the right transverse sinus	13	1.6	1.6	1.6
Continuity of sinus rectus with the left transverse sinus	29	3.6	3.6	3.6
Total	814	100.0	100.0	

Table 6: Occipital sinus variations

Occipital sinus				
Valid	**Frequency**	**Percentage**	**Valid percentage**	**Cumulative percentage**
No variation	787	96.7	96.7	96.7
Presence of right occipital sinus	20	2.5	2.5	2.5
Presence of left occipital sinus	2	0.2	0.2	0.2
Occipital sinus combined variation	5	0.6	0.6	0.6
Total	814	100.0	100.0	

setting.[6] 3D PC-MRV is an important benefit in evaluating dural sinus and cerebral venous structures, to prevent possible complications, such as surgical treatment of brain tumors, vascular disease, and radical neck dissections.

Goyal *et al*.[9] determined that the transverse sinuses were calculated 1 cm from the confluence sinuous and the sigmoid sinuses were measured 1 cm from the transverse sigmoid junctions. Their liner measurements were checked with the superior sagittal sinus. If the linear measurement was less than half the size of the superior sagittal sinus, it was evaluated hypoplastic and if not displayed, it was considered aplastic or atrectic sinus. In our study, hypoplasia and other variations were evaluated by comparing TSs with each other and comparing the SSS. The most common variation in dural venous structures was the drain of the superior sagittal sinus to the right transverse sinus.

Alper *et al*.[12] revealed that 21 of 105 patients (20%) had left TS sinus aplasia, 41 (39%) left sinus hypoplasia, 33 (31%) left sinüs aplasia, 6 (6%) right sinus hypoplasia, and 4 (4%) right sinus aplasia. In addition, right transverse sinus dominance was found in 62 (59%) patients, and left transverse sinus dominance in 10 (9.5%) patients. Ayanzen *et al*.[13] demonstrated that 59% of 100 patients had right transverse sinus, 25% left TS dominance, and 16% had codominant transverse sinus. Durgun *et al*.[7] determined that including 189 patients, 82 patients were found to have right transverse sinus, 36 patients left transverse sinus dominance, and 71 patients codominant.

In our study, TS was found to be right-dominant in 224 (27.5%) and left dominance in 76 (9.3%) patients. Codominance was detected in 342 (58%), and the combined form of these variations was observed in 42 (5.2%) cases. In some studies, right TS dominance was determined more frequently, while others stated that codominance was more common. In our study, the number of codominant cases was found to be 58% higher. Literature shows that there is heterogeneity in the distribution in terms of TS dominance.

Dora and Zileli[14] studied that occipital sinus was found in 53 of 163 cases. In 10 cases (6.6%) were found to drain the confluent sinuum. Kopuz *et al*.[8] showed, included 33 cadaveric cases, that occipital sinus was found in all cases. Ayanzen *et al*.[13] stated, included 100 cases ranging from 9 to 83 years, that occipital sinus was found in 10% of the cases. Ruíz *et al*.[15] reported that occipital sinus was found in one of 12 cadavers with an average age of 85. In addition, Widjaja and Griffiths[5] demonstrated that the occipital sinus was detected in 9 out of 50 patients and bilateral in 5 and unilateral occipital sinus in 4. They stated not to detect occipital sinus in children older than 9 years. We indicated that the occipital sinuses were observed in 27 (3.3%) cases. Right occipital sinus was observed in 20 (2.5%), left occipital sinus in 2 (0.2%), and both right and left occipital sinus in 5 (0.6%) patients in our study.

Goyal *et al*.[9] found that the most common variation of the SSS was atresia of the front one-third (15 cases, 0.9%), hypoplasia of the central part of the SSS (13 cases, 0.7%), hypoplasia of the front one-third (6 cases, 0.4%), hypoplasia of the front two-thirds (3 cases, 0.2%), and hypoplasia of the front half (1 case, 0.1%) in their study. In our study, the most common variation of SSS was atresia of anterior one-third SSS 19 (2.3%). Other variations were hypoplasia of the anterior half of SSS 2 (0.2%), atresia of posterior one-third of SSS (7, 0.9%), and combined variation of SSS (13, 1.6%).

Goyal *et al*.[9] evaluated that straight sinus hypoplasia was detected in 4 patients (0.2%).

In our study, straight sinus was observed 3 types of variations 42 (5.2%) of 814 patients. The continuity of the sinus rectus with the right transverse sinuses was observed in 13 (1.6%) patients, and the continuity of the sinus rectus with the left transverse sinuses was observed in 29 (3.6%) patients. Superior localization of straight sinus was also present in one patient.

Conclusion

In this study, unlike other studies, we evaluated the dural sinus variations in all age groups with 3D PCA MRV. We think that our study will take its place in the literature in this respect. In addition, we have identified a new variation as "the superior location of the straight sinus" in our study. Other studies did not mention this variation and we think that we would contribute to the literature with this variation.

Financial support and sponsorship

Nil.

Conflicts of interest

There are no conflicts of interest.

References

1. Larson AS, Lanzino G, Brinjikji W. Variations of ıntracranial dural venous sinus diameters from birth to 20 years of age: An MRV-based study. AJNR Am J Neuroradiol 2020;41:2351-7.
2. Iqbal N, Sharma A. Cerebral venous thrombosis: A mimic of brain metastases in colorectal cancer associated with a better prognosis. Case Rep Oncol Med 2013;2013:109412.
3. Patchana T, Zampella B, Berry JA, Lawandy S, Sweiss RB. Superior sagittal sinus: A review of the history, surgical considerations, and pathology. Cureus 2019;11:e4597.
4. Xiao Z, Zheng Y, Li J, Chen D, Liu F, Cao D. Four-dimensional CT angiography (4D-CTA) in the evaluation of juvenile nasopharyngeal angiofibromas: Comparison with digital subtraction angiography (DSA) and surgical findings. Dentomaxillofac Radiol 2017;46:20170171.
5. Widjaja E, Griffiths PD. Intracranial MR venography in children: Normal anatomy and variations. AJNR Am J Neuroradiol 2004;25:1557-62.
6. Ozturk K, Soylu E, Parlak M. Dural venous sinus thrombosis: The combination of noncontrast CT, MRI and PC-MR venography to enhance accuracy. Neuroradiol J 2018;31:473-81.
7. Durgun B, Ilglt ET, Cizmeli MO, Atasever A. Evaluation by angiography of the lateral dominance of the drainage of the dural venous sinuses. Surg Radiol Anat 1993;15:125-30.
8. Kopuz C, Aydin ME, Kale A, Demir MT, Corumlu U, Kaya AH. The termination of superior sagittal sinus and drainage patterns of the lateral, occipital at confluens sinuum in newborns: Clinical and embryological implications. Surg Radiol Anat 2010;32:827-33.
9. Goyal G, Singh R, Bansal N, Paliwal VK. Anatomical variations of cerebral MR venography: Is gender matter? Neurointervention 2016;11:92-8.
10. Eisová S, Píšová H, Velemínský P, Bruner E. Normal craniovascular variation in two modern European adult populations. J Anat 2019;235:765-82.
11. Osborn A. Diagnostic Neuroradiology. St. Louis: Mosby; 1994.
12. Alper F, Kantarci M, Dane S, Gumustekin K, Onbas O, Durur I. Importance of anatomical asymmetries of transverse sinuses: An MR venographic study. Cerebrovasc Dis 2004;18:236-9.
13. Ayanzen RH, Bird CR, Keller PJ, McCully FJ, Theobald MR, Heiserman JE. Cerebral MR venography: Normal anatomy and potential diagnostic pitfalls. AJNR Am J Neuroradiol 2000;21:74-8.
14. Dora F, Zileli T. Common variations of the lateral and occipital sinuses at the confluens sinuum. Neuroradiology 1980;20:23-7.
15. Ruíz DS, Yilmaz H, Gailloud P. Cerebral developmental venous anomalies: Current concepts. Ann Neurol 2009;66:271-83.

Original Article

The Impact of Tri (2-ethylhexyl) Trimellitate on Renal Functions in Sprague–Dawley Rats

Ayesha Zafar Rajpoot, Humaira Fayyaz Khan[1], Fatima Iqbal[1], Rubab Rameez[2], Tayyaba Anis[1], Ayesha Shahid[3], Shazia Ali[1], Hassan Mumtaz[4]

Departments of Physiology and [3]Anatomy, Hitec IMS Taxila, [1]Department of Physiology, Riphah International University, Rawalpindi, [2]Department of Physiology, Islamabad Medical and Dental College, [4]Innovation, Implementation, and Partnership Unit, Association for Social Development, Islamabad, Pakistan

Abstract

Background: Globally, there is a growing concern over the excessive use of plasticizers and their hazardous effects on human's organs particularly kidney. **Aims and Objectives:** This study aims to determine the effects of TOTM on renal functions so it may get used in medical equipment, toys, and food packaging with full knowledge regarding its repercussions. The objective is to determine the levels of serum urea, creatinine, cystatin C and endothelial nitric oxide synthase of Sprague Dawley rats exposed to different doses of TOTM to reach viable results. **Materials and Methods:** A total number of 30 rats were randomly divided into three groups. Each group comprised of 10 male rats divided as one control group (I) given normal saline with rat pellets, group II 300 mg/kg/day of TOTM and group III 1000 mg/kg/day TOTM in the form of rat pellets. Rats of experimental groups II and III were given TOTM with doses of 300 mg/kg/day and 1000mg/kg / day throughout the experiment via oral route for about four weeks. **Results:** The result showed an increase in serum urea, creatine and cystatin C level in a dose dependent manner. **Conclusion:** The study finds an association between exposure to TOTM plasticizer on renal function in proportion to dose.

Keywords: *Di (2-ethylhexyl) phthalate, renal functions, tri (2-ethylhexyl) trimellitate*

Introduction

Environmental chemicals have long been known to have a detrimental effect on public health and clinical well-being. However, growing evidence suggests that the general public has increasingly been exposed unknowingly to a wide variety of chemicals due to everyday consumer activities.[1] One example of such harmful agents is plasticizers. Long-term exposure to plasticizers escalates the risk of nephrotoxicity and exacerbation of chronic kidney diseases. Plasticizers are routinely added to Polyvinyl chloride (PVC) products to increase their flexibility. They get utilized in producing a wide range of consumer goods, ranging from the automobile industry to medical devices.[2]

One of the emerging plasticizers is tri (2-ethylhexyl) trimellitate (TOTM) from the trimellitate group. It gets used in the manufacturing of consumer goods for food packaging, contact material, cosmetics, emollients, and lotions.[3] In hospital settings, it is used in the mass production of various infusion equipment, tunings, and blood storage bags.[4] It is a colorless, pale liquid with high viscosity and low volatility.[5]

TOTM is poorly absorbed and metabolized in the body.[6] The parent compound is unmetabolized and excreted in the feces. The urinary metabolites of TOTM are 2-ethylhexanol and 2-ethylhexanoic acid. The parent compound does not get eliminated through urine. About 5% of TOTM leaves the body through feces, 16% gets excreted in the urine, and 1.9% evaporates as carbon dioxide.

TOTM is a weak inducer of peroxisome proliferation and causes a reduced induction of peroxisomes-associated enzymes.[7] In comparison with the compounds of other plasticizers, TOTM is less toxic in action due to its decreased leachability from the products, it gets used for manufacturing.

Limited toxicological data are available for TOTM. However, it does have less toxic potential than other plasticizers out there.[8] Some studies have revealed that it may promote injurious and estrogenic

How to cite this article: Rajpoot AZ, Khan HF, Iqbal F, Rameez R, Anis T, Shahid A, *et al.* The impact of tri (2-ethylhexyl) trimellitate on renal functions in Sprague–Dawley rats. J Anat Soc India 2024;73:323-7.

Article Info

Received: 05 September 2023
Revised: 06 October 2024
Accepted: 16 December 2024
Available online: 28 December 2024

Address for correspondence:
Dr. Hassan Mumtaz, Association for Social Development, Lahore, Pakistan. E-mail: hassanmumtaz.dr@gmail.com

Access this article online

Website: https://journals.lww.com/joai

DOI: 10.4103/jasi.jasi_94_23

Quick Response Code:

activity in the cell.[9] However, little to almost no data is available regarding its renal toxicity.

The inevitable exposure of plasticizers and their adverse effects on renal functions means that the topic needs to be searched more. In terms of safety profile, TOTM has proved to be less toxic than other plasticizers. As a high-molecular-weight monomeric plasticizer, TOTM has reduced mobility, and thus, its cumulative amounts in the blood are lower than di (2-ethylhexyl) phthalate (DEHP) under the same conditions.

Few studies are available in the literature about the effect of TOTM on renal functions. Therefore, it is vital to dig deeper into their various effects on renal functions. This study aims to determine the effects of TOTM on renal functions, so it may get used in medical equipment, toys, and food packaging with full knowledge regarding its repercussions. The objective is to determine the levels of serum urea, creatinine, cystatin C, and endothelial nitric oxide synthase of Sprague–Dawley rats exposed to different doses of TOTM to reach viable results.

Materials and Methods

Chemicals

TOTM in the liquid form with 99% purity was purchased from ATS Synthetic Pvt. Ltd., Lahore, India.

Preparation of solutions

TOTM in liquid form was weighed first on an electronic weighing scale according to a dose of 300 mg/kg/day and 1000 mg/kg/day. This was administered to each rat in the form of a rat pellet.

A randomized controlled trial was executed in the Department of Physiology and Multidisciplinary Research Laboratory of Islamic International Medical College (IIMC), Rawalpindi, in association with the Animal House at National Institutes of Health (NIH), Islamabad, Pakistan.

The study was approved by the Ethical Review Committee of IIMC, Riphah International University, Islamabad, and was accomplished under the guidelines, stated by the National Institute for animal experimentations.

Sample size

A total of 50 male Sprague–Dawley rats were included in the study. The sample size was selected according to the resource equation approach.[10]

Sample selection

Healthy 6- to 8-week-old male adult rats with an approximate weight of 250 g to 300 g were included in the study. Rats of <6 weeks and more than 8 weeks of age, with weight below 250 g and above 300 g, were excluded from the study.

Materials

Tri (2-ethylhexyl) trimellitate

TOTM in liquid form with 95% purity was procured from the ATS Synthetic Pvt. Ltd., Lahore.

Laboratory environment and nutrition regime

Rats were kept in cages under the supervision of the Animal house of NIH, Chak Shahzad, Islamabad. A total number of 50 rats weighing (250–300 g) were kept under the standard temperature at 22°C ± 0.5°C. They were shifted into clean stainless steel cages under 12-h light and dark cycle with 50% humidity. They were given food and water *ad libitum* for 7 days to acclimatize. Rat pellets and water were used as food during the whole experiment.

Experimental protocol

A total number of 30 rats were randomly divided into three groups. Each group comprised 10 male rats divided as one control: Group (I) given normal saline with rat pellets, Group II 300 mg/kg/day of TOTM, and Group III 1000 mg/kg/day of TOTM in the form of rat pellets.

On the 1st day of the study, the presample was carried out by drawing blood samples from the lateral tail vein of rats. Then, rats of the control group were given normal saline. Rats of experimental Groups II and III were given TOTM with doses of 300 mg/kg/day and 1000 mg/kg/day throughout the experiment through oral route for about 4 weeks.

Extraction of serum and storage

The labeled gel tubes having the blood samples were placed in a centrifuge machine and centrifuged at a speed of 3000 rpm for 15 min, until the serum was separated. It was then stored in Eppendorf tubes for further analysis and ensured that the temperature is maintained at −15°C to −20°C.

Statistical analysis

All the experimental data were analyzed using the SPSS software version 21 (SPSS, Chicago, Illinois USA) and expressed as mean ± standard deviation (SD). Data were analyzed by repeated-measure ANOVA and comparison among groups was made by *post hoc* Tukey test. $P < 0.05$ was considered statistically significant.

Table 1: Mean and standard deviation of serum creatinine (mg/dL) of all the groups on days 0,15 and 30

Variable (creatinine) points in time	Control I	Group II - TOTM 300	Group III - TOTM 1000
Day 0	0.49±0.15	0.51±0.18	0.53±0.16
Day 15	0.48±0.15	0.54±0.23	0.59±0.13
Day 30	0.5±0.17	1.3±0.25	1.77±0.52

TOTM: Tri (2-ethylhexyl) trimellitate

Results

A total of 30 rats were included in the study. The rats were divided into three groups each containing ten rats (n = 10).

Effect of tri (2-ethylhexyl) trimellitate on serum creatinine

To observe the effect of TOTM on serum creatinine, samples were assessed on days 0, 15th, and 30th days. The mean and SD of serum creatinine (mg/dL) of all the groups on days 0, 15, and 30 are shown in Table 1. A significant increase in serum creatinine was observed in Group III on day 30, as shown in Figure 1. When comparison was made among Groups III showed maximum increase in serum creatinine, as shown in Figure 2.

Effect of di (2-ethylhexyl) phthalate and tri (2-ethylhexyl) trimellitate on serum urea

After 30 days of exposure to DEHP and TOTM, serum urea of all the groups was measured. Mean and SD of serum urea (mg/dL) of all the groups was measured on days 0, 15, and 30. Group III (TOTM 1000) showed a maximum increase in the serum urea level among all other groups, as shown in Figures 3 and 4.

Effect of tri (2-ethylhexyl) trimellitate on serum cystatin C

Serum urea levels of the rats were determined at three different points during the experiment. Administration of a low dose of TOTM (300 mg/kg/day) in Group II showed no significant increase after 30 days of exposure. Group III (TOTM 10000) resulted in a significant increase in levels of cystatin C from day 0 to 30 [Figures 5 and 6].

Discussion

The kidney is a vital organ of the body that performs several important functions, including the conservation of homeostasis, detoxification and excretion of drugs, and harmful metabolites. The high exposure of chemicals to the body may lead to deterioration of renal structure and function. One such chemical commonly used chemical is a class of plasticizers such as DEHP and TOTM.

TOTM is one of the alternatives to DEHP. Due to its stable structure and minimal leachability, it may be considered a viable alternative to DEHP. However, we have limited data available at present to comment on its toxicological profile. Our meticulously researched study aims to determine the effects of TOTM on the renal functions of Sprague–Dawley rats and compare their toxicological profiles. It will help us make better choices in future about the manufacturing of consumer materials, particularly in food and medical devices.

The level of deterioration in renal function following exposure to TOTM was measured using serum creatinine levels in rats. Serum creatinine is the most widely and routinely used marker for renal function. An increase in the levels of creatinine is indicative of renal injury or dysfunction.[11,12]

Our data showed that creatinine level increases from baseline values with increasing doses of TOTM in Sprague–Dawley rats. In our study, the rats exposed to a low dose of TOTM (300 mg/kg/bw) showed no increase in serum creatinine at day 15. A high dose of TOTM (1000 mg/kg/bw) showed raised creatinine levels at days 15 and 30. So far, limited data are available about the toxicity of TOTM on renal structure and biomarkers. Recently, Murawski *et al*. conducted a study in Germany on children and adults to detect the metabolites of TOTM in urine. The study reported that metabolites of TOTM were scarce in the urine samples of the participants.[13] Another study conducted to detect the plasticizer exposure of infants during cardiac surgery also suggested similar findings. No metabolites of TOTM were traced in the urine samples of

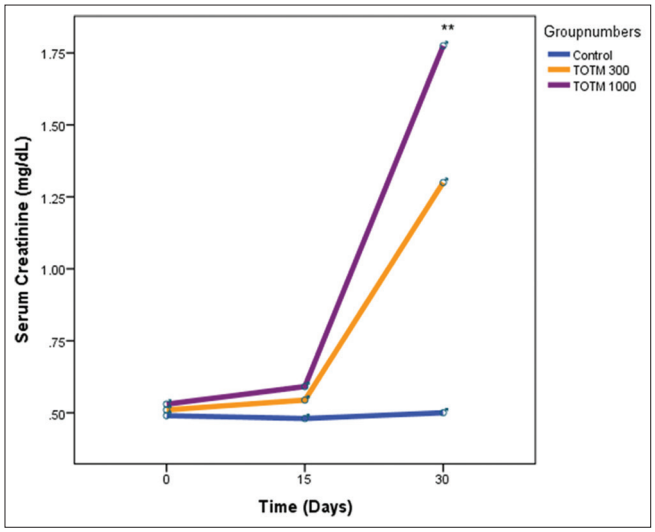

Figure 1: Dose-dependent changes in serum creatinine (mg/dL) following administration of different of tri (2-ethylhexyl) trimellitate at days 0, 15, and 30 in Sprague–Dawley rats. TOTM: Tri (2-ethylhexyl) trimellitate

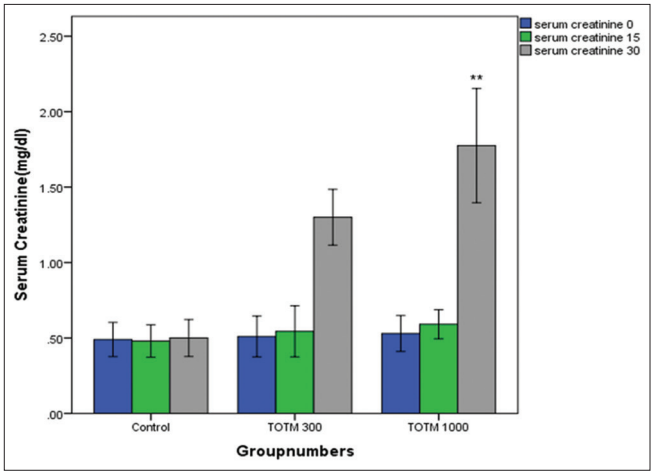

Figure 2: Comparison of means of serum creatinine (mg/dL) following ministration of different concentrations of tri (2-ethylhexyl) trimellitate on day 0, 15, and 30

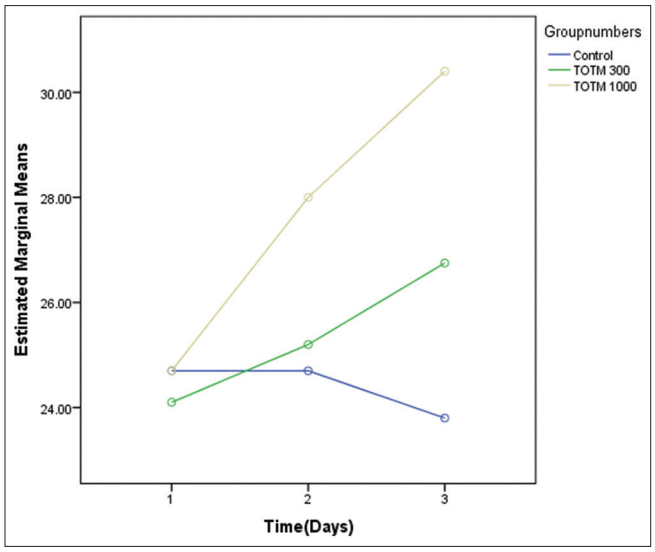

Figure 3: Mean of serum urea (mg/dL) of all the groups on days 0, 15 and 30

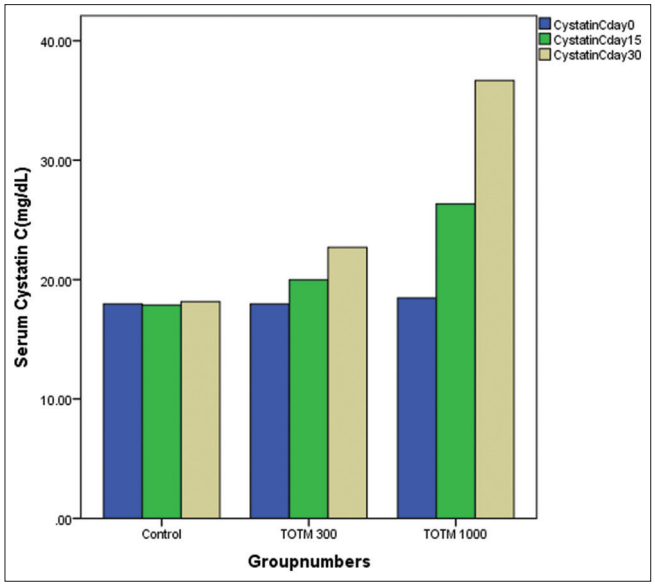

Figure 5: Administration of a low dose of TOTM showing increase after 30 days of exposure

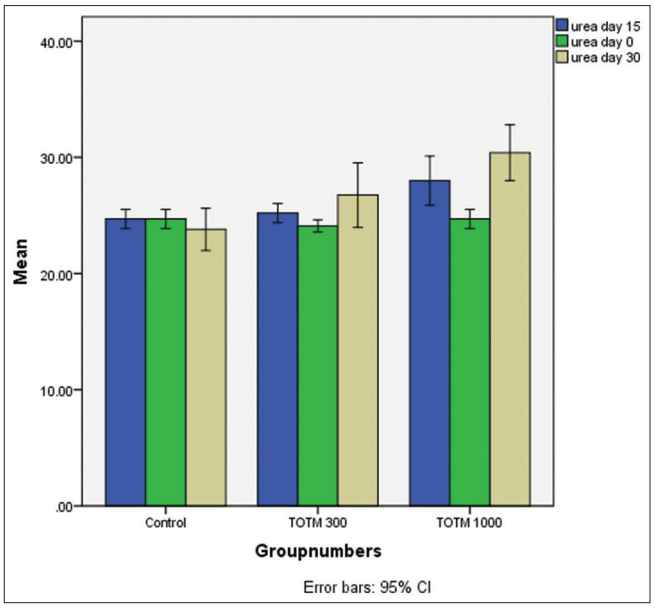

Figure 4: Group I numbers association with increase in serum urea level from day 0 to 30

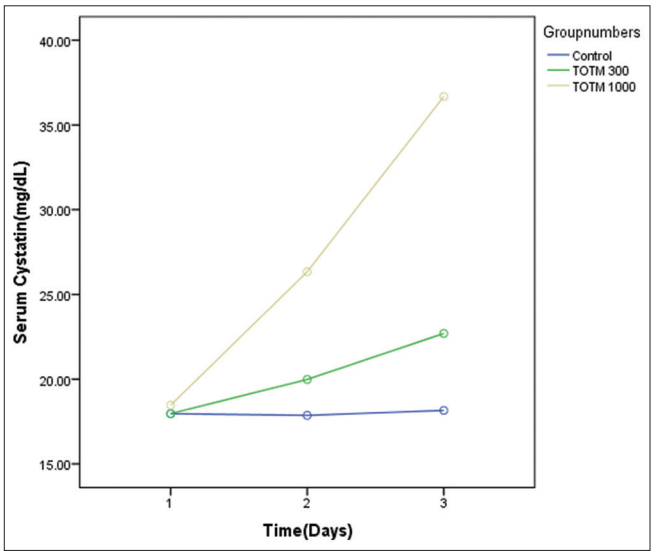

Figure 6: Group numbers association with levels of cystatin C from day 0 to 30

the participants.[14] These studies did not observe the effect of renal biomarkers in the patient.

TOTM, we measured the serum urea levels. In the current study, TOTM exposed group (300 mg/kg/bw) exhibited no significant increase in urea. However, a high dose of TOTM (1000 mg/kg/bw) showed an increase in urea levels at the end of the experiment. To the best of our knowledge, no study has reported the effects of serum urea levels in TOTM exposed rats. Chen *et al*. determined the hepatotoxic potential of TOTM in 6-week mice by injecting TOTM intravenously (100, 200, and 400 mg/kg/bw) for 5 consecutive days reporting a significant increase in hepatic biomarkers (aspartate aminotransferase, alanine aminotransferase, and inflammatory cytokines) in a dose-dependent manner.[15] This was consistent with our finding that toxicity of TOTM increases with increasing dose of chemical. The impact of TOTM on rat hepatocytes has been evaluated by a research. The study concludes that TOTM induces mild changes in histological, ultrastructure, and immunohistochemical levels in adult male albino rats.[16]

The serum cystatin C levels were measured to determine whether the effects of TOTM have altered glomerular function. Cystatin C is a reliable biomarker for determining nephrotoxicity and glomerular filtration rate. The study conducted on TOTM showed that a low dose of TOTM (300 mg/kg/BW) influenced no change in cystatin C level. An increase in cystatin C levels was observed on day 30 in the high-dose exposure group of

TOTM. A study on rats has reported its reproductive toxic effects such as decreased spermatocytes and spermatids on 300 and 1000 mg/kg/bw of TOTM. However, no effects on the weight of reproductive organs were recorded.[6]

Conclusion

The study finds an association between exposures to TOTM plasticizer on renal function. TOTM has shown toxic potential in a dose-dependent manner.

Financial support and sponsorship

Nil.

Conflicts of interest

There are no conflicts of interest.

References

1. Wu CF, Hsiung CA, Tsai HJ, Tsai YC, Hsieh HM, Chen BH, *et al*. Interaction of melamine and di-(2-ethylhexyl) phthalate exposure on markers of early renal damage in children: The 2011 Taiwan food scandal. Environ Pollut 2018;235:453-61.
2. Rahman M, Brazel CS. The plasticizer market: An assessment of traditional plasticizers and research trends to meet new challenges. Prog Polym Sci (Oxford) 2004;29:1223-48.
3. Iwase H, Oiso S, Kariyazono H, Nakamura K. Biological effects of the plasticizer tris (2-Ethylhexyl) trimellitate. Clin Pharmacol Biopharm 2014;S2:004. [doi: 10.4172/2167-065X.S2-004].
4. Malarvannan G, Onghena M, Verstraete S, van Puffelen E, Jacobs A, Vanhorebeek I, *et al*. Phthalate and alternative plasticizers in indwelling medical devices in pediatric intensive care units. J Hazard Mater 2019;363:64-72.
5. Münch F, Höllerer C, Klapproth A, Eckert E, Rüffer A, Cesnjevar R, *et al*. Effect of phospholipid coating on the migration of plasticizers from PVC tubes. Chemosphere 2018;202:742-9.
6. Testai E, MS Scientific Committee SCENIHR Electronic Address, SANTE-C2-SCENIHR@Eceuropaeu, Hartemann P, Rastogi SC, Bernauer U, Piersma A, *et al.* The safety of medical devices containing DEHP plasticized PVC or other plasticizers on neonates and other groups possibly at risk (2015 update). Regul Toxicol Pharmacol 2016;76:209-10.
7. Kambia N, Renault N, Dilly S, Farce A, Dine T, Gressier B, *et al.* Molecular modelling of phthalates – PPARs interactions. J Enzyme Inhib Med Chem 2008;23:611-6.
8. Johnson PD, Besselsen DG. Practical aspects of experimental design in animal research. ILAR J 2002;43:202-6.
9. Kambia K, Dine T, Gressier B, Dupin-Spriet T, Luyckx M, Brunet C. Evaluation of the direct toxicity of trioctyltrimellitate (TOTM), di(2-ethylhexyl) phthalate (DEHP) and their hydrolysis products on isolated rat hepatocytes. Int J Artif Organs 2004;27:971-8.
10. Arifin WN, Zahiruddin WM. Sample size calculation in animal studies using resource equation approach. Malays J Med Sci 2017;24:101-5.
11. Keppler A, Gretz N, Schmidt R, Kloetzer HM, Groene HJ, Lelongt B, *et al.* Plasma creatinine determination in mice and rats: An enzymatic method compares favorably with a high-performance liquid chromatography assay. Kidney Int 2007;71:74-8.
12. Wasung ME, Chawla LS, Madero M. Biomarkers of renal function, which and when? Clin Chim Acta 2015;438:350-7.
13. Murawski A, Schmied-Tobies MI, Rucic E, Schmidtkunz C, Küpper K, Leng G, *et al.* Metabolites of 4-methylbenzylidene camphor (4-MBC), butylated hydroxytoluene (BHT), and tris (2-ethylhexyl) trimellitate (TOTM) in urine of children and adolescents in Germany – Human biomonitoring results of the German Environmental Survey GerES V (2014-2017). Environ Res 2021;192:110345.
14. Eckert E, Müller J, Höllerer C, Purbojo A, Cesnjevar R, Göen T, *et al.* Plasticizer exposure of infants during cardiac surgery. Toxicol Lett 2020;330:7-13.
15. Chen XH, Ma L, Hu YX, Wang DX, Fang L, Li XL, *et al.* Transcriptome profiling and pathway analysis of hepatotoxicity induced by tris (2-ethylhexyl) trimellitate (TOTM) in mice. Environ Toxicol Pharmacol 2016;41:62-71.1.
16. Shehata AS, El-Rehim Mohamed ZA, El-Haleem MRA, Samak MA. Effects of exposure to plasticizers Di-(2-Ethylhexyl) phthalate and trioctyltrimellitate on the histological structure of adult male albino rats' liver. J Clin Toxicol 2013;3:169. [doi:10.4172/2161-0495.1000169].

Original Article

A Clinicoanatomical Study of Perforators of the Posterior Tibial Artery in Distal One-third of the Leg

Saba Anjum, Jyoti Chopra, Sushma Tomar, Rakesh Kumar Diwan, Brijesh Mishra[1]

Departments of Anatomy and [1]Plastic Surgery, King George Medical University, Lucknow, Uttar Pradesh, India

Abstract

Introduction: The posterior tibial artery (PTA) is the terminal branch of the popliteal artery. PTA flap has gained widespread clinical importance in reconstructive surgeries. Perforator flap procedures will be complicated without thorough knowledge of the anatomy of the underlying vasculature. Various areas of the body can be used to develop different types of flaps that can be used effectively to increase the survival of the flaps and thereby minimize morbidity and the quality of life the patients. **Materials and Methods:** The study was conducted on 29 lower limbs of 15 adult fresh frozen cadavers. There were 9 males and 6 females who voluntarily donated their bodies to the Department of Anatomy, King George's Medical University UP, Lucknow. Latex mixed with red paint was injected into the femoral artery. We measured the diameter, length, and distance of the perforator of PTA from the medial tibial border (MTB) and medial malleolus (MM) in the distal one-third of the leg. **Results:** The mean distance of all septocutaneous perforators from MTB and MM was 25.6 ± 2.4 mm and 72.6 ± 27.1 mm, respectively. The mean length and diameter of the perforator were 16.6 ± 4.4 mm and 0.64 ± 0.11 mm, respectively. **Conclusion:** The best flaps can be harvested from the distal one-third of the leg as it has a large piece of the skin and a long pedicle. Hence, for designing these flaps, the knowledge regarding location, type, length and caliber of the perforator as well as the area of skin it is supplied by it is mandatory.

Keywords: *Perforator flap, reconstructive surgery, septocutaneous*

Introduction

Knowledge of vascular anatomy plays an essential role in the success of any reconstructive surgery. Perforator flap procedures will be complicated without thorough knowledge of the anatomy of the underlying vasculature. To have quintessential to have depth knowledge of the anatomy of underlying vasculature for flawless perforator flap procedures. Hence, in order to develop different types of flaps in various parts of the body, that can be effectively used to increase the survival of the flaps. Doing so will minimize morbidity and increase the quality of life patients.[1]

The term "perforator flap" describes the vascularized region of the skin and subcutaneous tissue that receives its blood supply from one or more perforators or blood vessels starting from a source vessel beneath the deep fascia. These vessels go directly or indirectly via the target tissue and the deep fascia before reaching the subdermal plexus. There are direct and indirect perforators. Perforators that originate from the source artery and then pierce the deep fascia without crossing any deep structures are known as direct perforators. Direct perforators can be subclassified as direct cutaneous and septocutaneous (SC). If the perforators arising from the source artery reach directly to the skin, they are termed as direct cutaneous; whereas if they traverse the septa between the muscles and then reach the skin, then they are called as SC. The perforators that pass through the structures lying deep to the deep fascia formerly reaching the skin are termed as indirect perforators. The most common type of indirect perforators is musculocutaneous or myocutaneous (MC), these are the perforators that runs through the muscle and reaches to the skin. They may be major or minor.[2]

The posterior tibial artery (PTA) is the terminal branch of the popliteal artery. It originates at the distal border of the popliteus muscle between the tibia and fibula. It descends medially in the flexor

How to cite this article: Anjum S, Chopra J, Tomar S, Diwan RK, Mishra B. A clinicoanatomical study of perforators of the posterior tibial artery in distal one-third of the leg. J Anat Soc India 2024;73:328-32.

Article Info

Received: 02 August 2023
Accepted: 11 August 2024
Available online: 28 December 2024

Address for correspondence:
Dr. Saba Anjum,
633/47 Khalid's Villa,
Beside Gulzar Masjid,
Gulzar Colony, Chinhat
Tiraha, Lucknow - 226 028,
Uttar Pradesh, India.
E-mail: drsabarhanjum2023@gmail.com

Access this article online

Website: https://journals.lww.com/joai

DOI: 10.4103/jasi.jasi_79_23

Quick Response Code:

compartment and terminates deep tot the abductor hallucis, midway between the medial malleolus (MM) and calcaneal tubercle into medial and lateral planter arteries.[3]

The perforator-based flaps are used in reconstructive surgeries. Hong *et al*. in 1989 defined the use of PTA flap (PTAF) for the reconstruction of foot and leg defects.[4] The reconstructive surgery of soft tissue defects of the distal third of the leg, ankle, and heel are complicated due to scarcity of soft tissue in the region. Various kinds of PTAF are used for these surgeries nowadays.[5] For designing these flaps, it is mandatory to have a detailed knowledge of the perforators pertaining to their location, type, length, caliber, and area of skin supplied by them.

Materials and Methods

The present study was a collaborative study between the Department of Anatomy and the Department of Plastic Surgery, King George's Medical University UP, Lucknow. The study was conducted on 29 lower limbs of 15 adult fresh frozen cadavers on 9 males and 6 females bodies who voluntarily donated their bodies to the Department of Anatomy, King George's Medical University UP, Lucknow after approval from the Institutional Ethical Committee of KGMU UP, Lucknow with Reference code IV PGTSC-IIA/P43.

Inclusion criteria

The bodies of adult donors which were not embalmed and were kept at 20°C.

Exclusion criteria

Cadavers were excluded from the study due to following reasons:

- Cadavers who were <18 years of age
- If the death was due to peripheral vascular disease
- If there was the presence of scar, bedsore, or any surgery was done in the area of interest of the lower limb.

Methodology

The cadaver was taken out from the cold room (at −20°C), 24 h prior to the dissection to thaw it. Femoral artery was cannulated with nasogastric tube and latex (mixed with red paint) was injected. Then, for the curing, the cadaver was kept at −20°C for 48–72 h. The length of the leg was measured from the tibial tuberosity to the midpoint between the medial and lateral malleolus [Figure 1].[6] The leg was divided into proximal 1/3rd, middle 1/3rd, and distal 1/3rd, and the dissection was proceeded from the distal 1/3rd of the leg [Figure 1].[7] The flexor retinaculum was identified behind the MM and PTA was located deep to it. The PTA was traced upward observing the origin of perforators. According to the course, the perforators were categorized; if it was traversing the intermuscular septae before reaching the skin it was termed SC and if it was passing through the muscle, then was called MC [Figure 2].[2] The length of each perforator was measured from its point of origin till the point of fascial penetration [Figure 3]. Accompanying veins of each perforator were also counted. The origin point of each perforator was measured from the medial border of the tibia and MM.[8] The diameter of the perforators was measured at the point of origin [Figure 4].

Statistical analysis

The IBM SPSS Statis (Statistical Package for the Social Sciences) Version 21.0 was used. Number (%) and mean ± standard deviation were used to display the values.

Results

Morphometric measurements of PTA were taken on 15 cadavers. Out of these 15 cadavers, 9 (60.0%) were males and 6 (40.0%) were females. One cadaver had left leg amputated; therefore, 15 right legs and 14 left legs were used for measurements [Table 1].

Out of 29 legs, no major perforator in distal one-third of the leg was observed in 1 (3.4%) leg, one major perforator

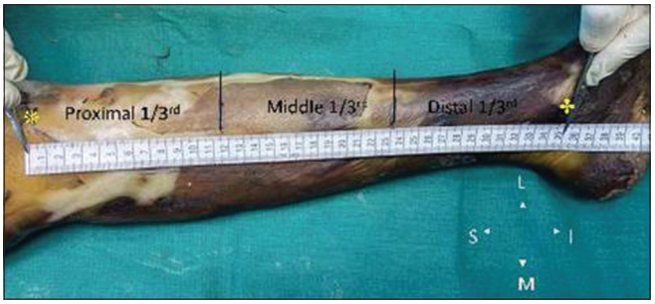

Figure 1: The division of the total left leg length tibial tuberosity medial malleolus

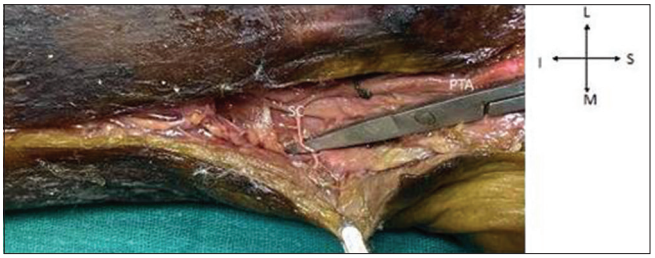

Figure 2: The septocutaneous perforator in the distal one third of the left lower limb

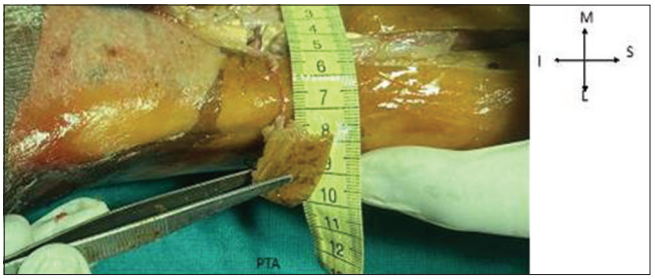

Figure 3: The length of septocutaneous perforator from its origin to its fasical penetration in the left lower leg

in 5 (17.2%), two in 12 (41.4%), three in 9 (31.0%), and four and five in 1 (3.4%) each leg.

The mean length, diameter, and distances from the medial tibial border (MTB) and MM of major perforators in the distal one-third of the leg were 16.6 ± 4.4 (range: 10–32) mm; 0.64 ± 0.11 (range: 0.50–0.91) mm; 25.6 ± 2.4 (20–31) mm and 72.6 ± 27.1 (19–82) mm, respectively [Table 2].

Out of 29 legs, no minor perforator in the distal one-third of the leg was observed in 3 (10.3%) legs, one minor perforator in 8 (27.6%) legs, 2 minor perforators in 13 (44.8%) legs, in 3 minor perforators 4 (13.8%), 5 minor perforators in 1 (3.4%) 5 were observed.

The mean length, diameter, and distances from MTB and MM of minor perforators in the distal one third of the leg were 16.4 ± 5.5 (range: 10-34) mm; 0.37 ± 0.07 (range: 0.25–0.49) mm; 27.1 ± 2.6 (21–32) cm and 51.9 ± 25.0 (15–116) mm, respectively.

Table 1: Characteristics of major perforators in the distal one-third of the leg

Characteristics	Statistics, *n* (%)		
Number of perforators in distal 1/3rd of each leg	37.9		
None	1 (3.4)		
One	5 (17.2)		
Two	12 (41.4)		
Three	9 (31.0)		
Four	1 (3.4)		
Five	1 (3.4)		
Characteristics (mm)	**Minimum**	**Maximum**	**Mean±SD**
Length	10	32	16.6±4.4
Diameter	0.5	0.91	0.64±0.11
Distance from MTB	20	31	25.6±2.4
Distance from MM	19	82	72.6±27.1

MTB: Medial tibial border, MM: Medial malleolus, SD: Standard deviation

Table 2: Characteristics of minor perforators in the distal one-third of the leg

Characteristics	Statistics, *n* (%)		
Number of minor perforators in distal 1/3rd) in each leg			
None	3 (10.3)		
One	8 (27.6)		
Two	13 (44.8)		
Three	4 (13.8)		
Five	1 (3.4)		
Characteristics (mm)	**Minimum**	**Maximum**	**Mean±SD**
Length	10	34	16.4±5.5
Diameter	0.25	0.49	0.37±0.07
Distance from MTB	21	32	27.1±2.6
Distance from MM	15	116	51.9±25

MTB: Medial tibial border, MM: Medial malleolus, SD: Standard deviation

All the major and minor perforators were SC type and all of them were accompanied by vein [Tables 3 and 4].

According to laterality and gender, no significant difference was found in the perforators of PTA in the distal one-third of the leg.

Discussion

The largest terminal branch of the popliteal artery is the PTA and is primary source of blood flow to the foot. It provides mostly SC perforators. Each perforator serves the posteromedial portion of the lower extremities and is accompanied by two comitant veins.[2] PTAF is used for the reformation of foot and leg defects as well as in the head-and-neck region for the restoration of total esophagus defect after corrosive injury.[9]

The present study found major PTA perforators in the distal one-third of the leg in 28/29 (96.6%) cases. Multiple perforators were seen in 22/29 (75.9%) cases. There were 11 (37.9%) cases with three or more perforators. The mean length, diameter, and distance from MTB and MM were recorded as 16.6 ± 4.4, 0.64 ± 0.11, 25.6 ± 2.4, and 72.6 ± 27.1 mm, respectively. Minor PTA perforators were seen in 26/29 (89.7%) cases. There were 18 (62.1%) cases with two or more minor perforators in the distal one-third of the leg. The mean length, diameter, and distance from MTB and distance from MM for minor perforators was 16.4 ± 5.5, 0.37 ± 0.07, 27.1 ± 2.7, and 51.9 ± 25.0 mm, respectively. The average number of major and minor perforators was 2.24 and 1.76, respectively. No significant differences in perforator characteristics were seen between the males and females and for the right or left sides.

With respect to length of perforators, in the present study, we measured it in relation to the MTB and MM. However, Hupkens *et al*. measured it in as the length between the source vessel to the level of the superficial fascia[10,11] and reported it to be 28 mm for distal third perforators of PTA[10] and 37.6 mm as an average length of perforators originating from anterior tibial, peroneal, and popliteal arteries respectively.

Compared to the present study, Kapoor *et al.*[12] found the average number of PTA perforators to be only 1.7 with a relatively higher average in males (1.8) as compared

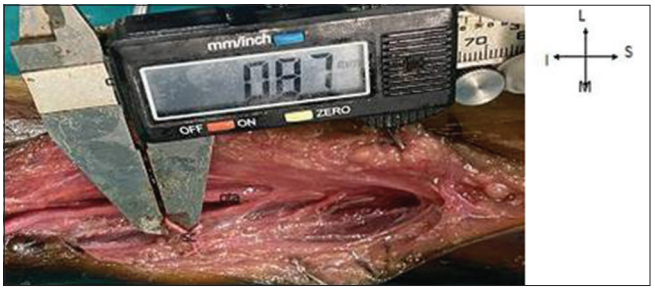

Figure 4: The septocutaneous major perforator in the distal one third of the right leg

Table 3: Gender wise comparison of major and minor perforators

Type of perforator	Parameter	Female		Male		Student's *t*-test	
		n	Mean±SD	*n*	Mean±SD	*t*	*P*
Major	Length	26	1.65±0.49	37	1.66±0.40	−0.026	0.979
	Diameter	26	0.65±0.11	37	0.64±0.11	0.184	0.854
	Distance from MTB	26	2.52±0.25	37	2.59±0.24	−1.174	0.245
	Distance from MM	26	7.50±6.46	37	8.16±2.72	−0.558	0.579
Minor	Length	21	1.59±0.49	30	1.67±0.59	−0.536	0.594
	Diameter	21	0.38±0.07	30	0.36±0.07	0.648	0.520
	Distance from MTB	21	2.65±0.24	30	2.75±0.27	−1.283	0.205
	Distance from MM	21	5.20±2.18	30	5.18±2.74	0.032	0.974

MTB: Medial tibial border, MM: Medial malleolus, SD: Standard deviation

Table 4: Laterality wise comparison of major and minor perforators

Type of perforator	Parameter	Right		Left		Student's *t*-test	
		n	Mean±SD	*n*	Mean±SD	*t*	*P*
Major	Length	30	1.68±0.46	33	1.64±0.42	0.363	0.718
	Diameter	30	0.64±0.11	33	0.65±0.11	0.230	0.819
	Distance from MTB	30	2.55±0.23	33	2.57±0.26	−0.369	0.714
	Distance from MM	30	9.01±5.94	33	6.88±2.66	1.873	0.066
Minor	Length	27	1.76±0.63	24	1.50±0.42	1.746	0.087
	Diameter	27	0.37±0.07	24	0.37±0.08	0.005	0.996
	Distance from MTB	27	2.68±0.27	24	2.74±0.25	−0.765	0.448
	Distance from MM	27	5.34±2.82	24	5.02±2.14	0.452	0.653

MTB: Medial tibial border, MM: Medial malleolus, SD: Standard deviation

to that in the females (1.3) in the upper and middle third of the leg as compared to the distal third of the leg in the present study. However, Hupkens *et al*.[10] reported the mean number of PTA perforators in the distal third of the leg to be 2.8. In the present study, the average of total number of PTA perforators was 4 when major as well as minor perforators were combined collectively. No such discrimination between major and minor perforators was made in these studies. The mean diameter of major perforators in the present study was 0.64 mm which is comparable to 0.8 mm reported by Hupkens *et al*.[10] in their study. Dependence of thickness of PTA perforators may be dependent on the location and may also be slightly different in live as compared to cadaveric assessment. In a study conducted in alive subjects, the mean thickness (caliber) of 0.8, 1.1, and 1.2 mm, respectively, for proximal, middle, and distal thirds.[13] Bulla *et al*.[8] in a study similar to ours measured the distance between distal perforator and MTB and reported the mean length as 12.3 mm which is much shorter than that observed for major perforators (16.6 mm) as well as minor perforators (16.4 mm) in the present study. Our study shows a relatively smaller diameter of both major (0.64 mm) and minor (0.37 mm) perforators as compared to the other studies. While difference in thickness of distal-third perforators in the study by Vaienti *et al*.[13] could be attributed to their live status, Bulla *et al*.[8] who conducted their study in cadavers reported the mean caliber to be 0.77 mm which is also larger than that in the present study. As such there are few studies from India evaluating the distal third PTA perforators. Kapoor *et al*.[12] who carried out anatomical study of upper and middle third leg perforators reported the average diameter in 0.8–1.29 mm for medial sural, posterior tibial SC, lateral sural and peroneal SC perforators. As such the morphological measurements in the present study are distinct and may be considered as representative of Indian population. Further studies to correlate and confirm the findings of the present study are recommended.

The literature review revealed that there are no studies pertaining to the minor perforators as they are considered insignificant as far as flap surgeries are concerned. However, from the anatomical point of view, we made an effort to trace and describe the minor perforators in the distal one third of the leg. The findings of the present study, with respect to minor perforators thus provide a reference to which further works may be performed.

In the present study, we did not find a significant impact of sex or side (laterality) of the perforator characteristics. On reviewing the literature, we did not come across any such study reporting effect of sex or side on the perforator characteristics. This implies that from clinical application point of view sex or side do not pose an issue with respect to generalization of these results.

One of the limitations of the present study was sample size, though most of the earlier studies, particularly cadaver studies, have been carried out in a small sample size; hence, generalization of the results needs a caution. Further

studies on a larger sample size, particularly those focusing on minor perforators, are recommended.

Conclusion

The knowledge of the morphometry of the PTA and its major and minor SC perforators based on gender and laterality will be helpful for the plastic surgeons in selecting the flap according to its size and type of the flap that is required in the patients. It will also help in the dissection and will prevent the accidental damage of the perforators that survive the flap.

Financial support and sponsorship

Nil.

Conflicts of interest

There are no conflicts of interest.

References

1. Cormack G, Lamberty B. The Arterial Anatomy of Skin Flaps. 2nd ed. London: Churchill Livingstone; 1994. p. 87,94,413.
2. Bradow BP. Fundamentals of perforator flaps: Perforator flaps. In: Janis JE. Essentials of Plastic Surgery. 2nd ed., Vol. 2. Florida: Karen Berger; 2014. p. 45-7.
3. Standring S. Gray's Anatomy. 41 ed. Churchill Livingstone: Elsevier; 2016. p. 1413-4.
4. Hong G, Steffens K, Wang FB. Reconstruction of the lower leg and foot with the reverse pedicled posterior tibial fasciocutaneous flap. Br J Plast Surg 1989;42:512-6.
5. Tanaka K, Matsumura H, Miyaki T, Watanabe K. An anatomic study of the intermuscular septum of the lower leg; branches from the posterior tibial artery and potential for reconstruction of the lower leg and the heel. J Plast Reconstr Aesthet Surg 2006;59:835-8.
6. Wu WC, Chang YP, So YC, Yip SF, Lam YL. The anatomic basis and clinical applications of flaps based on the posterior tibial vessels. Br J Plast Surg 1993;46:470-9.
7. Ozdemir R, Kocer U, Sahin B, Oruc M, Kilinc H, Tekdemir I. Examination of the skin perforators of the posterior tibial artery on the leg and the ankle region and their clinical use. Plast Reconstr Surg 2006;117:1619-30.
8. Bulla A, De Luca L, Campus GV, Rubino C, Montella A, Casoli V. The localization of the distal perforators of posterior tibial artery: A cadaveric study for the correct planning of medial adipofascial flaps. Surg Radiol Anat 2015;37:19-25.
9. Mashrah MA, Mai L, Wan Q, Huang Z, Wang J, Lin Z, *et al*. Posterior tibial artery flap with an adipofascial extension: Clinical application in head and neck reconstruction with detailed insight into septocutaneous perforators and donor-site morbidity. Plast Reconstr Surg 2020;145:142e-152e.
10. Hupkens P, Westland PB, Schijns W, van Abeelen MH, Kloeters O, Ulrich DJ. Medial lower leg perforators: An anatomical study of their distribution and characteristics. Microsurgery 2017;37:319-26.
11. Hupkens P, Schijns W, Van Abeelen M, Kooloos JG, Slater NJ, Ulrich DJ. Lateral lower leg perforator flaps: An anatomical study to localize and classify lateral lower leg perforators. Microsurgery 2015;35:140-7.
12. Kapoor A, Chattopadhyay D, Nath A, Gaur N. Anatomical study of perforators of posterior upper and middle third of leg to assess feasibility of combined gastrocnemius flaps. Indian J Clin Anat Physiol 2020;7:219-23.
13. Vaienti L, Cottone G, De Francesco F, Borelli F, Zaccaria G, Amendola F. The suprafascial course of lower leg perforators: An anatomical study. Arch Plast Surg 2020;47:165-70.

Original Article

Analysis of the Relationship between the Angular Characteristics of the Femur and the Dimensions of the Intercondylar Fossa

Burhan Yarar, Aysun Nur Yilmaz

Department of Anatomy, Atatürk University, Medical Faculty, Erzurum, Turkey

Abstract

Introduction: It has been reported in the literature that when the intercondylar fossa (ICF) is narrow, injuries to the anterior cruciate ligament (ACL) are common and the risk of osteoarthritis increases. In addition, the ICF has been reported to have some advantages in determining the depth of distal femoral resection in total knee arthroplasty. The aim of this study was to investigate whether femoral angular characteristics, which influence hip and knee joint kinematics, affect ICF dimensions. **Materials and Methods:** This study was performed on 74 dry femurs, 36 right and 38 left. Angular parameters were measured on digital images using ImageJ. The ICF parameters were measured using a digital caliper. **Results:** The anatomic lateral distal femoral angle and mechanic lateral distal femoral angle were found to be greater on the left side. A positive correlation was found between both anatomic lateral distal femoral angle and mechanic lateral distal femoral angle and ICF width on the right side and in all cases. A positive correlation was found between the anterior femoral bowing angle (AFBA) and ICF width on the right side. **Conclusion:** As a result, low anatomic lateral distal femoral angle, mechanic lateral distal femoral angle, and AFBA may lead to a narrower ICF, which may predispose to ACL injury and osteoarthritis. The results of this study may help orthopedic surgeons in knee surgery and cruciate ligament reconstruction.

Keywords: *Angular parameters, femur, intercondylar fossa, ligament, osteoarthritis*

Introduction

The intercondylar fossa (ICF) is a notch or pit at the distal end of the femur to which the anterior cruciate ligament (ACL) and posterior cruciate ligament, the intracapsular ligaments of the knee joint, are attached.[1] It has been reported that there is a relationship between ICF geometry and ACL injury and that the narrowness of this fossa has a predisposing effect on ACL injury.[2-4] In a study of the relationship between ICF dimensions and knee osteoarthritis, the ICF width index was found to be smaller in patients with medial compartment osteoarthritis than in healthy individuals.[5] ICF is an important landmark in cruciate ligament surgery and knee arthroscopy.[6] In addition, the ICF has been found to have some advantages in determining the limit of distal femoral resection in total knee arthroplasty.[7]

Many angular properties (such as femoral neck-shaft angle, femoral anteversion/torsion angle, femoral mechanical–anatomical angle, anatomical and mechanical distal femoral angle, femoral bowing angle [FBA], and condylar twist angle [CTA]) are defined on the femur in the literature.[8-10] The angular characteristics of the femur in particular the femoral neck shaft angle (NSA) and the femoral torsion angle (FTA) are important factors in the kinematics of the hip and knee joints.[11] In one study, NSA and FTA were shown to have a strong association with some distal femoral parameters.[10] It has been reported that NSA above 134.4° poses a serious risk of knee osteoarthritis.[12] Another study found that a large FTA can cause ACL tears during excessive internal rotation of the hip joint.[11] In addition to these angles, other femoral angles have been shown to be associated with many clinical conditions. It has been noted that accurate estimation of the mechanical–anatomical femoral axis angle is necessary for appropriate distal femoral resection in total knee arthroplasty.[13] In atypical femur fractures, the lateral bowing angle was found to be closely related to the localization of the fracture.[8] It was also emphasized that anatomical and mechanical lateral distal femoral angles (mLDFAs) are

How to cite this article: Yarar B, Yilmaz AN. Analysis of the relationship between the angular characteristics of the femur and the dimensions of the intercondylar fossa. J Anat Soc India 2024;73:333-40.

Article Info

Received: 01 April 2024
Revised: 29 October 2024
Accepted: 18 November 2024
Available online: 28 December 2024

Address for correspondence:
Dr. Burhan Yarar, Department of Anatomy, Medicine Faculty, Atatürk University, Erzurum 25240, Turkey.
E-mail: drburhan25@gmail.com

Access this article online

Website: https://journals.lww.com/joai

DOI: 10.4103/jasi.jasi_39_24

Quick Response Code:

important for proper femorotibial alignment.[9] Considering all these angular features, we asked whether the ICF geometry associated with ACL injury and knee osteoarthritis was influenced by these angular characteristics.

There have been many studies of ICF dimensions and their relationship to various femoral parameters.[5,6,14] However, there are few studies that examine the relationship between femoral angular parameters and ICF dimensions, which are particularly influential on both hip and knee joint mechanics, and these studies are related to NSA and FTA.[15,16] Therefore, the aim of our study was to investigate the relationship between femoral angular characteristics and ICF dimensions.

Materials and Methods

This study was carried out on 74 (36: right, 38: left) dry femurs in the anatomy laboratory of our faculty. The bones with deformations such as fractures, cracks, or dents that would affect the measurements were excluded from the study. There was no record of the age and sex of the people to whom the bones belonged. The right and left femur bones could not be matched to determine if they belonged to the same person.

Ethical approval

This study was approved by the Non-Interventional Clinical Research Ethics Committee (Date: December 29, 2022, Decision No: 19) of our university.

Imaging methods

Anteroposterior, craniocaudal, lateromedial, and condylar images of the bones were taken using a tripod-fixed digital camera (CANON EOS 1200) [Figures 1-3]. A metal tape measure was placed next to the bones for calibration during imaging.

Anteroposterior imaging

The femur was placed on the table so that the greater trochanter and both condyles were in contact with the table surface. The femoral head was brought to the internal rotation in contact with the table. The images were taken from 50 cm above, with the camera lens at the midpoint of the femoral body [Figures 1 and 2A].

Craniocaudal imaging

The femur was placed on the table so that the greater trochanter and both condyles were in contact with the table surface and the femoral neck axis was parallel to the edge of the table. The images were taken from the lateral side with the camera lens at the midpoint of the femoral neck, at the level of the table edge, and perpendicular to the table edge [Figure 3A].

Lateromedial imaging

The femur was placed on the table so that the greater trochanter and both condyles were in contact with the surface of the table and the lateral border of the femoral body was parallel to the edge of the table. The images were taken with the camera lens at the midpoint of the femoral body, at the level of the table edge, and perpendicular to the table edge [Figure 2B].

Condyles imaging

The femur was placed on the table so that the greater trochanter and both condyles were in contact with the surface of the table and the femoral condyles were parallel to the edge of the table. The images were taken with the camera lens at the level of the ICF, at the level of the table edge, and perpendicular to the table edge [Figure 3B].

Definition of femoral axes

These axes were defined according to previous studies[10,13,17] [Figures 1-3].

Anatomical axis: The line joining the proximal diaphysis midpoint at the level of the lower edge of the lesser trochanter and the distal diaphysis midpoint at the level of the upper edge of the condyles.

Mechanical axis: The line between the center of the femoral head and the center of the distal femur.

Proximal axis of the femur: The line joining the midpoints of the proximal diaphysis at the level of the inferior edge of the lesser trochanter and 5 cm below this level.

Distal axis of the femur: The line joining the midpoints of the distal diaphysis at 5 cm and 10 cm above the distal articular surface of the condyles.

Transepicondylar axis: The line between the most protruding points of the medial and lateral epicondyles.

Posterior condylar axis: The transverse axis passing through the posterior surfaces of the condyles.

Femoral neck axis: The line joining the center of the femoral head and the midpoint of the intertrochanteric line.

Measurement of angular parameters of the femur

Measured parameters were defined according to previous studies.[8-10,15,17]

Angle measurements were performed on digital images using ImageJ software (Rasband, WS, ImageJ, US National Institutes of Health, Bethesda, Maryland, USA, https://imagej.nih.gov/ij/, 1997–2018).

NSA: The angle between the femoral anatomical axis and the femoral neck axis. It was measured on the anteroposterior digital images [Figure 1].

Femoral torsion angle (FTA): The angle between the femoral neck axis and the posterior condylar axis. It was measured on the craniocaudal digital images [Figure 3A].

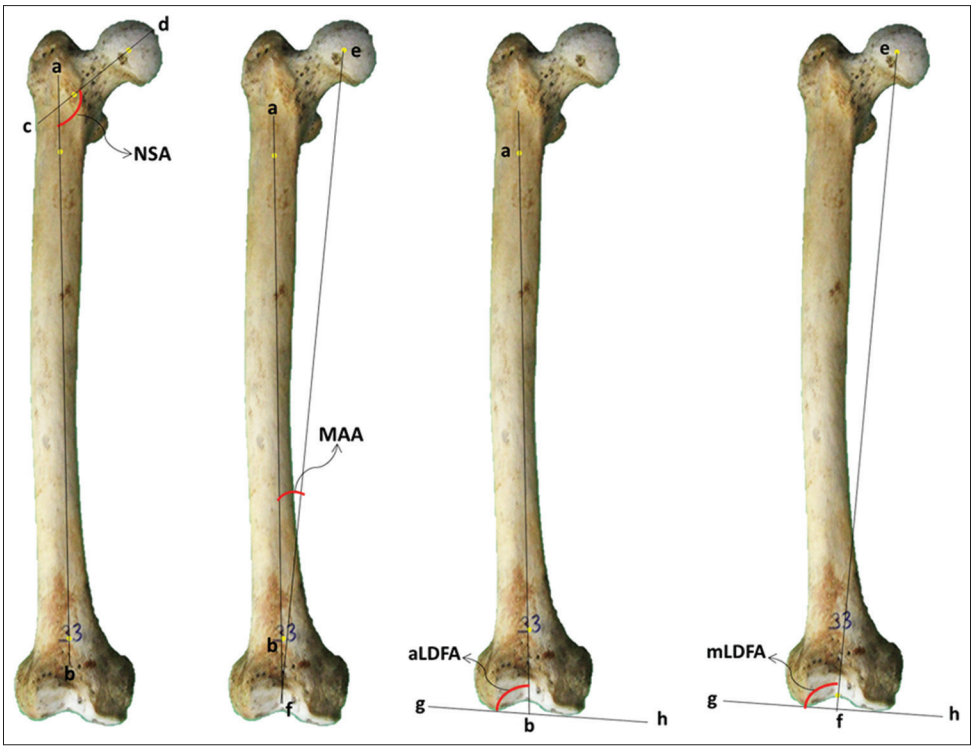

Figure 1: Anteroposterior images. ab: Anatomical axis of the femur, cd: Neck axis of the femur, ef: Mechanical axis of the femur, gh: Distal condylar line, NSA: Neck shaft angle, aLDFA: Anatomical lateral distal femoral angle, mLDFA: Mechanical lateral distal femoral angle, MAA: Mechanical–anatomical axis angle

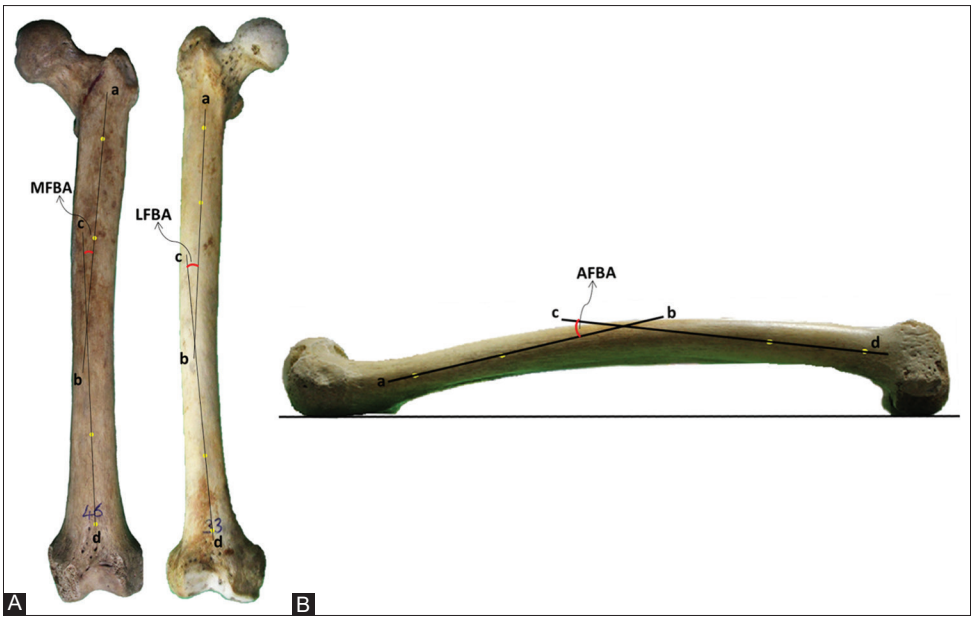

Figure 2: (A) Anteroposterior image, (B) lateromedial image. ab: Proximal axis of the femur, cd: Distal axis of the femur, MFBA: Medial femoral bowing angle, LFBA: Lateral femoral bowing angle, AFBA: Anterior femoral bowing angle

CTA: The angle between the posterior condylar axis and the transepicondylar axis. It was measured on the condylar digital images [Figure 3B].

Anatomical lateral distal femoral angle (aLDFA): The lateral angle formed between the anatomical axis of the femur and the line joining the distal articular surfaces of the condyles. It was measured on the anteroposterior digital images [Figure 1].

mLDFA: The lateral angle formed between the mechanical axis of the femur and the line joining the distal articular surfaces of the condyles. It was measured on the anteroposterior digital images [Figure 1].

Mechanical–anatomical axis angle (MAA): The angle between the mechanical and anatomical axes of the femur. It was measured on the anteroposterior digital images [Figure 1].

Anterior femoral bowing angle (AFBA): The angle between the proximal and distal axes of the femur in the sagittal plane. It was measured on the lateromedial digital images [Figure 2B].

Lateral femoral bowing angle (LFBA): The angle between the proximal and distal axes of the femur in the coronal plane. The convexity of the bowing is towards the lateral. It was measured on the anteroposterior digital images [Figure 2A].

Medial femoral bowing angle (MFBA): The angle between the proximal and distal axes of the femur in the coronal plane. The convexity of the bowing is toward the medial. It was measured on the anteroposterior digital images [Figure 2A].

Measurement of the intercondylar fossa parameters

The ICF dimensions were measured with a digital caliper.

Width of the intercondylar fossa (ICFW): The distance measured transversely between the condyles at the widest part of the ICF [Figure 4].

Anteroposterior diameter of the intercondylar fossa (ICFap): The distance between the midpoint of where the ICF meets the articular surface in front of the femur and the midpoint of the linea intercondylaris in the back [Figure 4].

Depth of the intercondylar fossa (ICFD): The distance between the posterior condylar axis and the deepest point of the ICF [Figure 4].

All measurements were made by two independent observers at different times. The final result was determined by calculating the average of these two measurements for each parameter.

Statistical analysis

IBM SPSS Statistics v25 (IBM Corp., Armonk, New York, USA) was used for statistical analysis. Means and standard deviations (SDs) of the measured variables were calculated. The Student's *t*-test was used to analyze the differences between the right and left sides. The distribution of the data was evaluated using the Kolmogrow–Simirnow test for normal distribution. Pearson correlation test was used to show the correlation between the angular parameters of the femur and the ICF dimensions. $P < 0.05$ was considered statistically significant.

Results

The mean values of the femoral angle and ICF parameters with their SDs are given in Table 1. ALDFA and mLDFA were found to be greater on the left side ($P < 0.001$). The difference between the right and left side for the other parameters was not statistically significant [Table 1].

The correlation values between ICF parameters and femoral angle parameters are given in Table 2. A moderate positive correlation was found between aLDFA, mLDFA, AFBA values and ICFW on the right side ($r = 0.339$, $r = 0.330$, $r = 0.452$, respectively, $P < 0.05$). A weak positive correlation was found between aLDFA, mLDFA values and ICFW in all cases ($r = 0.271$, $r = 0.264$, respectively, $P < 0.05$). No correlation was found between other angular parameters and ICF parameters [Table 2].

Discussion

A narrow ICF has been reported to increase the risk of ACL damage and osteoarthritis of the knee joint.[5] The ICF

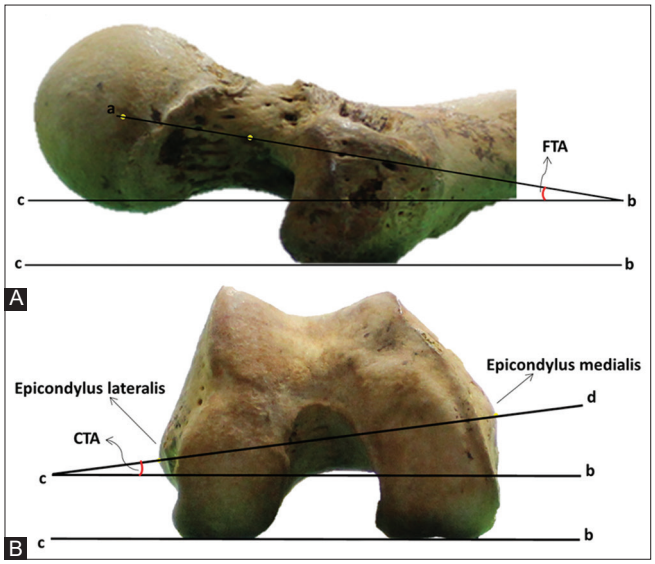

Figure 3: (A) Craniocaudal image, (B) condylar images. ab: Neck axis of the femur, cb: Posterior condylar axis of the femur, cd: Transepicondylar axis of the femur, FTA: Femoral torsion angle, CTA: Condylar twist angle

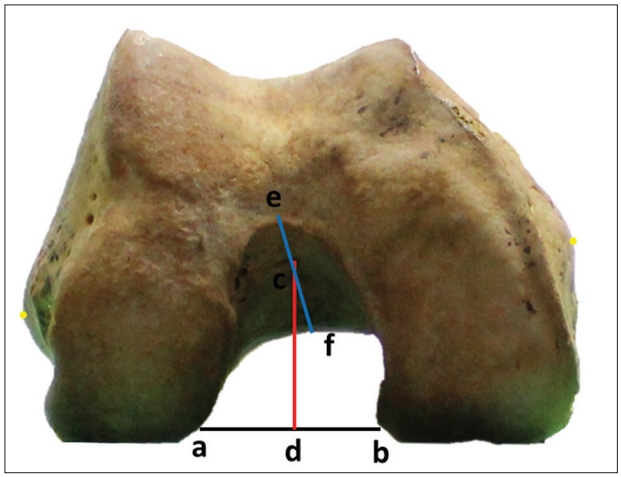

Figure 4: Intercondylar fossa dimensions. ab: Width of the intercondylar fossa, cd: Depth of the intercondylar fossa, ef: Anteroposterior diameter of the intercondylar fossa

Table 1: Mean and standard deviations of the angular parameters of the femur (°) and - intercondylar fossa parameters (mm)

Parameters	Side		
	Right (*n*=36), mean±SD	Left (*n*=38), mean±SD	Total (*n*=74), mean±SD
Angular parameters of the femur (°)			
NSA	129.47±6.70	127.08±5.98	128.24±6.41
FTA	8.42±6.38	8.91±8.60	8.67±7.55
CTA	5.40±3.00	4.38±2.17	4.87±2.64
aLDFA*	82.12±3.52	87.78±6.23	85.02±5.81
mLDFA*	87.05±3.88	93.84±6.12	91.02±5.89
MAA	5.93±0.98	6.07±0.92	6.00±0.94
AFBA	15.98±3.01	14.75±3.79	15.35±3.46
LFBA			
Right (*n*=28)	3.79±3.40	4.04±4.10	3.86±3.56
Left (*n*=11)			
MFBA			
Right (*n*=8)	3.70±2.63	5.81±3.68	5.33±3.55
Left (*n*=27)			
ICF parameters (mm)			
ICFW	21.92±2.92	22.43±3.19	22.18±3.05
ICFap	23.82±2.31	23.70±2.09	23.76±2.19
ICFD	25.77±2.27	25.16±2.17	25.46±2.22

*P<0.001 (the difference between right and left side). *n*: Number of cases, ICF: Intercondylar fossa, NSA: Neck shaft angle, FTA: Femoral neck torsion/anteversion angle, aLDFA: Anatomical lateral distal femoral angle, mLDFA: Mechanical lateral distal femoral angle, MAA: Mechanical –anatomical axis angle, AFBA: Anterior femoral bowing angle, LFBA: Lateral femoral bowing angle, MFBA: Medial femoral bowing angle, CTA: Condylar twist angle, ICFD: Deepth of the ICF, ICFap: Anteroposterior diameter of the ICF, ICFW: Widht of the ICF, SD: Standard deviation

Table 2: Correlation coefficients between angular parameters of the femur and intercondylar fossa parameters

ICF parameters	Angular parameters of the femur								
	NSA	FTA	CTA	aLDFA	mLDFA	MAA	AFBA	LFBA	MFBA
ICFW									
Right	0.027	0.172	−0.120	0.339*	0.330*	−0.090	0.452*	0.058	0.528
Left	0.032	−0.053	0.096	0.238	0.223	−0.129	0.065	0.160	−0.140
Total	0.013	0.037	−0.037	0.271*	0.264*	−0.018	0.203	0.090	0.045
ICFap									
Right	0.130	−0.264	−0.030	0.078	0.069	−0.009	0.129	0.076	0.402
Left	−0.050	0.060	0.036	0.080	0.114	0.219	−0.004	−0.407	0.279
Total	0.052	−0.081	0.003	0.051	0.66	0.097	0.060	−0.059	0.329
ICFD									
Right	0.110	−0.088	−0.278	0.231	0.252	−0.168	0.229	−0.162	0.472
Left	−0.029	0.052	−0.160	−0.034	−0.000	0.227	−0.016	−0.493	0.051
Total	0.069	−0.012	−0.193	−0.016	−0.013	0.185	0.130	−0.218	0.140

*P<0.05. ICF: Intercondylar fossa, NSA: Neck shaft angle, FTA: Femoral neck torsion/anteversion angle, CTA: Condylar twist angle, aLDFA: Anatomical lateral distal femoral angle, mLDFA: Mechanical lateral distal femoral angle, MAA: Mechanical–anatomical axis angle, AFBA: Anterior femoral bowing angle, LFBA: Lateral femoral bowing angle, MFBA: Medial femoral bowing angle, ICFW: Width of the ICF, ICFap: Anteroposterior diameter of the ICF, ICFD: Depth of the ICF

with narrower dimensions may reduce the visibility of the side walls of the fossa, especially when viewed from the anterolateral portal, which may affect knee surgery.[4] In addition, the ICF has been reported to be more advantageous than the condylar reference for determining the depth of distal femoral resection in total knee arthroplasty, and the thickness of the distal femoral osteotomy recorded using computer navigation for total knee arthroplasty is more consistent in the intercondylar notch region.[7] The present study investigated the relationship between ICF dimensions and femoral angular characteristics, which affect both hip and knee joint mechanics.

In our study, ICFW was 22.18 ± 3.05 mm, ICFap was 23.76 ± 2.19 mm and ICFD was 25.46 ± 2.22 mm, and the side difference was not statistically significant [Table 1]. van Eck *et al*.[4] mentioned three types of shape features (A, U, W

shape) for ICF and reported that type A fossa is narrower. In the same study, both ICF width and ICF height (depth) were found to be lower than in our study for all shapes.[4] Petermann *et al*.[18] found the ICF depth to be 3.4 cm and the ICF width to be 2.63 cm, which were greater than our findings. The same study reported that the gender difference in ICF dimensions was not significant.[18] Murshed *et al*.[3] studied 200 knee joints of people aged 18–78 years on MRI images and showed that ICF sizes were smaller in women and that ICF sizes decreased with age. Farrow *et al*.[6] reported that ICF depth was lower in women. In their study, 200 dry femurs were used and the ICF depth was measured to be 23.3 mm in all cases, which is close to our results.[6] In the literature, the ratio of ICF width to femoral condyle width is defined as NWI (notch width index).[2] A previous study compared patients with ACL injuries to healthy individuals and showed that the NWI was significantly lower in those with ligament damage.[2] Wada *et al*.[5] measured the ICF width to be 9.00 mm and the ICF depth to be 20.00 mm in cases without ACL. These results are smaller than our study results. In the same study, the ICF depth was measured to be 25.00 mm in patients with grade 3 and 4 osteoarthritis, and this finding is compatible with our study.[5] Measurement differences between our study and other studies may be due to differences in materials and methods. Our study was conducted on dry bones, and the lack of cartilage structure in dry bones may cause measurements to differ from other studies.

When examining the relationship between femoral angular characteristics and ICF dimensions; NSA and FTA are important femoral angular parameters that influence hip and knee joint motion characteristics. The NSA is the angle formed between the femoral neck axis and the femoral body axis and averages 135° (125–140).[1] It is also known in the literature as the collodiaphyseal angle or the inclination angle.[15,16] This angle increases in cerebral palsy, polio, hip dislocation, and congenital subluxation and decreases in the slipped capital femoral epiphysis, Perthes disease, intertrochanteric fracture, and congenital coxa vara.[19] It has been reported that NSA above 134.4° poses a serious risk of the knee joint osteoarthritis.[12] Another study reported that there was no association between the ACL rupture and the NSA.[20] The FTA is the angle formed between the femoral neck axis and the line passing behind the femoral condyles in the axial plane and averages 10°–15°.[1] Abnormal conditions associated with FTA can lead to femoroacetabular impingement, hip joint dysplasia, and hip joint osteoarthritis.[21] If the FTA is larger than normal, it causes the femoral head to look further forward in the acetabulum, and in this case, the thigh is brought into internal rotation to ensure hip joint harmony. It has been stated that internal rotation of the femur affects the knee joint kinematics, creating a risk of cruciate ligament injury.[11] In addition, it was reported that lower-than-normal FTA causes varus alignment in the knee joint and increases the risk of medial knee osteoarthritis.[22]

In our study, the mean NSA was 128.06° ±6.50° and the mean FTA was 8.74° ±7.32°, and the side difference for both parameters was not statistically significant [Table 1]. No significant correlation was found between both NSA and FTA and ICF parameters [Table 2]. Few studies have examined the relationship between NSA and FTA and ICF parameters.[15,16] These studies were observed to be methodologically similar to our study. In the study performed by Babacan and Deniz[15] on 33 dry femurs, the average NSA was 134.11°, FTA was 17.28°, ICFW was 18.61 mm and ICFD was 23.23 mm. The NSA and FTA values in their study were larger than our results, while the ICFW and ICFD were smaller. In the same study, no correlation was found between NSA, FTA, and ICF parameters, similar to our study.[15] Şenol[16] examined 65 dry femurs and found no correlation between NSA and ICF parameters, but unlike our study, there was a moderate positive correlation between FTA (anteversion angle-AA in their study) and ICF height (depth).

CTA is an angular characteristic of the distal femur and is the angle between the transepicondylar axis and the posterior condylar axis.[10] This angle also affects the rotational geometry of the distal femur. Changes in the rotational geometry of the distal femur may cause conditions such as knee pain, patellofemoral instability, and knee osteoarthritis.[23]

The mean CTA was found to be 4.87° ±2.64° and the side difference was not significant in our study [Table 1]. Cieliński *et al*.[24] examined CT images of 75 patients and found that the average CTA was 6.4° and was reported to be greater in women than in men. In the study performed by Chang *et al*.,[23] CT images of 211 individuals were examined, and the average CTA was found to be 7.4° in normal individuals, 10.2° in those with valgus knee joint, and 6.6° in those with varus knee joint. It has been stated that cartilage erosion occurs in the medial femoral condyle when the knee joint is varus and in the lateral femoral condyle when the knee joint is valgus.[23] Therefore, a large CTA can cause lateral knee osteoarthritis, and a small CTA can cause medial knee osteoarthritis. The results of these two studies were larger than our study, and it was thought that this might be due to differences in materials and methods. No significant correlation was found between CTA and ICF parameters in our study [Table 2]. In the literature review, no study was found that examined the relationship between CTA and ICF dimensions.

aLDFA and mLDFA were defined as the lateral angle between the anatomical and mechanical axis of the femur and the line passing through the distal articular surface of the femoral condyles, respectively.[9,17] MAA is the angle between the anatomical and mechanical axes or the difference between aLDFA and mLDFA.[25,26] It has been emphasized that these angular parameters are particularly

important in determining the angle of distal femoral resection in total knee arthroplasty.[26] A neutral alignment is aimed by performing a resection perpendicular to the mechanical axes of the femur and tibia in total knee arthroplasty. In order for this procedure to be successful, care must be taken that the resection angle is the same as the MAA.[25]

The mean aLDFA was 85.02° ±5.81°, mLDFA was 91.02° ±5.89°, and MAA was 6.00° ±0.94° in our study [Table 1]. Our results were similar to those of previous studies.[27,28] Side differences for aLDFA and mLDFA were statistically significant, and these parameters were greater on the left side [Table 1]. There was no significant correlation between MAA and ICF parameters, but aLDFA and mLDFA parameters showed a positive correlation with ICFW both on the right side and in all cases [Table 2]. Accordingly, low aLDFA and mLDFA can lead to the narrowing of the ICF, which can increase the risk of knee osteoarthritis and ACL injury. In the literature review, no study was found that examined the relationship between these parameters and the ICF dimensions.

It is seen that the body of the femur is generally not straight, but is curved both anteriorly and laterally (medially or laterally). Anterolateral curvature of the femoral shaft has been associated with atypical femoral fractures and the level of this fracture.[29] In addition, this slope also affects the position of the intramedullary guide and implant placed for distal femoral resection in total knee arthroplasty.[28] Among these curvatures, the angle formed by the anterior curvature in the sagittal plane is defined as the sagittal FBA (sFBA), and the angle formed by the lateral curvatures in the coronal plane is defined as the coronal FBA (cFBA).[28] In the literature, it is also referred to as the AFBA instead of the sFBA and the LFBA instead of the cFBA.[30] Since the curvature of the femoral shaft in the sagittal plane is anterior in all bones, the angle created by this curvature was defined as AFBA in our study. The femoral body is inclined medially or laterally in the coronal plane. The medial tilt angle was accepted as negative, the lateral tilt angle was accepted as positive, and both angles together were defined in the literature as the FBA.[13] In our study, if the curvature in the coronal plane was outward, it was defined as LFBA, and if it was inward, it was defined as MFBA, and it was observed that 39 femurs had lateral curvature and 35 femurs had medial curvature [Table 1].

The mean AFBA was 15.35° ±3.46°, LFBA was 3.86° ±3.56°, and MFBA was 5.33° ±3.55°, and the side difference for these parameters was not statistically significant [Table 1]. While the AFBA value in our study was compatible with the sFBA value (15.08 ± 3.79) in the radiographic study of Bao *et al*.,[28] it was greater than the AFBA value (9.7 ± 2.3) in the radiographic study of Maruyama *et al*.[30] In our study, the inclinations of the femoral body in the coronal plane were considered separately as LFBA and MFBA. Since both aspects are evaluated together in the literature, no comparison has been made in terms of LFBA and MFBA. While there was no correlation between anterior, lateral, and medial bowing angles and ICF parameters in all cases and on the left side, a moderate positive correlation was found between AFBA and ICFW on the right side in this study [Table 2]. According to this finding, the decrease in the anterior curvature of the femoral shaft may cause the ICF to become narrower. This increases the risk of ACL injury and osteoarthritis of the knee joint. No study was found in the literature that analyzed the relationship between these parameters and ICF parameters.

There were very few studies in the literature that examined the relationship between ICF parameters and femoral angular parameters. In fact, no study was found that examined the relationship between many angular parameters and the ICF. This situation limits the discussion in this study. At the same time, this study was carried out on dry bones. Due to the lack of cartilage structure on the articular surface in dry bones, there may be differences between measurements on cadaver and radiological images and measurements on dry bones. For this reason, it was thought that similar studies on radiological images and cadavers were needed to obtain better results.

Conclusion

As a result, this study showed that the anteroposterior diameter and depth of the ICF are not related to the angular characteristics of the femur, and the width of the ICF may be affected by some angular characteristics of the femur. A positive correlation was found between the angles defined as aLDFA, mLDFA, and AFBA and the ICF width. If these angles are small, it may cause narrowing of the ICF, which may predispose to ACL injury and knee osteoarthritis. The results of this study may help guide orthopedic surgeons in the evaluation of patients with knee joint problems and knee surgeries such as total knee arthroplasty and cruciate ligament reconstruction.

Financial support and sponsorship

This study was supported by the Ataturk University BAP unit (scientific research project unit).

Conflicts of interest

There are no conflicts of interest.

References

1. Standring S. Grays Anatomy: The Anatomical Basis of Clinical Practice. 41st ed. New York: Elsevier Limited; 2016. p. 1362, 1390.
2. Hoteya K, Kato Y, Motojima S, Ingham SJ, Horaguchi T, Saito A, *et al.* Association between intercondylar notch narrowing and bilateral anterior cruciate ligament injuries in athletes. Arch Orthop Trauma Surg 2011;131:371-6.
3. Murshed KA, Ciçekcibaşi AE, Karabacakoğlu A, Seker M, Ziylan T. Distal femur morphometry: A gender and bilateral

comparative study using magnetic resonance imaging. Surg Radiol Anat 2005;27:108-12.
4. van Eck CF, Martins CA, Vyas SM, Celentano U, van Dijk CN, Fu FH. Femoral intercondylar notch shape and dimensions in ACL-injured patients. Knee Surg Sports Traumatol Arthrosc 2010;18:1257-62.
5. Wada M, Tatsuo H, Baba H, Asamoto K, Nojyo Y. Femoral intercondylar notch measurements in osteoarthritic knees. Rheumatology (Oxford) 1999;38:554-8.
6. Farrow LD, Chen MR, Cooperman DR, Victoroff BN, Goodfellow DB. Morphology of the femoral intercondylar notch. J Bone Joint Surg Am 2007;89:2150-5.
7. Liu DW, Martinez Martos S, Dai Y, Beller EM. The femoral intercondylar notch is an accurate landmark for the resection depth of the distal femur in total knee arthroplasty. Knee Surg Relat Res 2022;34:32.
8. Chen LP, Chang TK, Huang TY, Kwok TG, Lu YC. The correlation between lateral bowing angle of the femur and the location of atypical femur fractures. Calcif Tissue Int 2014;95:240-7.
9. Cherian JJ, Kapadia BH, Banerjee S, Jauregui JJ, Issa K, Mont MA. Mechanical, anatomical, and kinematic axis in TKA: Concepts and practical applications. Curr Rev Musculoskelet Med 2014;7:89-95.
10. Wright SJ, Boymans TA, Grimm B, Miles AW, Kessler O. Strong correlation between the morphology of the proximal femur and the geometry of the distal femoral trochlea. Knee Surg Sports Traumatol Arthrosc 2014;22:2900-10.
11. Kaneko M, Sakuraba K. Association between femoral anteversion and lower extremity posture upon single-leg landing: Implications for anterior cruciate ligament injury. J Phys Ther Sci 2013;25:1213-7.
12. Coskun Benlidayi I, Guzel R, Basaran S, Aksungur EH, Seydaoglu G. Is coxa valga a predictor for the severity of knee osteoarthritis? A cross-sectional study. Surg Radiol Anat 2015;37:369-76.
13. Kim JM, Hong SH, Kim JM, Lee BS, Kim DE, Kim KA, *et al.* Femoral shaft bowing in the coronal plane has more significant effect on the coronal alignment of TKA than proximal or distal variations of femoral shape. Knee Surg Sports Traumatol Arthrosc 2015;23:1936-42.
14. Shepstone L, Rogers J, Kirwan JR, Silverman BW. Shape of the intercondylar notch of the human femur: A comparison of osteoarthritic and non-osteoarthritic bones from a skeletal sample. Ann Rheum Dis 2001;60:968-73.
15. Babacan S, Deniz M. Femur morphometry and correlation between proximal and distal parts. Cukurova Med J 2022;47:50-61.
16. Şenol GT. The relationship of inclination and anteversion angles in the femur with other osteometric parameters: Femur inclination and anteversion angle. IJCMBS 2023;3:82-8.
17. Kenneth A, Krockow M. The measurement and analysis of axial deformity at the knee. Mahwah, New Jersey: Homer Skyter centre, Skyter; 2008.
18. Petermann J, Reinecke J, Ishaque BA, Walthers EM, Gotzen L. Practice-orientated classification of the intercondylar fossa of the knee joint. Eur J Trauma 1999;25:215-3.
19. Isaac B, Vettivel S, Prasad R, Jeyaseelan L, Chandi G. Prediction of the femoral neck-shaft angle from the length of the femoral neck. Clin Anat 1997;10:318-23.
20. Devgan A, Barman C, Malhotra M, Rohilla R, Yadav P. Evaluation of risk factors of anterior cruciate ligament (ACL) injury: A prospective comparative analysis. Indian J Orthop 2018;4:354-61.
21. Botser IB, Ozoude GC, Martin DE, Siddiqi AJ, Kuppuswami S, Domb BG. Femoral anteversion in the hip: Comparison of measurement by computed tomography, magnetic resonance imaging, and physical examination. Arthroscopy 2012;28:619-27.
22. Puthumanapully PK, Harris SJ, Leong A, Cobb JP, Amis AA, Jeffers J. A morphometric study of normal and varus knees. Knee Surg Sports Traumatol Arthrosc 2014;22:2891-9.
23. Chang MJ, Jeong HJ, Kang SB, Chang CB, Yoon C, Shin JY. Relationship between coronal alignment and rotational profile of lower extremity in patients with knee osteoarthritis. J Arthroplasty 2018;33:3773-7.
24. Cieliński Ł, Kusz D, Wójcik M, Kamiński J, Kusz M. Variation in the posterior condylar angle. Ortop Traumatol Rehabil 2016;18:549-61.
25. Deakin AH, Basanagoudar PL, Nunag P, Johnston AT, Sarungi M. Natural distribution of the femoral mechanical-anatomical angle in an osteoarthritic population and its relevance to total knee arthroplasty. Knee 2012;19:120-3.
26. Nam D, Maher PA, Robles A, McLawhorn AS, Mayman DJ. Variability in the relationship between the distal femoral mechanical and anatomical axes in patients undergoing primary total knee arthroplasty. J Arthroplasty 2013;28:798-801.
27. ALShammari SA, Choi KY, Koh IJ, Kim MS, In Y. Total knee arthroplasty in femoral bowing: Does patient specific instrumentation have something to add? A randomized controlled trial. BMC Musculoskelet Disord 2021;22:321.
28. Bao Z, Qiao L, Qin J, Xu J, Zhou S, Chen D, *et al*. The assessment of femoral shaft morphology in the sagittal plane in Chinese patients with osteoarthritis-a radiographic analysis. J Orthop Surg Res 2017;12:127.
29. Lee YK, Yeom J, Jang BW, Nho JH, Suh YS, Koo KH. Reliability of measuring lateral bowing angle of the femur in patients with atypical femur fractures. J Orthop Surg (Hong Kong) 2019;27:1-5.
30. Maruyama M, Feinberg JR, Capello WN, D'Antonio JA. The Frank stinchfield award: Morphologic features of the acetabulum and femur: Anteversion angle and implant positioning. Clin Orthop Relat Res 2001;393:52-65.

Original Article

A Cadaveric Investigation of Human Middle Meningeal Artery Variations and their Clinical Significance

Abstract

Introduction: The middle meningeal artery (MMA) is a critical blood vessel supplying the dura mater of the skull. While traditionally described with a consistent origin, recent studies suggest anatomical variations exist. This study aimed to investigate these variations in human cadavers and assess their clinical significance. **Materials and Methods:** A series of 46 human cadaver heads were dissected. The MMA course, origin (maxillary artery or other sources), and branching patterns were documented. The data were statistically analyzed to determine the prevalence of each variation. Clinical implications of the variations, particularly for neurosurgical procedures and interpretation of neuroimaging, were explored. **Results:** The study identified a spectrum of MMA variations. The most common origin was the maxillary artery 50%, but variations including accessory branches and origins from the accessory meningeal artery 27% or ascending pharyngeal artery 13% were observed. The course and branching patterns also displayed variability, with 10%. These findings were statistically analyzed to determine the significance of each variation. The clinical significance of the variations was discussed, highlighting potential challenges during surgical procedures such as skull base surgeries and the need for careful preoperative imaging evaluation. **Conclusion:** This cadaveric study revealed a significant degree of variation in the human MMA anatomy. Understanding these variations is crucial for neurosurgeons, radiologists, and other health-care professionals to ensure safe and accurate surgical planning and interpretation of neuroimaging studies.

Keywords: *Artery, cadaver, meningeal artery, variation*

Abhimanu Kumar, Nidhi Puri[1], V. V. G. Patnaik[2], Pratibha Gupta[3]

Department of Anatomy, Ram Krishna Medical College Hospital and Research Centre, Bhopal, Madhya Pradesh, [1]Department of Anatomy, AIIMS, Bilaspur, Himachal Pradesh, [2]Department of Anatomy, MMIMSR, Ambala, Haryana, [3]Department of Anatomy, GIMSH, Durgapur, West Bengal, India

Introduction

The middle meningeal artery (MMA) is one of the most important arteries supplying the dura mater, the tough, protective outer layer of the brain. It is typically found on either side of the head, arising from the maxillary artery, a major branch of the external carotid artery. However, the origin and course of the MMA can vary significantly from person to person. Cadaveric studies can be used to study the variations of the MMA. In a cadaveric study, researchers dissect the head-and-neck region of a deceased donor to examine the anatomy of the blood vessels, including the MMA. This type of study can provide valuable information about the normal anatomy of the MMA as well as the variations that can occur. By understanding the variations of the human MMA, doctors can better plan for surgery, diagnose and treat conditions such as head trauma, and develop new treatments for neurological disorders. Understanding these variations is crucial for neurosurgeons, as the MMA is a major source of bleeding during intracranial surgeries. Variations of the MMA origin in about half of all cases, the MMA has an accessory meningeal artery arising from it. Less commonly, the ophthalmic artery, which supplies blood to the eye, may arise as a branch of the MMA. In rare cases, the MMA may originate from the internal carotid artery (ICA), the ophthalmic artery, or the lacrimal artery.[1] The course of MMA typically courses upward through the foramen spinosum, a hole in the sphenoid bone, and then enters the middle cranial fossa. From there, it divides into anterior and posterior branches that supply the dura mater of the frontal, temporal, and parietal lobes of the brain. The course of the MMA can vary depending on its origin. For example, if the MMA arises from the ICA, it may course through the carotid canal along with the ICA. Clinical significance: Variations in the origin and course of the MMA can have important clinical implications. For example, knowledge of these variations is essential for neurosurgery:[2] As mentioned earlier,

How to cite this article: Kumar A, Puri N, Patnaik VV, Gupta P. A cadaveric investigation of human middle meningeal artery variations and their clinical significance. J Anat Soc India 2024;73:341-6.

Article Info

Received: 03 June 2024
Revised: 16 July 2024
Accepted: 11 August 2024
Available online: 28 December 2024

Address for correspondence:
Dr. Abhimanu Kumar, Department of Anatomy, Ram Krishna Medical College Hospital and Research Centre, Bhopal - 462 042, Madhya Pradesh, India.
E-mail: akanatomyresearch@gmail.com

Access this article online

Website: https://journals.lww.com/joai

DOI: 10.4103/jasi.jasi_76_24

Quick Response Code:

the MMA is a major source of bleeding during intracranial surgeries. If a surgeon is not aware of a variation in the MMA's anatomy, they may accidentally injure the artery and cause serious bleeding. Interventional neuroradiology: Interventional neuroradiologists use minimally invasive techniques to treat conditions such as brain aneurysms and arteriovenous malformations. Understanding the variations of the MMA is important for these procedures as well, as the MMA can be involved in some of these conditions. Head trauma: The MMA can be damaged in head trauma, which can lead to epidural hematomas, a collection of blood between the dura mater and the skull. Knowing the location of the MMA can help doctors diagnose and treat epidural hematomas.

Injuries to middle meningeal artery

Injuries to the MMA are most commonly caused by head trauma, such as from a car accident, fall, or assault. When the MMA is injured, it can bleed, leading to a serious condition called an epidural hematoma.

Epidural hematoma

An epidural hematoma is a collection of blood between the dura mater (the tough, outer layer of the brain) and the skull. It can cause a variety of symptoms, including headache, nausea, vomiting, confusion, seizures, and coma. If left untreated, an epidural hematoma can be fatal.

Symptoms of an epidural hematoma

The symptoms of an epidural hematoma can vary depending on the size and location of the bleed. However, some of the most common symptoms include:

- Headache: This is usually the first symptom of an epidural hematoma. The headache may be severe and worsen over time
- Nausea and vomiting
- Confusion
- Drowsiness
- Seizures
- Weakness or paralysis on one side of the body
- Loss of consciousness.[3]

Treatment of an epidural hematoma

Treatment for an epidural hematoma typically involves surgery to remove the blood clot and stop the bleeding. In some cases, medication may be used to reduce swelling in the brain.

Other injuries of the middle meningeal artery

- Subdural hematoma: This is a collection of blood between the dura mater and the arachnoid mater, the middle layer of the meninges
- Intracerebral hemorrhage: This is bleeding within the brain tissue itself
- Arteriovenous fistula: An abnormal connection between an artery and a vein
- Aneurysm: A ballooning out of the wall of the artery.

Variations of middle meningeal artery

There are variations in both the origin and course of the MMA. Understanding these variations is crucial for neurosurgeons, as the MMA is a major source of bleeding during intracranial surgeries.

Variations of origin

- Accessory meningeal artery: In about half of all cases, the MMA has an accessory meningeal artery arising from it
- Ophthalmic artery: Less commonly, the ophthalmic artery, which supplies blood to the eye, may arise as a branch of the MMA
- Rare origins: In rare cases, the MMA may originate from the ICA, the ophthalmic artery, or the lacrimal artery.[4]

Variations of course

The MMA typically courses upward through the foramen spinosum, a hole in the sphenoid bone, and then enters the middle cranial fossa. From there, it divides into anterior and posterior branches that supply the dura mater of the frontal, temporal, and parietal lobes of the brain. The course of the MMA can vary depending on its origin. For example, if the MMA arises from the ICA, it may course through the carotid canal along with the ICA.

Materials and Methods

Sources of research data were obtained from PubMed and Google Scholar databases. The article search was limited to the English language. The 46 Skull (with Meningeal) cadaveric specimen was obtained from the Department of Anatomy, Ram Krishna Medical College Hospital and Research Centre, Bhopal, willed body program intended for the purpose of medical student dissection. This case report is based on the dissection of a 50–75-year-old male and female donor of Bhopal region.[5]

Instrument

Hammer, Scalpel, Surgical Blade, Cotton, Surgical Gloves, Tooth Forceps, Blunt Forceps, cotton

Specimens

This study utilized a series of 46 human cadaver heads obtained from a reputable anatomical donation program or institutional morgue.

Inclusion criteria for the cadaver heads could include:

- Age range (e.g., adults 50–75 years old)
- Absence of known cranial trauma or neurological disorders.

Dissection technique

- Dissection was performed under proper sterile conditions

- Soft tissues of the face and scalp were reflected to expose the cranium
- The infratemporal fossa was carefully dissected to identify the maxillary artery and its branches
- The MMA was traced from its origin at the maxillary artery to its entry point through the foramen spinosum of the sphenoid bone
- Within the cranium, the MMA's course, branching patterns.

Data collection

Standardized data collection forms were used to record detailed observations about the MMA anatomy. This could include:

- Origin (variations from the maxillary artery)
- Course (e.g., straight, tortuous)
- Foramen spinosum size and shape
- Branching patterns (anterior, posterior, accessory branches)
- Presence of anatomical anomalies (e.g., duplicated MMA, hypoplastic MMA).

Classification of variations

Established anatomical nomenclature was employed to classify the observed variations in the MMA. References to existing classification systems for MMA variations can be cited here.

Statistical analysis

- Descriptive statistics was used to report the prevalence of each type of MMA variation
- Depending on the research question, appropriate statistical tests (e.g. Chi-square test) could be performed to assess potential associations between specific variations and relevant clinical parameters.[6]

Discussion

This cadaveric investigation of the human MMA [Figures 1 and 3] and its variations has provided valuable insights into the clinical significance of anatomical deviations from the typical course. The observed prevalence of 30% variations underscores the necessity for surgeons to be aware of this anatomical variability during procedures involving the cranium.

Figure 1: Superior view of maningial artery

Clinical implications of variations

- Discuss the potential impact of identified variations on surgical approaches. For example, a tortuous MMA course might necessitate a modified craniotomy for safe access to underlying structures
- Explore how specific variations could influence intraoperative complications. For instance, the presence of an accessory meningeal artery might increase the risk of bleeding during tumor resection
- Briefly mention any observed variations that might have implications for neurological outcomes. For example, a hypoplastic MMA could potentially limit blood flow to the dura mater and contribute to postoperative complications.

Comparison to existing research

- Compare your findings with previous cadaveric studies on MMA variations. Discuss any similarities or discrepancies in the prevalence of specific variations reported in the literature
- Acknowledge any limitations of existing research, such as a lack of focus on clinical significance. Explain how your study addresses this gap by exploring the potential impact of variations on surgical procedures and patient outcomes.

Strengths and limitations

- Highlight the strengths of your cadaveric approach, such as the ability to directly visualize and measure anatomical structures
- Acknowledge the inherent limitations of cadaveric studies. These may include:
  - Potential differences in vascular anatomy between living humans and cadavers
  - Inability to assess the functional consequences of variations on blood flow dynamics
- Mention the limitations of your specific study design, such as sample size or potential selection bias in the cadaver population.[7]

Future directions

Propose future research directions to build upon your findings. This could involve:

- Utilizing advanced imaging techniques, such as angiography, to investigate the functional implications of specific variations in living patients
- Conducting larger-scale clinical studies to establish definitive correlations between MMA variations and surgical outcomes
- Investigating the potential link between MMA variations

and susceptibility to specific neurological conditions, such as epidural hematomas.[8]

Review of Literature

A strong foundation for your cadaveric investigation requires a review of existing literature on MMA variations. Here is a roadmap to get you started.

Prevalence of variations

- Discuss the established understanding of MMA origin and course as presented in standard anatomical texts
- Cite relevant studies that have documented the frequency of variations in origin (e.g., ophthalmic artery and persistent stapedial artery) and course within the middle cranial fossa.[9]

Clinical significance

- Highlight the importance of precise MMA anatomy knowledge in neurosurgical procedures, emphasizing the risks of vascular injury and bleeding during skull base or meningeal surgeries if variations are undetected
- Discuss the role of MMA variations in neurointerventional procedures such as embolization for intracranial hemorrhage. Explain how variations might influence catheter navigation
- Mention the association of MMA rupture with head trauma, particularly in children.

Limitations of existing literature

- Identify any gaps in current knowledge regarding MMA variations
- Mention limitations of previous studies, such as small sample size, or a lack of data on specific variations you plan to investigate.[10]

Search resources

- Utilize medical databases such as PubMed, Scopus, and Web of Science
- Search for terms such as "middle meningeal artery variations," "MMA anatomy variations," and "clinical significance of MMA variations,".
- Reference key neuroanatomy textbooks and relevant articles published in neurosurgical journals.[11]

Din Klisoveic *et al*. Variations of the MMA Significance for Surgery and Practice We examined 186 macerated skulls (128 male and 58 female).[18] Variations were classified into nine types. Some of the previously ignored communications of the branches of MMA with other arteries of the external carotid systems such as the deep temporal a., deep auricular a., occipital a., and anterior tympanic a., are described.[12]

Anna MAFS *et al*. Anatomy of the MMA is a relevant structure for the understanding of neurosurgical diseases.[19] In conclusion, every neurosurgeon must know the anatomy of the MMA sufficiently to correlate it with the diagnosed pathology, thus obtaining treatment effectiveness and preventing brain lesions.[13]

Bonasia *et al*. The MMA is the major human dural artery. Its origin and course can vary a great deal in relation, not only with the embryologic development of the hyostapedial system, but also because of the relationship of this system with the ICA, ophthalmic artery, trigeminal artery, and inferolateral trunk.

Results

Investigation

- This study likely uses cadavers (deceased human bodies) to examine variations in the MMA
- The MMA supplies blood to the skull's lining (meninges). Understanding its variations is crucial for neurosurgeons.

Variations

- The study might report how often the MMA deviates from its usual origin point (typically a branch of the maxillary artery)
- It could explore other variations in size, branching patterns, or course within the skull.

Clinical significance

- Knowing these variations is important because the MMA can be damaged during head injuries
- Unusual anatomy can make surgery more complex or increase bleeding risk during procedures near the artery
- The study might highlight specific variations that surgeons should be aware of for improved patient outcomes.[14]

The describes nine variations (Type I–IX) in the branching patterns of the MMA, a blood vessel supplying the skull. The MMA typically divided into three branches:

- Frontal branch: Supplies the upper part of the skull
- Parietal branch: Supplies the side of the skull
- Petrosquamous branch: Supplies the lower part of the skull.

The most common pattern (Type I, 50% of cases) has well-developed frontal and parietal branches, with the petrosquamous branch being underdeveloped and located near the base of the skull [Figures 2 and 3].

Here is a breakdown of the less frequent variations (Types II–IX):

- Type II (22%): Well-developed petrosquamous branch, with a missing or very small parietal branch
- Type III (7%): Two separate, high-positioned parietal branches
- Type IV (6%): Parietal branch originates low and curves upward. Underdeveloped petrosquamous branch
- Type V (5%): Single or double petrosquamous branches present with a combined parieto-petrosquamous trunk
- Type VI (5%): Both branches are positioned high in their respective regions

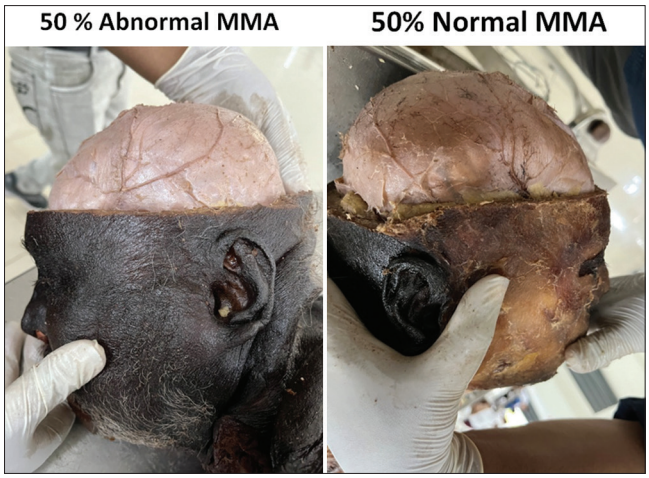

Figure 2: Lateral view of maningial artery (Right & Left)

- Type VII (3%): Parietal branch along the middle ridge, with an absent or near-base petrosquamous branch
- Type VIII (1%): Rare and unique pattern where the ophthalmic artery (another head artery) contributes to the branching
- Type IX (1%): Similar to Type VIII, the ophthalmic artery supplies only the frontal branch, while the other branches arise normally from the MMA.

Conclusion

This cadaveric investigation into the variations of the human MMA has shed light on the prevalence and clinical significance of these anatomical deviations. Our findings demonstrate that the MMA course and origin exhibit a wider range of variability than previously described in textbooks.

Key points regarding variations

- The origin of the MMA displayed a notable departure from the textbook description, with a significant portion arising from sources other than the maxillary artery
- The course of the MMA within the middle cranial fossa also deviated from the standard anatomical description, presenting in various configurations.[15]

Clinical significance

These variations hold considerable importance in several clinical scenarios:

- Neurosurgery: Precise knowledge of MMA location and course is crucial during surgical procedures on the skull base and meninges. Unidentified variations could increase the risk of vascular injury and bleeding
- Neurointervention: Minimally invasive procedures such as endovascular embolization for treating intracranial hemorrhage require detailed understanding of the MMA's course to navigate catheters safely and effectively
- Head Trauma: MMA rupture is a serious complication of head trauma, particularly in children. Awareness of potential variations can aid in diagnosing and managing these injuries.[16]

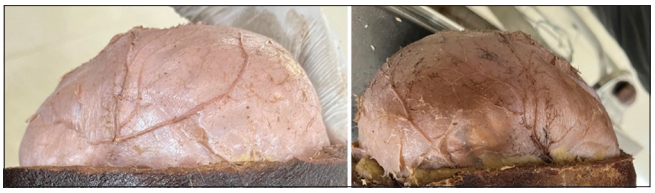

Figure 3: Lateral view of middle maningeal artery

Future directions

Further research avenues based on this study include:

- Developing a larger dataset to confirm the prevalence of the observed variations
- Investigating the potential impact of these variations on blood flow patterns within the skull
- Correlating specific MMA variations with clinical outcomes in patients undergoing relevant procedures.[17]

By incorporating the findings from this study and future investigations, anatomical references and surgical guidelines can be refined to account for the spectrum of human MMA variations. This will ultimately enhance patient safety and improve outcomes in neurosurgical procedures, neurointerventions, and management of head trauma.

Financial support and sponsorship

Nil.

Conflicts of interest

There are no conflicts of interest.

References

1. Salamon G, Faure J, Raybaund C, Grisoli F. The external carótida internal. In: Newton, Potts DG. Radiology of The Skull Brain. Angiography. New York, United States: Mosby CVSaint Louis; 1974. p. 1246-75.
2. Goss CM. Gray Anatomia. 29th ed. Rio de Janeiro Guanabara Koogan; 1977.
3. Kainz J, Stammberger H. The roof of the anterior ethmoid: A place of least resistance in the skull base. Am J Rhinol 1989;3:191-9.
4. Newton TH. The anterior and posterior meningeal branches of the vertebral artery. Radiology 1968;91:271-9.
5. Royle G, Motson R. An anomalous origin of the middle meningeal artery. J Neurol Neurosurg Psychiatry 1973;36:874-6.
6. Ustun ME, Buyukmumcu M, Ulku CH, Guney O, Salbacak A. Transzygomatic-subtemporal approach for middle meningeal-to-P2 segment of the posterior cerebral artery bypass: An anatomical and technical study. Skull Base 2006;16:39-44.
7. Vasconcelos C, Xavier J, Almeida-Pinto J, Cruz R. Vascularization of the skull base – Review of the literature and illustrative cases. Acta Med Port 2001;14:33-42.
8. Richter HP, Schachenmayr W. Preoperative embolization of intracranial meningiomas. Neurosurgery 1983;13:261-8.
9. Penfield W, McNaughton F. Dural headache and innervation of the Dura mater. Arch Neurol Psychiatry 1940;44:43-75.

10. Maeda S, Aizawa Y, Kumaki K, Kageyama I. Variations in the course of the maxillary artery in Japanese adults. Anat Sci Int 2012;87:187-94.
11. Fiorella D, Arthur AS. Middle meningeal artery embolization for the management of chronic subdural hematoma. J Neurointerv Surg 2019;11:912-5.
12. Haldrup M, Ketharanathan B, Debrabant B, Schwartz OS, Mikkelsen R, Fugleholm K, *et al*. Embolization of the middle meningeal artery in patients with chronic subdural hematoma-a systematic review and meta-analysis. Acta Neurochir (Wien) 2020;162:777-84.
13. Plummer SC. III. Research on the surgical anatomy of the middle meningeal artery. Ann Surg 1896;23:540-72.
14. Margolis MT, Newton TH. Collateral pathways between the cavernous portion of the internal carotid and external carotid arteries. Radiology 1969;93:834-6.
15. Shah A, Choudhri O, Jung H, Li G. Preoperative endovascular embolization of meningiomas: Update on therapeutic options. Neurosurg Focus 2015;38:E7.
16. Link TW, Boddu S, Marcus J, Rapoport BI, Lavi E, Knopman J. Middle meningeal artery embolization as treatment for chronic subdural hematoma: A case series. Oper Neurosurg (Hagerstown) 2018;14:556-62.
17. Dubel GJ, Ahn SH, Soares GM. Contemporary endovascular embolotherapy for meningioma. Semin Intervent Radiol 2013;30:263-77.
18. Klisović D, *et al*. Variations of the middle meningeal artery: Significance for surgery and practice. First published: 1993;6:28994.
19. Muzumdar D, *et al*. Neurosurgery in the Past and Future. An Appraisal, Ann Med Surg (Lond) 2012;1:135.

Original Article

Standardization of the Klingler Dissection Technique at 3400 m above Sea Level

Herminia Naveda, Yuri Vargas, Juan Condori, Alexander Montesinos[1], Franklin Miranda, Carlos Virto[1], Cristabel Rivas[1], Lugo Miranda, Yvan Gallegos[2], Iris Peralta[2], Hesed Virto-Farfan[1,2]

Basic Science and Amphitheater Laboratories, Andean University of Cusco, [1]Neuroscience Research Center (CENEURO), Andean University of Cusco, [2]Neuroscience Research Circle, Andean University of Cusco, Cusco, Peru

Abstract

Introduction: This study aimed to evaluate the efficacy of different formaldehyde concentrations (5%, 8%, and 10%) on the Klingler dissection technique, specifically in the context of high-altitude (3400 m above sea level) bovine brain preparation. **Methods:** Forty bovine brains were prepared using various Klingler methods and were distinguished by formaldehyde concentrations. The brains were subjected to a standardized process of fixation, freezing, thawing, and dissection. The evaluation criteria included the ease of meningeal removal, tissue consistency, and the degree of encephalic tissue degradation, assessed through a Likert scale. The statistical analysis involved analysis of variance tests for group comparisons and Spearman correlations to explore relationships between evaluation metrics. The Ethics Committee of the Andean University of Cusco approved the protocol by RESOLUCIÓN N° 021-2023-VRIN-UAC. **Results:** Formaldehyde concentrations of 5% and 10% were significantly more effective than the 8% concentration at facilitating meningeal removal, enhancing tissue consistency, and reducing encephalic tissue degradation. Notably, the 5% concentration demonstrated superior outcomes in terms of dissection quality and tissue color preservation. Statistically significant differences were observed between groups, with *post hoc* analyses indicating that the 5% and 10% groups were superior to the 8% group. **Conclusions:** The Klingler technique revealed that a 5% formaldehyde concentration is most conducive for high-altitude bovine brain dissection. This concentration optimizes tissue preservation and dissection quality, potentially offering insights for anatomical studies and educational practices. Future research should explore the applicability of these results to human brain anatomy and consider additional environmental and procedural variables.

Keywords: *Brain anatomy, fiber dissection, Klingler, Klingler method, white matter*

Introduction

Neuroscience has become an important part of medical knowledge and has been the basis for understanding pharmacologic, surgical, psychiatric, and even technological advances. Neuroanatomy is an important topic in this field. However, neurophobia[1] (fear of clinical neurology caused by the inability to apply theoretical knowledge to practical clinical situations) has been observed not only among students but also among almost 30%[2] to 36%[3] of graduate physicians. The most important tools for approaching neuroanatomy have been the use of three-dimensional teaching tools and peer teaching tools,[4] which are part of any brain dissection technique but are particularly useful for the Klingler technique.

The COVID-19 pandemic has significantly affected the quality of neuroanatomy education in human medicine, particularly in practice. A survey involving 117 directors from American medical schools highlighted a marked reduction in hands-on learning, clinical correlations, and radiology teaching due to the pandemic, with 79% noting a negative impact on learning quality. This was attributed to reduced interactive learning and a lack of dissection opportunities. Similarly, a study from the University of Zaragoza revealed 74% student dissatisfaction with online neuroanatomy teaching, primarily due to interaction and connectivity issues. Teachers unanimously believed that in-person attendance was crucial for effective learning.

We must remember that the brain's white matter consists of myelinated nerve fibers. When these fibers share the same start and end points, they cluster into compact bundles known as fascicles or tracts. Diffusion magnetic resonance

How to cite this article: Naveda H, Vargas Y, Condori J, Montesinos A, Miranda F, Virto C, *et al.* Standardization of the Klingler dissection technique at 3400 m above sea level. J Anat Soc India 2024;73:347-52.

Article Info

Received: 07 May 2024
Revised: 25 May 2024
Accepted: 18 November 2024
Available online: 28 December 2024

Address for correspondence:
Dr. Hesed Virto-Farfan, Neuroscience Research Center (CENEURO), Andean University of Cusco, Cusco, Peru.
E-mail: hesedvirto@gmail.com

Access this article online

Website: https://journals.lww.com/joai
DOI: 10.4103/jasi.jasi_58_24
Quick Response Code:

imaging (dMRI) allows noninvasive mapping of these axon orientations, facilitating the exploration of white matter anatomy and cortical connections. However, these tracts through dMRI have already been confirmed by anatomical dissection.

Klingler's method of brain dissection, developed in 1935, has been a valuable tool for understanding the complex anatomical organization of cerebral hemispheres.[5] Klingler's work has had a significant impact on neuroscience, particularly in the field of neurosurgery, and has been influential in the development of stereotactic neurosurgery.[6] Currently, the predominant methods for anatomical dissection of white matter are based on variations of the original technique introduced by Klingler in 1935.[7] This method involves three key phases: first, extracting and fixing the brain; second, freezing a specimen; and third, thawing this specimen before dissecting the white matter tracts. Klingler described the first step in which 5% formalin solution was used for 4 weeks, the temperature was adjusted to −8°C to −10°C for 8 days, and the tissue was preserved during dissection in a 5% solution.[7]

However, multiple protocols have been used with different concentrations and durations of treatment. There are several protocols for accessing 4% formaldehyde solution,[8,9] 5% formaldehyde solution,[10,11] and 10% formaldehyde solution.[12-15]

The aim of the present study was to compare different formaldehyde concentrations in bovine brains measured via the Klingler Dissection Technique at 3400 m above sea level.

Methods

Materials and specimens

40 brains were extracted from bovine specimens since January 2023 to March 2023 according to the Klingler method.[7] The skin and skull were removed. Both cranial nerves and vessels were cut in an anterior-posterior fashion to extract the whole brain, including the brainstem and cerebellum, as shown in Figure 1. Careful cuts were made on the bony surface of the coil head with an emery cutter to avoid damaging the encephalic tissue.

Protocol

We separated the 39 brains into 3 groups at different concentrations of formaldehyde (5%, 8%, and 10%). The hermetic flasks were prepared for each group. The same 3 steps of fixation, freezing, and thawing were used for each group, but only the concentrations of the solutions were varied. Time and the rest of the variables were obtained from the Dziedzic literature review.[9]

Fixation

Fixation started 1–3 h after the death of the animal. For fixation, specimens were placed in 3 formalin solutions.

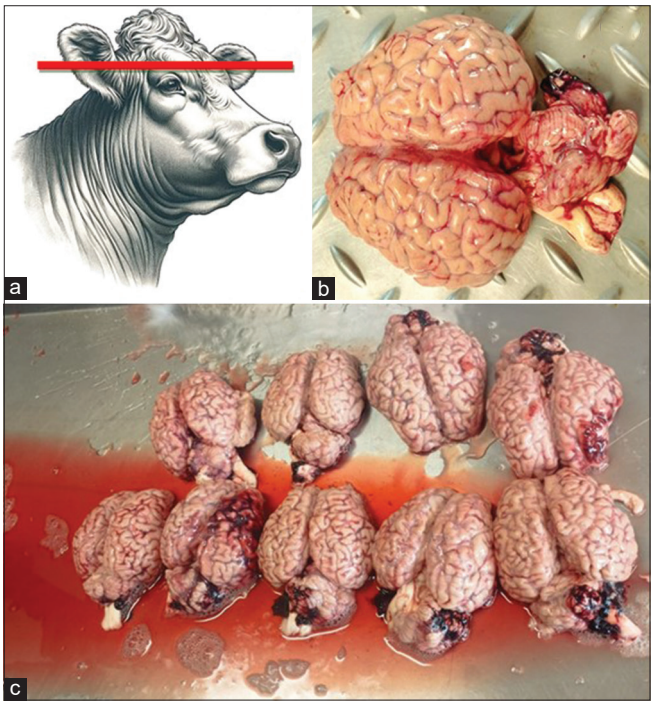

Figure 1: Bovine brain extraction. (a) Cutoff point for brain extraction, (b) Bovine brain before the start of Klingler technique, (c) Multiple brains extracted

The time for fixation was 4 weeks, and the formaldehyde solutions were changed every 2 weeks because when the brains were placed in the containers, they eventually released water and lipids, altering the concentrations. To avoid brain deformity during the fixation process, the brains were placed on gauze within the formalin solution and allowed to float freely. We subsequently washed out the formalin before starting the freezing steps. The reaction was performed with running water for 2 h for 2 days.

Freezing

Then, the formalized tissue was subjected to a temperature of 10°C–12°C below zero until it took rise to a brown color after approximately 9–10 days. The sections were covered entirely with plastic film. This process allows brain tissue, especially white fibers, to take on a nonsoft consistency and separate nerve fibers easily.

Thawing and dissection

Thawing was completed at room temperature under running water for 2–4 h. After thawing and during dissections, the specimen was kept in formalin. Finally, to perform the Klingler method, different equipment is used, the most important of which are detailed in Figure 2.

Microbiological analysis

The plastic containers containing the brains were identified in 5%, 8%, and 10% formaldehyde, and samples were taken from the surface and bottom of each container. The 5%, 8%, and 10% formaldehyde samples were cultured on

blood agar, salted mannitol, MacConkey, and Sabouraud plates. The culture media were incubated at a Temperature of 37°C for 24 and 48 h, and the other Sabouraud media were incubated at room temperature for 10 days for the development of filamentous fungi. Direct examination of the different concentrations of formaldehyde was performed to determine the presence of protozoa. This can be observed in Figure 3.

Evaluation of the brains

The success of each treatment was evaluated by assessing the difficulty of meningeal removal, the consistency of the encephalic tissue, and the degree of encephalic tissue degradation on a Likert scale ranging from 1 to 5. The difficulty level of meningeal removal was as follows: 1 – extremely difficult removal of the meninges to 5 – extremely easy removal of the meninges. The consistency level of the encephalic tissue was as follows: 1 – lower consistency of encephalic tissue to 5 – increased consistency of encephalic tissue. The level of encephalic tissue degradation was as follows: 1 – increased degradation of encephalic tissue to 5 – decreased degradation of encephalic tissue.

Sample

For the calculation of sample size, an *a priori* analysis was performed for tests of differences between more than 2 independent groups with the following parameters: effect size = 0.52, α levels = 0.05, power of contrast $1-\beta = 0.80$, and number of groups = 3. According to the software G*Power 3.1.9.7, SPSS (Statistical Package for the Social Sciences) is developed by IBM Corporation, based in Armonk, New York, United States which was developed by the University of Dusseldorf, a sample of 13 encephalons was obtained from each group, for a total of 39 samples for the experimental study.

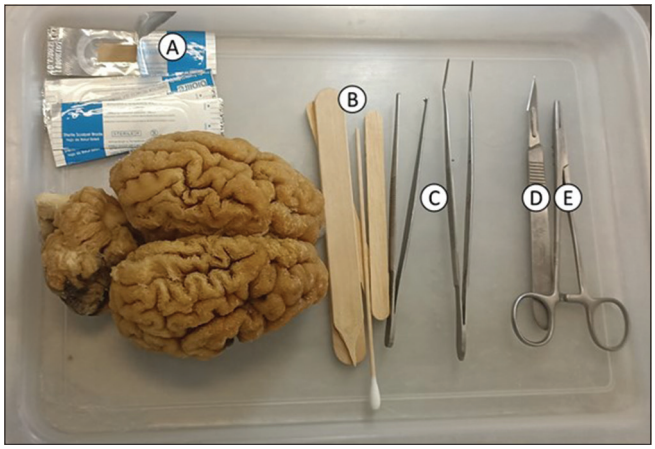

Figure 2: Equipment for performing the Klingler method. (A) Bisturi no 11, (B) Wooden paddles and Swab sticks, (C) Dissecting forceps, (D) Scalpel handle, (E) Needle holder

Results

The 39 brains achieved the final state of the Klingler technique without any missing tissue. The descriptive statistics of the difficulty level of meningeal removal, consistency level of encephalic tissue, and level of encephalic tissue degradation on a Likert scale ranging from 1 to 5 are shown in Table 1.

Analysis of variance was performed to determine the significance of the differences between groups [Table 2]. A significant difference was found between the groups, as shown in Figure 4, particularly between the 10% and 5% groups, which were similar to the 8% group. A *post hoc* analysis of Tukey's test was performed, where statistically significant differences were observed between these groups, as shown in Table 3. Finally, strong Spearman correlations were observed between the 3 measures, as shown in Table 4.

Observations

During the dissection for analysis of the degradation and consistency of the encephalic materials, we observed that the 10% group had a darker color than the 5% group [Figure 5]. Additionally, 5% of the patients in the group with the highest malleability for dissection of internal structures had fewer problems dissecting the internal configuration [Figure 6].

Microbiological analysis

After incubating for 72 h, no bacterial colonies developed, as indicated by the absence of filamentous fungi and yeasts in the Sabouraud cultures.

Discussion

The best groups had formaldehyde concentrations of 5% and 10%. However, the 5% group had better properties during the dissection step and a better color at the end of the technique.

The interpretation of the results obtained in this study sheds light on the significant impact of formaldehyde concentrations on the efficacy of the Klingler dissection technique, especially when applied to bovine brains at an altitude of 3400 m above sea level. By comparing three

Figure 3: Microbiological analysis

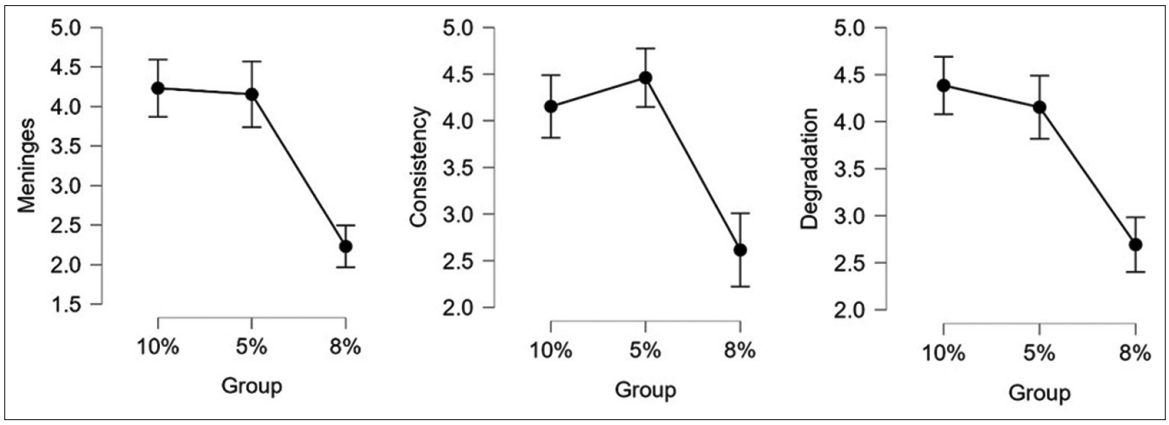

Figure 4: Analysis of variance test graphics

Table 1: Descriptive statistics

	Meninges			Consistency		Degradation		
	10%	**8%**	**5%**	**10%**	**8%**	**10%**	**8%**	**5%**
Median	4	2	4	4	3	4	3	4
Mean	4.231	2.231	4.154	4.154	2.615	4.385	2.692	4.154
SD	0.599	0.439	0.689	0.555	0.65	0.506	0.48	0.555
IQR	1	0	1	0	1	1	1	0
Shapiro–Wilk	0.766	0.533	0.811	0.733	0.772	0.628	0.592	0.733
P value of Shapiro–Wilk	0.003	<0.001	0.009	0.001	0.003	<0.001	<0.001	0.001

SD: Standard deviation, IQR: Interquartile range

Table 2: ANOVA test results

Cases	Sum of squares	df	Mean square	*F*	*P*
ANOVA - meninges					
Group	33.385	2	16.692	48.825	<0.001
Residuals	12.308	36	0.342		
ANOVA - consistency					
Group	25.436	2	12.718	38.154	<0.001
Residuals	12	36	0.333		
ANOVA - degradation					
Group	21.897	2	10.949	41.323	<0.001
Residuals	9.538	36	0.265		

Table 3: *Post hoc* comparisons - group

Evaluation criteria	%	Mean difference	SE	*t*	P_{tukey}
Meninges					
10%	5%	0.077	0.229	0.335	0.94
10%	8%	2	0.229	8.721	<0.001
5%	8%	1.923	0.229	8.385	<0.001
Consistency					
10%	5%	−0.308	0.226	−1.359	0.373
10%	8%	1.538	0.226	6.794	<0.001
5%	8%	1.846	0.226	8.152	<0.001
Degradation					
10%	5%	0.231	0.202	1.143	0.494
10%	8%	1.692	0.202	8.382	<0.001
5%	8%	1.462	0.202	7.239	<0.001

SE: Standard error

different concentrations of formaldehyde (5%, 8%, and 10%), the present study revealed statistically significant differences in several crucial aspects.

The study revealed that the 10% and 5% concentrations of formaldehyde presented similar and superior results compared to the 8% concentration in terms of ease of removal of meninges and tissue consistency. These results are particularly relevant because proper tissue preparation is critical for effective dissection and detailed visualization of brain structures. Efficient removal of the meninges without damaging the underlying tissue is a critical step in anatomic dissection, while adequate tissue consistency facilitates accurate dissection and minimizes damage to delicate brain structures.

The lower tissue degradation observed in the 10% and 5% groups suggested that these concentrations are more effective at preserving the integrity of brain tissue, which is essential for high-quality anatomical and neuroscientific studies. Tissue degradation not only hinders dissection and visualization of brain structures but also may compromise the validity of studies that rely on accurate brain morphology.

Other studies have already used a 5% formaldehyde concentration in Italy[16] to evaluate the arcuate fasciculus, superior and inferior longitudinal fasciculus, corona radiata, extreme and external capsule, claustrum, anterior commissure, and internal capsule. Additionally, in Turkey,[10] the corona radiata and tapetum were dissected. Using a similar solution technique in France,[17] myelin

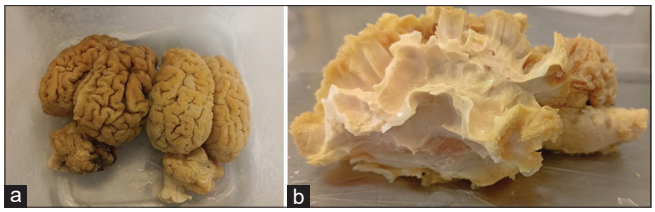

Figure 5: Images of groups 5% and 10%. (a) Left brain corresponds to the 10% concentration, right brain to the 5% concentration, (b) the dissection of white matter corresponds to the 5% group

Table 4: Spearman's correlations

	Spearman's rho	*P*	Effect size (Fisher's *Z*)
Meninges - consistency	0.669***	<0.001	0.808
Meninges - degradation	0.704***	<0.001	0.875
Consistency - degradation	0.714***	<0.001	0.895

***P<0.001

sheaths were preserved, allowing the maintenance of axonal integrity via the same preparation. Additionally, in France, six fiber tracts, such as the long, anterior, and posterior segments of the superior longitudinal fasciculus, the inferior fronto-occipital fasciculus, the inferior longitudinal fasciculus, and the uncinate fasciculus, have been reconstructed from cadaveric dissection.[18] Finally, our results confirm the use of the original Klingler technique with 5% formaldehyde[7,11] and similar times and concentrations at 3400 m above sea level.

The ultimate aim of fixation is to swiftly and evenly preserve the structure of cells and tissues, inhibit proteolytic enzymes, reinforce the specimen for subsequent steps, and guard against microbial contamination and decay.[19-21] However, we have observed that if the formaldehyde solution is not gradually changed, the fixation process displaces water, lipids, and intracellular material in the solution, giving rise to a biofilm on which microorganisms can grow. After the COVID-19 pandemic, we observed, to our surprise, that the cadavers we had left in the formaldehyde wells possessed an extensive layer of fungi and microorganisms in a superior biofilm film.

Clinically, high-altitude hypoxia exposure causes neurological deficits via formaldehyde accumulation.[22] However, this property at high altitudes might explain why a lower concentration of formaldehyde is more effective at 3400 m above sea level. The 5% and 10% groups showed better results than the 8% group; however, the 5% group was easily dissected and had a better color at the end of the protocol. Other tissue analyses at simulated high altitudes have shown that lower formaldehyde concentrations are needed for fixation (4%).[23]

High-altitude protocol

At high altitude, the best protocol should be as follows: fixation started 1–3 h after the death of the animal.

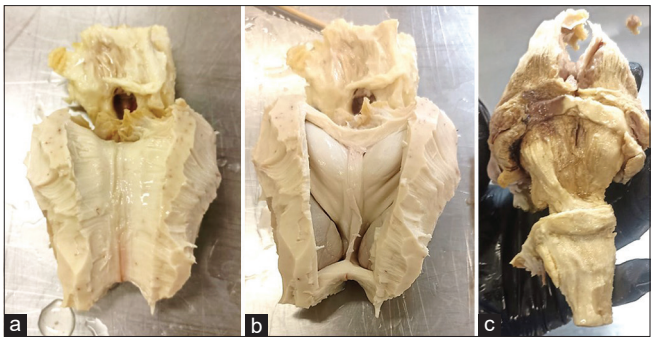

Figure 6: Dissection of the 5% group. (a) White matter configuration, (b) internal configuration, (c) Brainstem

A concentration of 5% formaldehyde was used. The time for fixation was 4 weeks, and the formaldehyde solution was changed every 2 weeks. To avoid brain deformity during the fixation process, the brain must be placed on gauze within the formalin solution and float freely. Afterward, the sections were washed out of formalin before the freezing steps started (2 h for 2 days). After freezing, the temperature must be 10°C–12°C below zero until it becomes brown, at approximately 9-10 days. The brain was covered entirely with plastic film. Thawing and dissection were performed at room temperature under running water for 2–4 h. After thawing and during dissections, the specimen was kept in 5% formalin.

Limitations

Nevertheless, it is imperative to acknowledge that while the findings of this study offer insightful guidance regarding the optimization of formaldehyde concentrations for the preparation of neural tissue, the direct application of these findings to clinical or educational contexts necessitates a cautious approach. The extrapolation of results derived from bovine cerebral specimens to human cerebral anatomy mandates a comprehensive examination of interspecies anatomical and histological variances. Moreover, the observed impact of altitude on the experimental outcomes underscores the potential significance of environmental variables in the preparation of neural tissue, warranting additional investigations to elucidate these effects comprehensively. Investigating the impact of other variables, such as fixation time and the need to mesh formaldehyde containers, on tissue preparation could be beneficial for further optimizing dissection protocols.

The Klingler dissection method is an important tool in research and is the basis for visualizing otherwise invisible fasciculi. For example, in combination with new imaging techniques, Klingler dissection has improved the visualization of longitudinal fascicules 2 and 3.[24]

Conclusions

The study compared the effects of different formaldehyde concentrations (5%, 8%, and 10%) on the Klingler

dissection technique, specifically for bovine brains at an altitude of 3400 m. In conclusion, 5% and 10% formaldehyde solutions yield superior outcomes in terms of ease of meningeal removal, tissue consistency, and reduced encephalic tissue degradation compared to the 8% solution. A 5% concentration, in particular, offers the best results during dissection, preserves tissue color more effectively, and facilitates the dissection of the internal ganglia. These findings suggest that environmental factors, such as altitude, significantly impact the effectiveness of tissue fixation and dissection processes. This study proposes an optimized high-altitude protocol that includes a 5% formaldehyde concentration for fixation and specific procedures for freezing and thawing, aimed at minimizing brain tissue deformation and ensuring effective dissection.

Acknowledgments

This study was funded by Universidad Andina del Cusco. We would like to express our gratitude to Micaela Rosaluz Manchego Jayo, Luciana Andrea Collantes Siancas, Luis Alejandro Montesinos Guerra, and Rosselyn Paloma Medina Velasco for their invaluable assistance in organizing the samples during the course of the study.

Financial support and sponsorship

This study was funded by Universidad Andina del Cusco RESOLUCIÓN N.° 183-CU-2023-UAC.

Conflicts of interest

There are no conflicts of interest.

References

1. Jozefowicz RF. Neurophobia: The fear of neurology among medical students. Arch Neurol 1994;51:328-9.
2. Saldaña-Inda I, Cisneros-Gimeno AI, Lambea-Gil A. Neurophobia among resident physicians in the emergency service. Rev Neurol 2023;77:285-91.
3. McDonough A, Chishimba L, Chomba M, Zimba S, Mwendaweli N, Asukile M, *et al.* Neurophobia in Africa: Survey responses from fifteen African countries. J Neurol Sci 2022;434:120161.
4. Sotgiu MA, Mazzarello V, Bandiera P, Madeddu R, Montella A, Moxham B. Neuroanatomy, the Achille's heel of medical students. A systematic analysis of educational strategies for the teaching of neuroanatomy. Anat Sci Educ 2020;13:107-16.
5. Wysiadecki G, Clarke E, Polguj M, Haładaj R, Żytkowski A, Topol M. Klingler's method of brain dissection: Review of the technique including its usefulness in practical neuroanatomy teaching, neurosurgery and neuroimaging. Folia Morphol (Warsz) 2019;78:455-66.
6. Agrawal A, Kapfhammer JP, Kress A, Wichers H, Deep A, Feindel W, *et al.* Josef Klingler's models of white matter tracts: Influences on neuroanatomy, neurosurgery, and neuroimaging. Neurosurgery 2011;69:238-52.
7. Klingler J. Facilitating macroscopic preparation of the brain through the freezing process. Zurich, Switzerland; 1935.
8. Sincoff EH, Tan Y, Abdulrauf SI. White matter fiber dissection of the optic radiations of the temporal lobe and implications for surgical approaches to the temporal horn. J Neurosurg 2004;101:739-46.
9. Dziedzic TA, Balasa A, Jeżewski MP, Michałowski Ł, Marchel A. White matter dissection with the Klingler technique: A literature review. Brain Struct Funct 2021;226:13-47.
10. Yakar F, Eroglu U, Peker E, Armagan E, Comert A, Ugur HC. Structure of corona radiata and tapetum fibers in ventricular surgery. J Clin Neurosci 2018;57:143-8.
11. Klingler J, Gloor P. The connections of the amygdala and of the anterior temporal cortex in the human brain. J Comp Neurol 1960;115:333-69.
12. Di Carlo DT, Benedetto N, Duffau H, Cagnazzo F, Weiss A, Castagna M, *et al.* Microsurgical anatomy of the sagittal stratum. Acta Neurochir (Wien) 2019;161:2319-27.
13. Baran O, Baydin S, Gungor A, Balak N, Middlebrooks E, Saygi T, *et al.* Surgical approaches to the thalamus in relation to the white matter tracts of the cerebrum. World Neurosurg 2019;128:e1048-86.
14. Capilla-Guasch P, Quilis-Quesada V, Regin-Neto M, Holanda VM, González-Darder JM, de Oliveira E. White matter relationships examined by transillumination technique using a lateral transcortical parietal approach to the atrium: Three-dimensional images and surgical considerations. World Neurosurg 2019;132:e783-94.
15. Flores-Justa A, Baldoncini M, Pérez Cruz JC, Sánchez Gonzalez F, Martínez OA, González-López P, *et al.* White matter topographic anatomy applied to temporal lobe surgery. World Neurosurg 2019;132:e670-9.
16. Bertolini G, La Corte E, Aquino D, Greco E, Rossini Z, Cardia A, *et al.* Real-time *ex-vivo* magnetic resonance image-guided dissection of human brain white matter: A proof-of-principle study. World Neurosurg 2019;125:198-206.
17. Zemmoura I, Blanchard E, Raynal PI, Rousselot-Denis C, Destrieux C, Velut S. How Klingler's dissection permits exploration of brain structural connectivity? An electron microscopy study of human white matter. Brain Struct Funct 2016;221:2477-86.
18. Zemmoura I, Serres B, Andersson F, Barantin L, Tauber C, Filipiak I, *et al.* FIBRASCAN: A novel method for 3D white matter tract reconstruction in MR space from cadaveric dissection. Neuroimage 2014;103:106-18.
19. Franco-Duarte R, Černáková L, Kadam S, Kaushik KS, Salehi B, Bevilacqua A, *et al.* Advances in chemical and biological methods to identify microorganisms-from past to present. Microorganisms 2019;7:130.
20. Latini F, Hjortberg M, Aldskogius H, Ryttlefors M. The use of a cerebral perfusion and immersion-fixation process for subsequent white matter dissection. J Neurosci Methods 2015;253:161-9.
21. Werner M, Chott A, Fabiano A, Battifora H. Effect of formalin tissue fixation and processing on immunohistochemistry. Am J Surg Pathol 2000;24:1016-9.
22. Wang X, Sun H, Cui L, Wang X, Ren C, Tong Z, *et al.* Acute high-altitude hypoxia exposure causes neurological deficits via formaldehyde accumulation. CNS Neurosci Ther 2022;28:1183-94.
23. Langmeier M, Maresová D. Intermittent hypobaric hypoxia during development--morphological and functional changes in the neocortex. Prague Med Rep 2005;106:275-82.
24. Taçyıldız AE, Barut O, Üçer M, Özgündüz Y, Bozyiğit B, Tanriover N. Improving the visualization of superior longitudinal fascicule-2 and superior longitudinal fascicule -3 using photoshop filters. World Neurosurg 2024;185:e1136-43.

Original Article

Gender- and Age-based Measurement of Morphometric Parameters around the Hip Joint: A Radiographic Study

Mohd. Arif Makdoomi, Shaheen Shahdaad, Javeed Ahmad Khan, Ghulam Mohammad Bhat, R Aijaz Ahmad Hakeem

Department of Anatomy, Government Medical College, Srinagar, Jammu and Kashmir, India

Abstract

Purpose: Morphometric parameters of structures around the hip joint are essential for surgeries around the area. The present study aimed to determine the mean values of the distance between the tip of the greater trochanter to the superior edge of the acetabulum and the mean values of medial femoral offset. **Materials and Methods:** Normal plain radiographs (anteroposterior view) of the pelvis with bilateral hip joints of 200 people between 20 and 50 years of age were used for the study. The X-rays were from (a) Patients complaining of Lower back ache or pain in the hip, who had no joint pathology based on radiological examination, (b) Patients of age group 20–50 years, and (c) Patients without any deformity of the hip joint. **Results:** The mean distance values between the tip of the greater trochanter to the superior margin of the acetabulum in females in 100 X-rays on the right side was 23.34 ± 1.25 mm, and on the left side, it was 23.04 ± 1.58 mm. In males, the mean value of this parameter in 100 X-rays on the right side was 25.83 ± 1.65 mm; on the left side, it was 25.31 ± 1.39 mm. All the above findings were statistically significant ($P < 0.001$). The mean values of medial femoral offset on the right side in females in 100 X-rays were 35.27 ± 2.22 mm; on the left, it was 35.01 ± 2.19 mm. In males, the mean value of this parameter in 100 X-rays on the right side was 38.62 ± 3.26 mm; on the left side, it was 36.52 ± 3.16 mm. All the above findings were statistically significant with $P < 0.001$. **Conclusion:** The results calculated provide essential information about gender, age, and side variations of the mean values of the distance between the tip of the greater trochanter to the superior edge of the acetabulum and the mean values of medial femoral offset for anatomists, radiologists, and orthopedic surgeons.

Keywords: *Acetabular margin, greater trochanter, hip joint arthroplasty, medial femoral offset*

Introduction

The hip joint is essential in the body owing to its stability and multi-axial nature. Its importance is increased as it may get involved in numerous pathologies and traumatic conditions such as the fracture neck of the femur and dislocation of the hip, which are widespread conditions, particularly in older people. Knowledge about the different morphometric parameters of the head and different dimensions of the neck of the femur is essential for orthopedic surgery. If not properly treated, these conditions may lead to malunion or nonunion, which can cause limping. The weight-bearing joints of the lower limb are more stable. The hip joint allows the same movements as the mobile shoulder joint, but the range of actions is restricted.[1] The hip joints are usually radiographed in the posterior view, with the heels slightly separated and the toes symmetrically directed forwards and medially. The femora are rotated somewhat medially in this position, but the femoral necks parallel the film.[2] As the greater trochanter is an essential landmark for the intraoperative limb length assessment, the distance between the superior edge of the acetabulum and the tip of the greater trochanter may minimize limb length discrepancy.[3]

Medial femoral offset

Medial femoral offset is the distance from the center of rotation of the femoral head to a line bisecting the long axis of the femur. The radiological measurement should be accurately performed as it varies according to hip rotation. The normal femoral offset varies between 41 and 44 mm.[4] The neck shaft angle determines the size of the anatomical femoral offset.[5] A decreased femoral offset would medially move the femur closer to the pelvis. This can lead to the impingement of greater trochanter in

How to cite this article: Makdoomi MA, Shahdaad S, Khan JA, Bhat GM, Hakeem RA. Gender- and age-based measurement of morphometric parameters around the hip joint: A radiographic study. J Anat Soc India 2024;73:353-8.

Article Info

Received: 04 July 2023
Revised: 17 September 2024
Accepted: 18 November 2024
Available online: 28 December 2024

Address for correspondence:
Dr. Ghulam Mohammad Bhat, Department of Anatomy, Government Medical College, Srinagar - 190 001, Jammu and Kashmir, India.
E-mail: gmbhat144@gmail.com

Access this article online

Website: https://journals.lww.com/joai
DOI: 10.4103/jasi.jasi_68_23

Quick Response Code:

extremes of movement. The medial movement would also result in soft-tissue relaxation. Both of these factors can lead to implant instability and possible dislocation. An increase in femoral offset moves the femur laterally, resulting in decreased chances of impingement, better tension in soft tissue, and better stability. Increasing the femoral offset also addresses issues such as improving hip abductor strength and increasing the range of motion.[6,7] Problems such as limping and the need for crutches are also reduced by increasing the femoral offset.[8] It is felt that offset restoration also decreases the cup strain and polyethylene wear.[9]

Total hip arthroplasty is regarded as the operation of the 21st century and is one of the most successful and cost-effective surgical procedures.[10] However, despite the overall success of total hip arthroplasty, approximately 7%–9% of patients are not satisfied with their hip function 1 year after the surgery.[11] After performing a successful total hip arthroplasty, patient satisfaction still conflicts about whether leg length is a predictor of functional outcome.[12] More focus has been given to gender-specific implants in arthroplasty in recent years. The present implant system is sufficient to solve male and female patients' size and offset requirements.[13] Literature is scarce regarding the effect of implant position and reconstruction of the center of rotation and offset, whether femoral or acetabular, on the outcome of total hip arthroplasty.[14] The aim of the present study was to determine the mean distance between the tip of the greater trochanter and the superior edge of the acetabulum and determine the mean values of medial femoral offset.

Materials and Methods

The present hospital-based observational study was conducted in the Department of Anatomy and Radiodiagnosis and Imaging, Government Medical College, ABC. Ethical clearance of the study was obtained from the Institutional Ethical Committee vide letter No. IEC/1422/2023/38, Dated: 22-05-2019. Normal plain radiographs of the pelvis with bilateral hip joints in anteroposterior view were used to study. The participants included males and females between 20 and 50 years of age. 200 X-rays (100 males and 100 females) were reviewed.

Instruments used

The instruments used are goniometer, measuring scale, divider, and markers [Figure 1].

Inclusion criteria

X-rays of patients (20–50 years old) complaining of lower back aches or hip pain with no hip joint pathology or deformity were defined based on radiological examination.

Exclusion criteria

Patients with a history of diseases such as osteoarthritis, tuberculosis, and fractures around the hip joint and or patients having a history of surgical intervention on the proximal femur, acetabulum, or pelvis.

Figure 1: The instrument used in the study

The technique of taking X-rays

Measurements used in the present study were obtained from standard pelvic radiographs. The anteroposterior view of radiographs was used while the patient was supine, and both the lower limbs were internally rotated at 15°. The focal film distance of these radiographs was 1.2 meters. The mid-point between the two anterior superior iliac spines and the upper boundary of the symphysis pubis was used for centralization.

Radiographs having the following features were included in the study: Symmetrical obturator foramen, lateralization of the Greater Trochanter, clarity of the pyriform fossa, pubis, and coccyx in the same plane and absence of hip joint arthrosis.

Parameter measured

1. Distance between the tip of the greater trochanter and superior acetabular margin. Two points on the X-ray were marked with the help of a marker; one on the tip of the greater trochanter and another at the superior edge of the acetabulum. A line connected the two points, and this line was measured in millimeters with the help of a measuring scale. This measurement gave us the distance between the tip of the greater trochanter and the superior acetabular margin [Figure 2a]
2. Medial femoral offset: It is the distance between the center of rotation of the femoral head to a line bisecting the long axis of the femur. Three lines were marked with the help of a marker, one passing through the center of rotation of the head of the femur and another line as a long axis of the shaft of the femur. A perpendicular was drawn from the femur's center of rotation to the femur's long axis. This perpendicular distance was measured in millimeters with a measuring scale and gave us the medial femoral offset [Figure 2b].

Statistical methods

The data were entered in a Microsoft Excel spreadsheet. The categorical variables were summarized as percentages. At the same time, continuous variables were summarized as

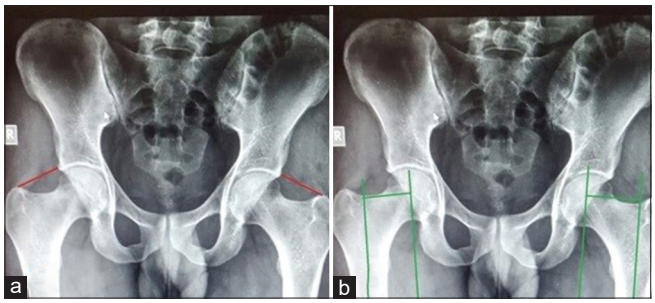

Figure 2: (a) An X-ray pelvis anteroposterior view showing the distance between the tip of the greater trochanter and superior acetabular margin, and (b) medial femoral offset

mean and standard deviation. An unpaired *t*-test was used to test whether any difference exists between male and female measurements. Measurements were compared across age groups using one-way ANOVA. Paired *t*-test was used to compare the difference in measurements between the right and left sides. Analysis was done using SPSS version 23 (IBM, Armonk, New York, USA). Two-sided *P* values were reported, and $P < 0.05$ was considered statistically significant.

Observation and Results

A total of 200 X-rays were included in the study, 100 males (50%) and 100 females (50%). All 200 X-rays were obtained from adult patients (20–50 years). Fifty-four X-rays (27%) of the total X-rays belonged to patients younger than 30. Similarly, the age group 31–40 years had 69 X-rays, making 34.5% of total X-rays. Age group 41–50 years, there were 77 X-rays (38.5%). The mean age study population was 37.3 years ± 8.7 years.

The mean distance on the right side was 24.58 ± 1.92 mm. The mean distance on the left side was 24.17 ± 1.97 mm. The mean of medial femoral offset on the right side was 36.94 ± 3.25 mm. The mean of the medial femoral offset on the left side was 35.76 ± 2.81 mm [Table 1].

The distance between the tip of the greater trochanter and the upper edge of the acetabulum and the mean values were close in both sexes' right and left hips. However, the mean values in males were about 2 mm higher than in females. The standard deviation of mean values of the right hip in females was about 1.25; on the left hip, it was 1.58. In males, there was a standard deviation of 1.65 on the right hip, and on the left hip, the standard deviation was 1.39. The association of females and males in the distance on the right and left sides was statistically significant, with a $P < 0.001$ [Table 2].

On the right side, the mean value of medial femoral offset observed in males was 38.62 mm with a standard deviation of ±3.26 and a standard error mean of 0.32. In comparison, on the left side, the medial femoral offset was 36.52 mm with a standard deviation of ± 3.16 and a standard error mean of 0.31 [Table 3].

In females, the mean value of medial femoral offset on the right side was 35.27 mm with a standard deviation of 2.22 and a standard error mean of 0.22. On the left side, the medial femoral offset was 35.01, with a standard deviation of ±2.19 and a standard error mean of 0.21. The association of females and males in MFO on the right and left sides was significant, with a $P < 0.001$ [Table 3].

These results showed that the mean value of medial femoral offset on the right side in males is higher than that of the left. While as in females, there is a slight difference in the medial femoral offset of the two sides. Furthermore, in males, the medial femoral offset on both sides is significantly higher than the mean medial femoral offset in females [Table 3].

The mean distance on the right side in the age group 20–30 years in 54 subjects was 24.81 ± 1.84 mm. The mean distance on the right side in the age group 31–40 years in 69 subjects was 24.87 ± 1.96 mm. The mean distance on the right side in the age group 41–50 years in 77 subjects was 24.16 ± 1.90 mm. The overall mean distance of all the 200 subjects on the right side was 24.58 ± 1.92 mm and was statistically insignificant with a $P = 0.052$. The overall mean distance of all the 200 subjects on the left side was 24.17 ± 1.87 mm and was not statistically significant, with a $P = 0.112$ [Table 4].

The mean MFO on the right side in the age group 20–30 years in 54 subjects was 36.70 ± 3.24 mm. The mean MFO on the right side in the age group 31–40 years in 69 subjects was

Table 1: The distribution of overall dimensions of various parameters in the study population

Parameters	Valid (*n*)	Missing (*n*)	Mean±SD	Minimum	Maximum
Distance-rt	200	0	24.58±1.92	21.0	30.0
Distance-lt	200	0	24.17±1.87	21.0	32.0
MFO-rt	200	0	36.94±3.25	31.0	47.0
MFO-lt	200	0	35.76±2.81	31.0	45.0

SD: Standard deviation, MFO: Medial femoral offset

Table 2: The association of distance with gender

	Sex	*n*	Mean	SD	SE	*P*
Distance_rt	Female	100	23.34	1.25	0.12	<0.001
	Male	100	25.83	1.65	0.16	<0.001
Distance_lt	Female	100	23.04	1.58	0.15	<0.001
	Male	100	25.31	1.39	0.13	<0.001

SE: Standard error, SD: Standard deviation

Table 3: The association of medial femoral offset with gender

	Sex	*n*	Mean	SD	SE	*P*
MFO_rt	Female	100	35.27	2.22	0.22	<0.001
	Male	100	38.62	3.26	0.32	<0.001
MFO_lt	Female	100	35.01	2.19	0.21	<0.001
	Male	100	36.52	3.16	0.31	<0.001

SE: Standard error, SD: Standard deviation, MFO: Medial femoral offset

37.62 ± 3.15 mm. The mean MFO on the right side in the age group 41–50 years in 77 subjects was 36.50 ± 3.29 mm. The overall mean MFO of all the 200 subjects on the right side was 36.94 ± 3.25 mm and was statistically insignificant with a *P* value of 0.095. The overall mean MFO of all the 200 subjects on the left side was 35.76 ± 2.81 mm and was not statistically significant, with a *P* = 0.725 [Table 5].

Discussion

The mean value of the distance from the tip of the greater trochanter to the superior margin of the acetabulum

In males, the mean value of the distance from the tip of the greater trochanter to the superior edge of the acetabulum on the right side was 25.83 ± 1.65, and on the left side, it was 25.31 ± 1.39. In females, the mean value of the distance from the tip of the greater trochanter to the superior margin of the acetabulum on the right side was 23.34 ± 1.25; on the left side, it was 23.04 ± 1.58. Thus, it was observed that there was no significant difference in the mean values on the right and left sides of both sexes, but a significant difference was observed when the corresponding values were compared with the opposite sex. Ates *et al*.[3] made a similar observation.

Medial femoral offset

Medial femoral offset values are essential in determining the abductor strength mechanism. Increasing the values improves the hip abductor strength and enhances the range of movements, thereby reducing limping and the need for crutches.[15] A computed tomography (CT) scan is the most accurate way of measuring medial femoral offset.[16] However, it is not feasible to have pre- and postoperative CT scans for the patient. Hence, plain radiography is the most cost-effective and readily available method with less radiation in evaluating the hip joint.[17,18] Restoring femoral offset after hip arthroplasty is associated with an increased range of movement and decreased postoperative complications.[19] It should also be remembered that hip rotation may influence the results of the femoral offset in plain radiographs.[20] However, since the patients with gross hip pathology were excluded from our study, this effect (e.g., impingement) did not influence our results. Significant limb length discrepancy and failure to obtain adequate femoral offset can compromise the biomechanics after total hip arthroplasty and may affect the patient's function and long-term surgical outcome.[21] It has been radiographically suggested that the hip axis and length of the femoral neck are becoming longer as years pass by, and these changes can increase the risk of fracture.[22] In our present study, the mean value of femoral offset in females was 35.27 ± 2.22 mm on the right side, and on the left side, it was 35.01 ± 2.19 mm. In males, the mean value of this parameter on the right side was 38.62 ± 3.26 mm, and on the left side, it was 36.52 ± 3.16 mm. Thus, the mean values of femoral offset observed on the right side in males were significantly higher than on the left side, whereas in females, the mean values on the two sides were

Table 4: The relationship of distance with age

	Age (years)	*n*	Mean	SD	SE	95% CI for mean		Minimum	Maximum	*P*
						Lower bound	Upper bound			
Distance_rt	≤30.0	54	24.81	1.84	0.25	24.31	25.31	21.0	30.0	0.052
	31–40	69	24.87	1.96	0.23	24.39	25.34	21.0	29.0	
	41.0+	77	24.16	1.90	0.21	23.73	24.60	21.0	28.0	
	Total	200	24.58	1.92	0.13	24.31	24.85	21.0	30.0	
Distance_lt	≤30.0	54	24.31	2.02	0.27	23.76	24.86	21.0	32.0	0.112
	31–40	69	24.44	1.85	0.22	24.00	24.89	21.0	28.0	
	41.0+	77	23.83	1.74	0.19	23.43	24.22	21.0	28.0	
	Total	200	24.17	1.87	0.13	23.91	24.43	21.0	32.0	

SE: Standard error, SD: Standard deviation, CI: Confidence interval

Table 5: The association of medial femoral offset with age

MFO	Age (years)	*n*	Mean	SD	SE	95% CI for mean		Minimum	Maximum	*P*
						Lower bound	Upper bound			
MFO_rt	≤30.0	54	36.70	3.24	0.44	35.81	37.58	31.0	47.0	0.095
	31.0–40.0	69	37.62	3.15	0.37	36.86	38.38	33.0	46.0	
	41.0+	77	36.50	3.29	0.37	35.75	37.25	31.0	46.0	
	Total	200	36.94	3.25	0.23	36.49	37.39	31.0	47.0	
MFO_lt	≤30.0	54	35.51	2.81	0.38	34.75	36.28	31.0	43.0	0.725
	31.0–40.0	69	35.92	3.24	0.39	35.14	36.70	31.0	45.0	
	41.0+	77	35.79	2.40	0.27	35.24	36.33	32.0	42.0	
	Total	200	35.76	2.81	0.19	35.37	36.15	31.0	45.0	

SE: Standard error, SD: Standard deviation, CI: Confidence interval, MFO: Medial femoral offset

almost similar. The mean values of medial femoral offset in males were correspondingly higher than in females. Analysis of medial femoral offset is still used in managing hip arthroplasty. Atkinson *et al*.[23] used 100 consecutive Caucasian patients (61 males and 39 females) to study the differences in hip morphology between the genders in patients undergoing hip resurfacing. In the study, they compared the femoral offset between the two genders. The mean medial femoral offset was 55 mm with a range of 42–68 mm, whereas in females, it was 48 mm with a range of 37–57 mm. There was no significant difference between the measurements of each patient on the right and left sides. Our study also showed similar results.

Unnanuntana *et al*.[24] studied cadaveric femora using digital photographs. They observed that the mean horizontal offset values were 42.66 ± 5.6 mm in males and 39.67 ± 6.02 mm in females, which was statistically significant and consistent with our present study. Preininger *et al*.[25] conducted a three-dimensional CT study of femoral offset in 100 subjects. They observed that the mean MFO in males was higher than in females, with a $P < 0.001$, and no side difference of femoral offset was observed in gender. Our study observed a significant difference in MFO values between the two sexes with a $P < 0.001$. The gender variation of our study is consistent with the above research, and the side variation is inconsistent. Similar observations were made by Roy *et al*.,[26] who reported a larger mean medial femoral offset in males (38.5 mm) compared to the females 35.7 mm) and is thus consistent with the present study.

Similarly, Takamatsu *et al*.[27] studied rotation center and femoral offset in 98 Japanese adults, obtaining mean values of 36.00 ± 5.8 mm for males and 33.4 ± 4.9 mm for females. This study shows a significant difference in femoral offset between the two genders, corroborating with the present study. Sengodan *et al*.[28] reported that the mean values of medial femoral offset were 39.84 mm in males and 35.40 mm in females. This difference between the two genders is statistically significant and consistent with our study. Similarly, while working on the medial femoral offset values, Ates *et al*.[3] observed a significant difference in the mean values of medial femoral offset in the two sexes.

Conclusion

The mean values of the distance between the tip of the greater trochanter to the superior edge of the acetabulum and the mean values of medial femoral offset were higher in males than in females. The gender variation of the mean value of the distance between the tip of the greater trochanter to the superior margin of the acetabulum and the mean values of medial femoral offset on both sides was statistically significant. The age variation of all the parameters on both sides was statistically insignificant. The variation reported in our study may be due to genetic, geographical, racial, and nutritional effects and physical stress. The results thus calculated provide essential information about gender, age, and side variations of these parameters around the hip joint for anatomists, radiologists, and orthopedic surgeons. Radiological knowledge of these parameters around the hip joint will help orthopedics diagnose and select various treatment modalities for fractures around the hip joint, dislocation, and other surgical procedures.

Financial support and sponsorship

Nil.

Conflicts of interest

There are no conflicts of interest.

References

1. Chaurasia BD. Human Anatomy Hip Joint Volume II; Lower Limb, Abdomen and Pelvis; 8th ed. New Delhi, India: CBS Publishers and Distributors Pvt. Ltd.; 2020. p. 162, 163. (Reprint 2021).
2. Hamilton WJ, Simon G. Surface and Radiological Anatomy for Students and General Practitioners. 4th ed. New Jersey, UK: Heffer, Rutgers University; 1958. p. 304-5.
3. Ates A, Aydin E, Maralcan G. Proximal femur morphology and radiological measurement of femuroacetabular distance. Glob J Res Anal 2019;8:2277-8160.
4. Lecerf G, Fessy MH, Philippot R, Massin P, Giraud F, Flecher X, *et al.* Femoral offset: Anatomical concept, definition, assessment, implications for preoperative templating and hip arthroplasty. Orthop Traumatol Surg Res 2009;95:210-9.
5. Charles MN, Bourne RB, Davey JR, Greenwald AS, Morrey BF, Rorabeck CH. Soft-tissue balancing of the hip: The role of femoral offset restoration. Instr Course Lect 2005;54:131-41.
6. Yamaguchi T, Naito M, Asayama I, Ishiko T. Total hip arthroplasty: The relationship between posterolateral reconstruction, abductor muscle strength, and femoral offset. J Orthop Surg (Hong Kong) 2004;12:164-7.
7. Spalding TJ. Effect of femoral offset on motion and abductor muscle strength after total hip arthroplasty. J Bone Joint Surg Br 1996;78:997-8.
8. Asayama I, Naito M, Fujisawa M, Kambe T. Relationship between radiographic measurements of reconstructed hip joint position and the Trendelenburg sign. J Arthroplasty 2002;17:747-51.
9. Devane P, Home G, Winemaker M, Bourne R, Rorabeck C. The effect of restoring femoral offset during total hip replacement on 3D volumetric wear. J Bone Joint Surg BR 1997;79 Suppl (4S):385.
10. Jenkins PJ, Clement ND, Hamilton DF, Gaston P, Patton JT, Howie CR. Predicting the cost-effectiveness of total hip and knee replacement: A health economic analysis. Bone Joint J 2013;95-B:115-21.
11. Anakwe RE, Jenkins PJ, Moran M. Predicting dissatisfaction after total hip arthroplasty: A study of 850 patients. J Arthroplasty 2011;26:209-13.
12. Whitehouse MR, Stefanovich-Lawbuary NS, Brunton LR, Blom AW. The impact of leg length discrepancy on patient satisfaction and functional outcome following total hip arthroplasty. J Arthroplasty 2013;28:1408-14.
13. Kostamo T, Bourne RB, Whittaker JP, McCalden RW, MacDonald SJ. No difference in gender-specific hip replacement

outcomes. Clin Orthop Relat Res 2009;467:135-40.
14. Müller ME. Total hip prostheses. Clin Orthop Relat Res 1970;72:46-68.
15. McGrory BJ, Morrey BF, Cahalan TD, An KN, Cabanela ME. Effect of femoral offset on range of motion and abductor muscle strength after total hip arthroplasty. J Bone Joint Surg Br 1995;77:865-9.
16. Pasquier G, Ducharne G, Ali ES, Giraud F, Mouttet A, Durante E. Total hip arthroplasty offset measurement: Is C T scan the most accurate option? Orthop Traumatol Surg Res 2010;96:367-75.
17. Mathews JD, Forsythe AV, Brady Z, Butler MW, Goergen SK, Byrnes GB, *et al.* Cancer risk in 680,000 people exposed to computed tomography scans in childhood or adolescence: Data linkage study of 11 million Australians. BMJ 2013;346:f2360.
18. Rubin PJ, Leyuraz PF, Aubaniac JM, Argenson JN, Esteve P, Roguin B. The morphology of the proximal femur. A three dimensional radiographic analysis. J Bone Joint Surg (Br) 1992;74-B: 28-32.
19. Charnley J. Total hip replacement by low-friction arthroplasty. Clin Orthop Relat Res 1970;72:7-21.
20. Maruyama M, Feinberg JR, Capello WN, D'Antonio JA. The Frank Stinchfield Award: Morphologic features of the acetabulum and femur: anteversion angle and implant positioning. Clin Orthop Relat Res 2001. p. 52-65.
21. Friberg O. Clinical symptoms and biomechanics of lumbar spine and hip joint in leg length inequality. Spine (Phila Pa 1976) 1983;8:643-51.
22. Nakamura T, Turner CH, Yoshikawa T, Slemenda CW, Peacock M, Burr DB, *et al.* Do variations in hip geometry explain differences in hip fracture risk between Japanese and white Americans? J Bone Miner Res 1994;9:1071-6.
23. Atkinson HD, Johal KS, Willis-Owen C, Zadow S, Oakeshott RD. Differences in hip morphology between the sexes in patients undergoing hip resurfacing. J Orthop Surg Res 2010;5:76.
24. Unnanuntana A, Toogood P, Hart D, Cooperman D, Grant RE. Evaluation of proximal femoral geometry using digital photographs. J Orthop Res 2010;28:1399-404.
25. Preininger B, Schmorl K, von Roth P, Winkler T, Matziolis G, Perka C, *et al.* Femoral offset (3D) in patients without osteoarthritis – Index values from 200 hip joints. Open Orthop J 2012;6:578-81.
26. Roy S, Kundu R, Medda S, Gupta A, Nanrah BK. Evaluation of proximal femoral geometry in plain anterior-posterior radiograph in Eastern-Indian population. J Clin Diagn Res 2014;8:C01-3.
27. Takamatsu T, Shishido T, Takahashi Y, Masaoka T, Tateiwa T, Kubo K, *et al.* Radiographic determination of hip rotation center and femoral offset in Japanese adults: A preliminary investigation toward the preoperative implications in total hip arthroplasty. Biomed Res Int 2015;2015:610763.
28. Sengodan VC, Sinmayanantham E, Kumar JS. Anthropometric analysis of the hip joint in South Indian population using computed tomography. Indian J Orthop 2017;51:155-61.

Original Article

Morphometric Study of Bicipital Groove in Dry Adult Human Cadaveric Humerus in Indian Population

Kesar Khanna, Hina Nafees, Dilshad Ahmad Usmani, Sanjeev Kumar Jain, Sonika Sharma

Department of Anatomy, TMMC and RC, TMU, Moradabad, Uttar Pradesh, India

Abstract

Introduction: An important anatomical feature on the ventral surface of the proximal section of the humerus is the "bicipital groove" (BG). Understanding the functional importance of the shoulder area requires a thorough understanding of the morphometric research of the bicipital groove. It is regarded as a significant turning point for humeral head replacement and shoulder prosthesis. The current study aims to investigate the bicipital groove's morphometry and show how variations in its parameters affect the way the surrounding structures operate. **Objectives:** Primary objective is to determine various morphometric parameters of bicipital groove and to calculate the medial and lateral angles of the dry humerus's bicipital groove. We also evaluate the anthropometric differences between intertubercular sulcus of the right side and the left side of humerus. **Materials and Methods:** The study was carried out at the Anatomy Department of TMMC and RC, TMU, Moradabad, and was descriptive in nature. Forty-one dried adult cadaveric humerus bones (19 Rt. Humerus, 22 Lt. Humerus) were used in the study. The bicipital groove's breadth and length as well as the medial and lateral wall angles were measured. It was noted that Meyers Ridge was present. A suitable test for statistics was used. **Results:** The biciptal groove measured 78.35 ± 4.5 mm on the right side and 78.21 ± 7.2 mm on the left. The calculated width of the same was 9.13 ± 1.1 mm on the left and 10.11 ± 1.2 mm on the right. The bicipital groove measured in this study has a depth of 5.39 ± 1.0 mm on the right side and 5.30 ± 1.0 mm on the left. The median wall angle of the right humerus measured 46.58 ± 6.5, whereas the left humerus measured 47 ± 5.8. The bicipital groove measurements for the right and left sides were 48.89 ± 5.8 and 49 ± 4.7, respectively, in terms of their lateral wall angles. The frequency of Meyer's supratubercular ridge on the right side of the humerus was determined to be 15.8%. **Conclusion:** The differences in the morphometry of the bicipital groove have been verified by this investigation. In the Indian population, these grooves were found to be slightly deeper and wider. Anatomists, orthopedic surgeons, and others who fabricate prosthesis based on native Indian bone measurements would greatly benefit from the data collected.

Keywords: *Bicipital groove, Meyers ridge, musculoskeletal disorders*

Introduction

A significant anatomical marker on the ventral surface of the proximal portion of the humerus is the "bicipital groove" (BG), also known as the intertubercular sulcus. A 5-centimeter long and 4–6-mm-deep intertubercular sulcus is present.[1] The morphometry of the shoulder area is essential to comprehending it functionally.[2] Prior research indicates that the morphology of the intertubercular sulcus is indicative of diseases in the biceps brachii muscle tendon and can be utilized to guide surgical interventions in that region.[3] When the sulcus width is less than the biceps tendon width, a small bicipital groove will cause attrition changes that cause degeneration, impingement, and inflammation. Similarly, a shallow groove will cause dislocation, and this subluxation will result in rupture and degenerative alterations to the biceps brachii tendon. Thus, for shoulder prosthesis and humeral head replacement, the intertubercular sulcus is regarded as a crucial landmark.[3,4] Studies have demonstrated that the greatest anatomic diversity of the bicipital groove is associated with lesions of the long-head tendon of the biceps brachii, which are the most common causes of shoulder discomfort and functional impairment.[5] In light of the practical significance of the bicipital groove and the anatomical variations found in its morphometry, the following research has been done to examine the morphometry of this groove and document any potential

How to cite this article: Khanna K, Nafees H, Usmani DA, Jain SK, Sharma S. Morphometric study of bicipital groove in dry adult human cadaveric humerus in Indian population. J Anat Soc India 2024;73:359-63.

Article Info

Received: 03 April 2024
Revised: 16 August 2024
Accepted: 19 November 2024
Available online: 28 December 2024

Address for correspondence:
Dr. Hina Nafees, Department of Anatomy, TMMC and RC, TMU, Moradabad, Uttar Pradesh, India.
E-mail: 786drhinanafees@gmail.com

Access this article online

Website: https://journals.lww.com/joai

DOI: 10.4103/jasi.jasi_43_24

Quick Response Code:

effects that variations in its length, width, breadth, and angle may have on the operation of nearby structures.

Materials and Methods

- Study design: Observational study
- Study type: Descriptive study
- Study location: The study was carried out at Teerthanker Mahaveer Medical College and Research Center in Moradabad, Uttar Pradesh, in the Department of Anatomy
- Study period: Present study has been approved from the Indian Council of Medical Research, ICMR-STS 2022 program. Reference ID: 202200287. The study was carried out for 2 months as part of the Short-term Studentship Program
- Sample size: The study was performed on 41 dried adult cadaveric humerus (consisting of 19 right humeri and 22 left humeri) collected at TMMC and RC from the departments of anatomy and forensic medicine
- Ethics approval: Approval was obtained from the Ethics Committee of TMU, Moradabad. The procedures used in this study adhere to the tenets of the Declaration of Helsinki.

Materials

Digital Vernier's Calliper by Aerospace (Least count: 0.01), Finger Goniometer by Bos Medicare (Least count: 1° or 1/2°).

Inclusion criteria

All bones available in the Department of Anatomy and Department of Forensic Medicine at TMMC and RC.[6]

Exclusion criteria

The investigation excluded the humeri that experienced any injury or abnormal alterations.[6]

Methodology

Once the Institutional Research Committee (Ref. No. IRB/73/2022) has granted approval. A total of 41 dry adult cadaveric humerus were obtained from the Anatomy and Forensic department, consisting of 19 right humerus and 22 left humerus. Vernier's calliper was used to measure the length, width, and depth of the groove, whereas a finger goniometer was used to measure the lateral and medial wall angles.

Measurement of length of "Bicipital Groove"

The distance between the most proximal and distal point of the groove using Vernier's Callipers [Figure 1].[6]

Measurement of width of "Bicipital Groove"

The width was measured as the maximum distance between medial and lateral lips of the groove using Vernier's Callipers [Figure 2].[6]

Measurement of depth of "Bicipital Groove"

The depth was measured as the distance between greater or lesser tubercle to floor of the groove using Vernier's Callipers [Figure 3].[6]

Figure 1: Measurement of length of intertubercular sulcus

Figure 2: Measurement of width of intertubercular sulcus

Figure 3: Measurement of depth of intertubercular sulcus

Measurement of Lateral and Medial Wall Angle of "Bicipital Groove"

A finger goniometer was used to measure the angle at which the lips' convergence finally stopped [Figure 4]. Tracing a line perpendicular to the groove angle center allowed us to measure the medial and lateral angles [Figures 5 and 6].[7]

The presence of supratubercular ridge of Meyer was observed.

The measurements of all these parameters were conducted with precision, and the average results were calculated. A paired *t*-test was employed to evaluate the disparity in measurements of the bicipital groove between the left and right sides. The acquired data were organized as mean ± standard error of the mean and subjected to statistical analysis. The frequency of supratubercular ridge present in both the left and right humerus was assessed using a one-sample Chi-square test.

Results

This study looks at the dimensions of the bicipital groove in the humerus of dry adult human cadavers from the Indian population, including its length, depth, width, medial angle, lateral angle, and groove angle. Both the right and left humerus exhibited the presence or absence of a supratubercular ridge.

The average length of the bicipital groove on the right side was measured to be 78.35 ± 4.5, whereas the average length on the left side was found to be 78.21 ± 7.2, based on the data shown in Table 1. The length variable produced a $P = 0.12$ after a paired *t*-test was run. On the right side, the bicipital groove measured an average depth of 5.39 ± 1.0, whereas on the left side, it measured 5.30 ± 1.0. After doing a paired *t*-test, the depth variable had a $P = 0.75$. The computed mean width values for the left and right sides were 9.13 ± 1.1 and 10.11 ± 1.2, in that order.

A paired *t*-test was conducted, yielding a $P = 0.73$ for the variable "width." On the right side, the mean medial angle was 46.58 ± 6.5, whereas on the left side, it was 47 ± 5.8. A paired *t*-test was conducted, yielding a $P = 0.79$ for the medial angle. On the right side, the mean value for the lateral angle was 48.89 ± 5.8, whereas on the left side, it was 49 ± 4.7. A paired *t*-test was conducted, yielding a $P = 0.44$ for the lateral angle. The mean groove angle values on the right side were 79.37 ± 7.9, whereas on the left side they were 73 ± 9.2. A paired *t*-test was conducted, yielding a $P = 0.28$ for the groove angle.

Table 1: Morphometrical parameters of bicipital groove of humerus

Parameters	Right humerus	Left humerus	*P*	*t*
Length of BG	78.35±4.5	78.21±7.2	0.12	−0.073
Depth of BG	5.39±1.0	5.30±1.0	0.75	−0.073
Width of BG	10.11±1.2	9.13±1.1	0.73	−2.579
Medial angle	46.58±6.5	47±5.8	0.79	0.216
Lateral angle	48.89±5.8	49±4.7	0.44	0.119
Groove angle	79.37±7.9	73±9.2	0.28	−2.328

BG: Bicipital groove

Figure 4: Measurement of groove angle

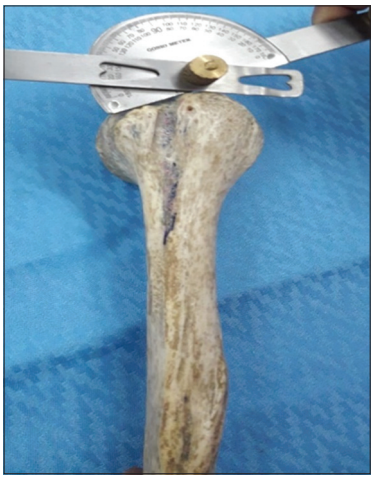

Figure 5: Measurement of lateral wall angle

Figure 6: Measurement of medial wall angle

The supratubercular ridge was exclusively observed in the right humerus. A Chi-square test was conducted on a single sample, revealing a prevalence rate of 15.8% for the right side humerus [Table 2].

Discussion

The World Health Organization has determined that musculoskeletal issues rank as the second-most important cause of disabilities worldwide. A painful musculoskeletal condition affects approximately 20%–33% of the population, depending on the age and diagnosis.[8] The bicipital groove and the transverse humeral ligament are essential for preserving stability within the shoulder joint and enabling the tendon of the long head of the biceps brachii muscle to operate as intended.[9] Gaining an understanding of the shoulder area's morphometry is essential to understanding its functions. This study's major goal was to assess the morphometrical and anatomical alterations in the humerus remains of deceased individuals' bicipital groove diameters.

A major factor for shoulder deficits is the existence of differences in the bicipital groove's architecture and morphometry. By focusing only on the critical region of the groove, Ueberham and Le Floch were able to confirm these variations. They determined factors including width, depth, and angle that could potentially jeopardize the stability of the tendon that connects the biceps brachii muscle.[10] Male cadavers had a significantly wider bicipital groove at its narrowest point than female cadavers, according to findings from a different study done by Anthony N. Baumann. However, when comparing the length and depth of the groove in male and female cadavers, the study found no differences.[11] Anthropometric measures were used in this investigation to ascertain the bicipital groove's length, depth, width, medial angle, lateral angle, and groove angle. The supratubercular ridge of Meyer has been identified by the examination of the discrepancy in measurements between the right and left bicipital grooves. The bicipital groove lengths measured in this study were 78.35 ± 4.5 mm on the right side and 78.21 ± 7.2 mm on the left. The length of the groove, regardless of side, was found to be 72.98 ± 7.54 mm by Kumar *et al*. in their investigation.[12] The present study's results are comparable to those of Bahiru Tenaw Goshu's study on the Ethiopian population,[6] but they are marginally lower than those of Murlimanju *et al*.'s[13] and Rajani and Man's[14] investigations. Significantly shorter bicipital groove lengths were reported by Kaur and Gupta[9] and Arunkumar *et al*.[15] which is in opposition to the results of the current study. The width of the bicipital groove measured in this study is 10.11 ± 1.2 mm on the right side and 9.13 ± 1.1 mm on the left, suggesting that the right side is slightly wider than the left. The study's findings are comparable to those published by Rajani and Man,[14] but they marginally outperform those of Bahiru Tenaw Goshu[6] Kaur and Gupta[9] and Arunkumar *et al*.[15] in their investigations of Ethiopians.

Table 2: Presence of supratubercular ridge of Meyer

Parameter	Total	Frequency (%)
Right	19	3 (15.8)
Left	22	0

The existence of the supratubercular ridge of Meyer has also been revealed by the analysis of the discrepancy in measurements between the right and left bicipital groove. The supratubercular ridge of Meyer in the present study was found in 15.8% in the right side and 0% in the left side. Hitchcock and Bechtol proposed that there exists a definitive relationship between the presence of supratubercular ridge and tendonitis.[5] This ridge was also observed by Cone *et al*.[16] in 50% of cases. Vettivel *et al*.[17] observed this ridge in 88% on the right side and 57% on the left side and also stated its importance on the right side than the left to prevent the medial displacement of long head of biceps brachii tendon from bicipital groove.

Conclusion

The length, depth, width, medial angle, lateral angle, and groove angle of the bicipital groove have all been studied in relation to its morphometric and anatomical features. It has been noted whether a supratubercular ridge is present or absent, and the sizes of the left and right bicipital groove's have been compared. The current study has confirmed the differences in the bicipital groove's morphometry that have been noted. According to this study, the Indian population possessed grooves that were marginally deeper and wider. The instability of the biceps tendon can also be attributed to the presence of the supratubercular ridge of Meyer and the medial and lateral wall angles. Bicipital groove (BG) levels can be evaluated morphometrically to gain important information about a patient's health and to help with shoulder reconstruction surgeries that are more successful.

Financial support and sponsorship

Research work approved by ICMR- STS 2022 program Reference ID: 202200287.

Conflicts of interest

There are no conflicts of interest.

References

1. Gupta S, Naqshi BF, Shah AB, Hassan N, Raina S, Khan HA, *et al*. Variations in the bicipital groove in North Indian population: A morphological and morphometric study and review of literature. Int J Health Sci Res 2015;5:220-6.
2. Moatshe G, Marchetti DC, Chahla J, Ferrari MB, Sanchez G, Lebus GF, *et al.* Qualitative and quantitative anatomy of the proximal humerus muscle attachments and the axillary nerve: A cadaveric study. Arthroscopy 2018;34:795-803.
3. Levinsohn EM, Santelli ED. Bicipital groove dysplasia and medial dislocation of the biceps brachii tendon. Skeletal Radiol 1991;20:419-23.

4. Khan R, Satyapal KS, Naidoo N, Lazarus L. Dimensional analysis of the bicipital groove and its associated pathology in a South African population. J Orthop 2020;19:128-31.
5. Hitchcock HH, Bechtol CO. Painful shoulder; observations on the role of the tendon of the long head of the biceps brachii in its causation. J Bone Joint Surg Am 1948;30A:263-73.
6. Goshu BT. Anatomical analysis of bicipital groove of dry adult human cadaveric humerus in Ethiopia. EC Clin Exp Anat 2019;2:311-5.
7. Wafae N, Atencio Santamaría LE, Vitor L, Pereira LA, Ruiz CR, Wafae GC. Morphometry of the human bicipital groove (sulcus intertubercularis). J Shoulder Elbow Surg 2010;19:65-8.
8. World Health Organization. worldHealth statistics 2016 [OP] Monitoring health for the Suatainable Development Goals (SDGs). World Health Organuzation; Geneva, Switzerland 2016.
9. Kaur M, Gupta R. Morphometric and morphological study of bicipital groove in North Indian population. Int J Basic Appl Med Sci 2015;5:48-53.
10. Ueberham K, Le Floch-Prigent P. Intertubercular sulcus of the humerus: Biometry and morphology of 100 dry bones. Surg Radiol Anat 1998;20:351-4.
11. Baumann AN, Talaski GM, Fiorentino A, Sidloski K, Rogers H, Oleson CJ, *et al.* Examining the dimensions of the bicipital groove: A human cadaveric study. Cureus 2023;15:e50895.
12. Kumar P, Saha S, Arora G, Aneja PS. Detailed morphometry and morphology of bicipital groove of humerus among North Indian Population. J Clin Diagn Res 2021;15.
13. Murlimanju BV, Prabhu LV, Pai MM, Shreya M, Prashanth KU, Kumar CG, *et al.* Anthropometric study of the bicipital groove in Indians and its clinical implications. Chang Gung Med J 2012;35:155-9.
14. Rajani S, Man S. Review of bicipital groove morphology and its analysis in North Indian population. ISRN Anat 2013;2013:243780.
15. Arunkumar KR, Manoranjitham R, Delhi Raj U, Shalini R. Morphometric study of bicipital groove in South Indian population and its clinical implications. Int J Anat Res 2016;4:2187-97.
16. Cone RO, Danzig L, Resnick D, Goldman AB. The bicipital groove: Radiographic, anatomic, and pathologic study. Am J Roentgenol 1983;141:781-8.
17. Vettivel S, Indrasingh I, Chandi G, Chandi SM. Variations in the intertubercular sulcus of the humerus related to handedness. J Anat 1992;180:321-6.

Review Article

Morphometric and Histological Changes of the Placenta in Hypertensive Disorders of Pregnancy

Jyothi N. Nayak[1], B. Sunitha[2], Hannahsugirthabai Rajilarajendran[3]

[1]Department of Anatomy, DAPM RV Dental College, Bengaluru Karnantaka, [2]Milan Fertility and Birthing center JP Nagar, Bengaluru Karnataka, [3]Chettinad Hospital and Research Institute, Kelambakkam, Tamil Nadu, India

Abstract

The placenta is the discoid foeto-maternal organ which maintains pregnancy and promotes normal foetal development. The human placenta is a hemo-chorial placenta where the maternal blood directly comes in contact with the foetal trophoblast. Functions of placenta include gas exchange, metabolic transfer, hormone secretion and foetal protection. Hypertension is a common complication of pregnancy which significantly contributes to the perinatal and maternal mortality and morbidity. 5 % to 8% of all maternal deaths are due to hypertension during pregnancy. Complications of hypertensive disorders of pregnancy are reflected in the placenta in a significant way both macroscopically and microscopically. Study of placenta is useful in understanding the pathophysiology of the placenta. Previous studies on preeclamptic placentae revealed a significant decrease in morphological parameters like weight, diameter, thickness, surface area, volume, and cotyledon number. Various histological changes like increased syncytial knots, cytotrophoblastic proliferation, fibrinoid necrosis, stromal fibrosis, and calcification were also noted in the placenta from preeclamptic cases. The changes in placental structure and function can have significant implications for the well-being and development of the fetus. This review gives an overview of both morphological and histological changes of placentae in hypertensive disorders of pregnancy.

Keywords: *Histology, hypertension, morphology, placenta, preeclampsia*

Introduction

The placenta is the most important organ of intrauterine life, which is essential for the proper growth and development of the fetus. It acts as a connecting link between mother and fetus and facilitates nutrient and gas exchange between mother and fetus.[1]

Hypertensive disorders are common complications of pregnancy, which complicate 5%–10% of all pregnancies. Hypertension is one of the leading causes of maternal mortality and morbidity both in developed and developing countries of the world. Hypertensive disorders of pregnancy are classified into preeclampsia and eclamptic syndrome, chronic hypertension, preeclampsia superimposed on chronic hypertension, and gestational hypertension. Young women are at risk of developing preeclampsia, whereas older women are at higher risk for chronic hypertension with superimposed preeclampsia.[2] Hypertensive disorders can affect the tissue component of the placenta and they are reflected in the placenta in a significant way, both macroscopically and microscopically.[3]

The placenta is the root cause of the development of preeclampsia. The onset, severity, and progression of preeclampsia are significantly affected by maternal response to placentally derived factors and proteins.[4] In preeclampsia, the maternal arteries fail to undergo physiological adaptations like that of normal pregnancy, which is required for sufficient placental perfusion.[5] The late onset of preeclampsia comprises more than 80% of all preeclampsia cases. The late onset of preeclampsia can be a maternal disease rather than a placental disease, it causes less morphological changes in the placenta.[6]

The well-being of the fetus mainly depends on the placental morphology, blood flow, and nutrient transport function.[7] The morphology and histology of the placenta vary with conditions such as hypertension, diabetes, and other maternal disorders.[8] The adverse pregnancy outcomes are associated with the placental growth restriction.[9] The examination of the placenta after delivery

How to cite this article: Nayak JN, Rajilarajendran H, Sunitha B. Morphometric and histological changes of the placenta in hypertensive disorders of pregnancy. J Anat Soc India 2024;73:364-7.

Article Info

Received: 28 March 2023
Revised: 02 March 2024
Accepted: 12 March 2024
Available online: 28 December 2024

Address for correspondence:
Dr. Hannahsugirthabai Rajilarajendran, Department of Anatomy, Chettinad Hospital and Research Institute, Chettinad Academy of Research and Education, Kelambakkam, Chennai - 603 103, Tamil Nadu, India.
E-mail: drrajianat@gmail.com

Access this article online

Website: https://journals.lww.com/joai
DOI: 10.4103/jasi.jasi_31_23
Quick Response Code:

provides a clear-cut picture of prenatal development, and maternal and fetal health and is also helpful for the management of future pregnancies.[10]

To the best of our knowledge, there is a very limited number of systematic reviews comparing the morphological and histological differences of the placenta between normotensive controls and hypertensive pregnancy cases. Considering this, we have developed a comprehensive systematic review of the current literature to critically examine the gross and microscopic findings associated with hypertensive pregnancy.

Materials and Methods

Literature search strategy

PubMed, Google Scholar, and other open-access articles related to morphometric and histological changes of the placenta in hypertensive disorders of pregnancy were searched online. The keywords used in the search engines included "Morphometric study of Placenta" AND "Hypertensive disorders," "Placenta histology" AND "Preeclampsia," or "Pregnancy-induced Hypertension." The literature review included articles from 2014 to 2022.

The research articles were collected according to the following criteria: (a) studies on the human placenta, (b) study of morphometry and histology of placenta affected by hypertension, and (c) comparative studies between normotensive and hypertensive placentae. Inclusion criteria: Both prospective and retrospective case-control studies were also included. Exclusion criteria: The studies on the placenta affected by gestational diabetes, thyroid, and other maternal disorders were excluded.

Methods

After the search, 20 articles met the inclusion criteria. Among them, two of them explained the normal anatomy and hypertensive disorders of pregnancy. Eight of them evaluated only morphological changes of the placenta in preeclampsia. Five of them explained only histological changes of hypertensive placentae. The rest of the articles evaluated both morphological and histological changes in hypertensive placentae and compared it with normotensive placentae.

Collected articles were assessed according to the following criteria: study design, sample size, number of pregnancies, age of the pregnant women, types of hypertension, changes that occurred in the placenta affected by hypertension and its comparison with the normal, and effect of disease in the health of mother and fetus. The changes in most important morphological and histological parameters such as placental weight, diameter, thickness, number of syncytial knots, stromal fibrosis, and fibrinoid necrosis were noted.

Discussion

Preeclampsia is a multifactorial and polygenic disorder.[11] The hereditary predisposition for preeclampsia results from interactions of genes that are inherited from both mother and father that control enzymatic and metabolic functions of the organ system. In normal pregnancy, the cytotrophoblastic invasion into the spiral arteries of intervillous spaces occurs deep into the myometrium, muscular, and elastic tissues of the arteries in a retrograde fashion. These are replaced by fibrinoid substances, which are responsible for the dilatation of the spiral arteries and the increase of uteroplacental blood flow.[12] In preeclampsia patients, these vascular changes are limited only to the decidua, which results in various degrees of placental ischemia.[13] Several studies have reported that due to maternal vasospasm, uteroplacental blood decreases in hypertensive pregnancies. This leads to constriction of fetal stem arteries, and fetal hypoxia and it may result in fetal death also.[14]

Many authors have reported significant morphometric and histological changes in hypertensive placentae compared to normotensive placentae.[3,5,15,16,18] The normal weight of the placenta is 400–800 g. Fetal maturity is mainly determined by important factors like placental weight. Various morphological parameters such as placental weight, diameter thickness, surface area, volume, and cotyledon numbers were significantly reduced in hypertensive placentae compared to normotensive[3,5,7,8,10-13,16] as shown in Table 1. This reduction in parameters is mainly because of placental insufficiency which is caused by reduced uteroplacental blood flow.[13,14] Higher incidence of infarction is common in hypertensive placentae. Infarctions are due to disturbance of intervillous circulation caused by thrombotic occlusion of uteroplacental arteries.[15] Calcification and infarction increase with the severity of hypertension. Calcification is considered evidence of placental degeneration, which occurs due to reduced vascularity to the placenta in conditions like hypertension or it may occur at the end of pregnancy as a result of the aging of the placenta.[16] A higher incidence of low fetal birth weight and intrauterine death of a fetus is reported in preeclamptic placentae with placental calcification and infarction.[13,14,18]

Histological changes of the placenta in hypertensive disorders

The histology of preeclamptic placentae showed a significant increase in number of syncytial knot formation, cytotrophoblastic proliferation, fibrinoid necrosis, calcification, villous hyalinization, and hypovascular villi Table 2.[8,12,14-16,19] The syncytial knot formation is usually seen in term and preterm placentae, but their number significantly increases in hypoxic conditions like hypertensive disorders of pregnancy.[17] A decrease in intervillous blood flow leads to increased syncytial knotting in the placental villi. Increased syncytial knotting indicates the disturbance of hormonal factors, which alters

Table 1: Comparison of placental morphometry in both normotensive and hypertensive cases

Parameter	Studies/authors	Mean±SD		*P*
		Normotensive	Hypertensive	
Weight of placenta	Bar *et al*.[3]	476.88±21.829	377.00±12.079	0.000
	Girish *et al*.[5]	423.11±45.85	357.45±61.66	<0.00
	Prathiba *et al*.[8]	461.75±99.08	421.8±120.09	<0.011
	Dixit Daksha *et al*.[10]	482.63±83.80	455.13±05.78	0.000151
	Wubale and Tolera[11]	499.4±11.89	456.20±19.13	0.0001
	Sarma *et al*.[20]	514.8±62.8	486.9±37.08	0.037
Diameter of the placenta	Bar *et al*.[3]	17.91±0.982	15.39±0.535	<0.005
	Girish *et al*.[5]	16.00±0.75	15.31±1.08	<0.0001
	Wubale and Tolera[11]	19.40±0.85	17.66±1.07	0.0001
	Sarma *et al*.[20]	15.60±0.40	14.76±0.33	<0.0001
Placental thickness	Bar *et al*.[3]	2.29±0.282	2.10±0.431	0.024
	Wubale and Tolera[11]	1.96±0.20	1.72±0.11	0.0001
	Sarma *et al*.[20]	1.76±0.19	1.48±0.15	<0.0001
	Salmani *et al*.[7]	2.78±0.23	2.74±0.28	<0.05
Number of cotyledons	Girish *et al*.[5]	17.04±2.06	14.07±2.04	<0.0001
	Dixit Daksha *et al*.[10]	22.37±4.94	19.39±3.78	0.00662
	Sree Ranga *et al*.[14]	19.1±1.2	16.1±2.5	<0.001
	Wubale and Tolera[11]	18.66±1.21	17.24±1.06	0.001
	Salmani *et al*.[7]	21.18±1.48	21.21±1.58	<0.05

SD: Standard deviation

Table 2: Changes in placental histology in hypertensive pregnancies

Histological findings	Studies	Effect on hypertensive pregnancy placenta
Calcification	Singh *et al*.,[16] Sree Ranga *et al*.,[14] Rana *et al*.,[15] Gore *et al*.,[17] Vijayanand *et al*.,[18] Chhatwal *et al*.[19]	Increased
Infarction	Sree Ranga *et al*.,[14] Rana *et al*.,[15] Gore *et al*.,[17] Vijayanand *et al*.,[18] Chhatwal *et al*.[19]	Increased
Syncytial knots	Singh *et al*.,[16] Prathiba *et al*.,[8] Sree Ranga *et al*.,[14] Rana *et al*.,[15] Gore *et al*.,[17] Vijayanand *et al*.,[18] Chhatwal *et al*.[19]	Increased
Fibrinoid necrosis	Singh *et al*.,[16] Prathiba *et al*.,[8] Sree Ranga *et al*.,[14] Gore *et al*.,[17] Vijayanand *et al*.,[18] Chhatwal *et al*.[19]	Increased
Cytotrophoblastic proliferation	Singh *et al*.,[16] Prathiba *et al*.,[8] Sree Ranga *et al*.,[14] Gore *et al*.,[17] Vijayanand *et al*.,[18] Chhatwal *et al*.[19]	Increased
Stromal fibrosis	Singh *et al*.,[16] Prathiba *et al*.,[8] Sree Ranga *et al*.,[14] Rana *et al*.,[15] Gore *et al*.,[15] Vijayanand *et al*.,[18] Chhatwal *et al*.[19]	Increased
Villous hyalinisation	Singh *et al*.,[16] Sree Ranga *et al*.,[14] Rana *et al*.,[15] Gore *et al*.,[17] Vijayanand *et al*.,[18] Chhatwal *et al*.[19]	Increased
Hypovascular villi	Singh *et al*.,[16] Sree Ranga *et al*.,[14] Rana *et al*.,[15] Gore *et al*.,[17] Vijayanand *et al*.,[18] Chhatwal *et al*.[19]	Increased

placental morphometry and results in *pregnancy-induced hypertension* to the mother.[14-18] Cytotrophoblastic proliferation leads to reduced intervillous blood flow, resulting in decreased blood supply to fetus and fetal growth retardation.[7,13] The increased incidence of stromal fibrosis is related to reduced uteroplacental blood flow as a result of obliterative endarteritis as seen in hypertensive placentae.[19]

Conclusion

Placenta is the only source of nutrition for the fetus. Placental studies are of great clinical importance. Examination of a placenta may provide valuable information about the effect of maternal disorders on the fetus, the cause of preterm delivery, and fetal growth restriction.[20] A placental examination is essential in case of fetal death. The hypertensive disorders of pregnancy like preeclampsia had an adverse effect on the morphology and histology of the placenta. These morphological and histological changes adversely influence the fetal outcome. Preeclampsia is a multisystem disorder, but its etiology and pathogenesis are still not understood. Hence, the examination of the placenta is helpful in understanding the pathophysiology of the placenta, identifying the cause for pathological changes, risk of recurrence, and also the management of future pregnancies.

Financial support and sponsorship

Nil.

Conflicts of interest

There are no conflicts of interest.

References

1. Saddler TW. Langman's Medical Embryology. 14th ed. New Delhi: Wolters Kluwer Pvt, Ltd; 2018.
2. American College of Obstercians and Gynaecologists. Issuing body II. Hypertension, Pregnancy Induced-Practice Guideline. Library of Congress in Cataloging-in –Publication Data. Washington: American College of Obstercians and Gynaecologists; 2013. p. ix, 2.
3. Bar PK, Ghosh S, Gayen P, Mandal S, De A. Morphological study of placenta in Hypertensive disorders in pregnancy. Trop J Path Micro 2019;5:366-73.
4. Abdel Salam GE, Alam OA, Ahmed UF, Al-Sherbeny MF. Light and elcetron microscopic study of placenta in Pre-eclampsia: A trial to define underlying changes and its clinical impact. Tata Med J 2015;43:134-45.
5. Girish BL, Nandagoapl KM, Padmini CP, Mahesh SH, Shivanna R, Srinath S. A morphometric comparative study of placenta in normal and preeclampsia pregnancies delivering at 36 to 38 weeks of gestation and its impact on birth weight. J Evol Med Dent Sci 2015;4:14444-50.
6. Askar E, Selim S, Sibai H. Histological changes of human placenta in early intrauterine growth restriction with and without preeclampsia. J Med Histol 2019;3:65-76.
7. Salmani D, Purushothaman S, Somashekara SC, Gnanagurudasan E, Sumangaladevi K, Harikishan R, *et al*. Study of structural changes in placenta in pregnancy induced hypertension. J Nat Sci Biol Med 2015;5:352-5.
8. Prathiba A, Einstien D, Subramanian V, Mahendranath P, Murugesan S. Comparative study of placental morphometry and histomorphology in normal and pre-eclamptic pregnancies. Int J Sci Stud 2016;4:96-9.
9. Vijayalakshmi B, Kittali S. Morphological changes of placenta in cases of pre-eclampsia and perinatal outcome. Int J Sci Stud 2015;3:137-42.
10. Dixit Daksha P, Vanitha, Virupaxi Rajendrakumar D. Study on placenta in hypertensive disorders of pregnancy. Indian J Anat 2018;7:4.
11. Wubale Y, Tolera A. Gross Morphological study of placenta in Preeeclampsia. Anat J Afr 2017;6:977-81.
12. Karmakar MK, Kar S, Kumar SM, Chattopadhyay SK, Vaid LK, Sen S. A study of histological changes of palcenta in rural population of Eastern India. Int J Reprod Contracept Obstet Gynecol 2018;7:3280-7.
13. Mehra S, Rathore SP. Morphology and Morphometry study of placenta in pregnancy-induced hypertension and its comparison with that of normal pregnancies. Int J Curr Res 2016;8:34714-6.
14. Sree Ranga MK, Adaline Thangam TF, Vasantha Mallika MC, Indira MV. Morphological and histological variations of human placenta in hypertensive disorders of pregnancy. Int J Anat Res 2017:5:3591-98.
15. Rana S, Diwan Y, Chauhan RS, Diwan D, Gupta A. Comparative study of histology of placenta in normotensive and hypertensive cases. JMSCR2017;5:18635-40.
16. Singh V, Ranjan K, Tewarson SL, Singh R, Yadav Y. Study of histological changes of placenta in pregnancy-induced hypertension in poorvanchal region of Uttar Pradesh, India. J Anat Soc India 2021;70:25-9.
17. Gore CR, Pandey A, Shetty A, Rao R, Paranjape S. A study on histopathological changes in placenta in pre-eclampsia/eclampsia: A case-control study in tertiary care center, Western India. Indian J Pathol Oncol 2018;5:385-90.
18. Vijayanand M, Geeta Anasuya D, Jeevamani SG, Sutha S. Comparative histological study of normal human placentae with hypertensive placentae in Western part of Tamilnadu state (Kongunadu region). Int J Anat Res 2021;9:7948-54.
19. Chhatwal J, Chaudhary DN, Chauhan N. Placental changes in hypertensive pregnancy: A comparison with normotensive pregnancy. Int J Reprod Contracept Obstet Gynecol 2018;7:3808-13.
20. Sarma GD, Sanyal R, Al Hossainin SS, Khemka VK, Mitra A. Study the morphology and morphometric measurements of placenta among normotensive and pregnancy induced hypertension pregnancies. Int J Health Clin Res 2021;4:142-7.

Case Report

An Atypical Case of Intracardiac Myxoma Fed by Extracardiac Arteries

Zeliha Coşgun, Süleyman Filiz[1]

Department of Radiology, Faculty of Medicine, Bolu Abant Izzet Baysal University, Bolu, [1]Department of Radiology, Gazi Mustafa Kemal Occupational and Environmental Diseases Hospital, Ankara, Turkey

Abstract

Myxoma is the most common type of primary benign heart tumor and is usually easily identified by echocardiography. Tumor vascularity is a rare finding in atrial myxomas and reported cases of the right atrial myxomas most frequently involve feeding vessels from the right coronary artery or, less frequently, from both coronary arteries. In this case report, an echocardiographic examination of a 74-year-old male, who was admitted to hospital with chest pain revealed an echogenic solid mass in the right atrium. A coronary angiography showed an arteriocavity fistula connecting the feeding artery to the cardiac chamber. In the computed tomography angiography examination performed, a mass was observed with intense vascularity, containing feeding vessels from the left circumflex artery, the right inferior phrenic artery, and the left hepatic artery; calcifications in the right atrium were also present. The mass was completely and successfully resected. Pathology results of the mass were compatible with cardiac myxoma. This was an atypical case of a right atrial myxoma due to the presence of intense vascularization and the feed from the cardiac and extracardiac arteries.

Keywords: *Atypic, computed tomography angiography, vascularity, myxoma*

Introduction

Myxoma is the most common type of primary cardiac tumor and is typically diagnosed by echocardiography.[1] However, some myxomas have rare characteristics that can lead to a misdiagnosis. In the literature, atypical attachment zones, multiple masses, coexistence with other heart diseases, recurrent masses, severe calcification, and necrosis have been reported as among these rare characteristics.[2] Tumor vascularity is also a rare finding in atrial myxomas and reported cases of the right atrial myxomas most frequently receive feeding vessels from the right coronary artery (RCA) or, less frequently, from both coronary arteries.[3,4] We aimed to report a case of a cardiac myxoma feeding by extracardiac vessels.

Case Report

A 74-year-old male patient was admitted to the cardiovascular surgery clinic with a complaint of chest pain over the previous 6 months. Echocardiographic examination revealed a 4.5 cm × 6 cm solid echogenic mass in the right atrium. While the coronary angiography showed fistulization from the circumflex artery to the right atrium, the coronary vessels were normal [Figure 1]. Multiphase computed tomography angiography (CTA) was then planned to evaluate both the mass and the possible fistulization. In the first phase obtained without contrast, scattered heterogeneous calcifications were seen in the right atrium. Cardiac CTA with large field-of-view performed after the contrast agent injection revealed a mass of 52 mm × 77 mm × 50 mm in the right atrium, attached to the interatrial septum, contained densely tortuous vascular structures [Figures 2 and 3]. The pulmonary CTA phase was also performed in the same session to better evaluate the margins of the mass. It was observed that the mass received feeding branches from the right inferior phrenic artery and the left hepatic artery [Figure 3]. The differential diagnosis also considered angiosarcoma since there are no known cases of cardiac myxoma fed by extracardiac arteries in a review of the literature, and because intensive vascularity is a rare finding in myxomas.

The patient was operated on through a median sternotomy. Following a right atriotomy, a 6 cm × 4.5 cm intracardiac solid mass originating from the interatrial

How to cite this article: Coşgun Z, Filiz S. An atypical case of intracardiac myxoma fed by extracardiac arteries. J Anat Soc India 2024;73:368-70.

Article Info

Received: 14 March 2024
Accepted: 18 November 2024
Available online: 28 December 2024

Address for correspondence:
Dr. Süleyman Filiz, Department of Radiology, Ankara Gazi Mustafa Kemal Occupational and Environmental Diseases Hospital, 06560, Yenimahalle, Ankara, Turkey.
E-mail: suleymanfilizz@gmail.com

Access this article online

Website: https://journals.lww.com/joai
DOI: 10.4103/jasi.jasi_34_24
Quick Response Code:

septum was explored [Figure 4], cardiac and extracardiac arteries feeding the mass were ligated, and the mass was completely excised. A subsequent interatrial septal defect was closed using a pericardial patch. The operation was completed in the standard fashion. No postoperative complications occurred, and the postoperative course was uneventful. A histopathological examination of the surgically resected mass showed a benign-looking lesion was characterized by stellate cells in a mucoid-myxoid matrix, which is compatible with a cardiac myxoma.

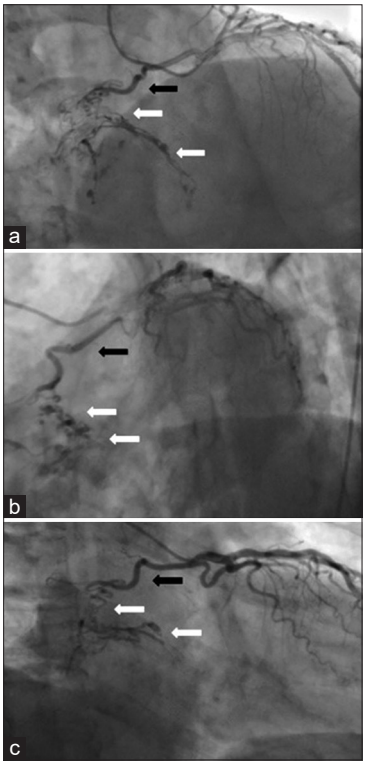

Figure 1: Selective coronary angiography of the patient. Feeding artery from the left circumflex artery in cranial right anterior oblique (a), left caudal (b), and caudal right anterior oblique (c) views of the left coronary artery. This cardiac myxoma has a feeding artery from the left circumflex coronary artery consisting of a vascular branch (black arrow), clusters of tortuous vessels, and an arteriocavity fistula (white arrow)

Discussion

We reported an atypical right atrial myxoma due to the presence of intense vascularization and the feed from the cardiac and extracardiac arteries. Until our case, there was no case of cardiac myxoma fed by extracardiac arteries in the literature. Myxoma is the most common primary benign cardiac tumor. About 80%–90% of myxomas are found in the left atrium, and most of these tumors attach to the interatrial septum.[5] Echocardiography is usually the first imaging method used to evaluate a suspected cardiac mass. In atypical cases, a cardiac CTA or magnetic resonance imaging is recommended. However, neovascularization revealed by imaging is extremely rare in a cardiac myxoma and reported cases of right atrial myxomas generally receive feeding vessels from the RCA or, less frequently, from the left coronary artery or both coronary arteries.[3,4] The myxoma in our case received feeding vessels from the right inferior phrenic artery and the left hepatic artery, as well as from the left circumflex artery.

In patients scheduled for surgery due to cardiac myxoma, detecting the presence of possible cardiac and extracardiac feeding vessels before the operation may be helpful in preventing complications that may develop during and after the operation.

Declaration of patient consent

The authors certify that they have obtained all appropriate patient consent forms. In the form, the patient has given his consent for his images and other clinical information to be reported in the journal. The patient understands that name and initials will not be published and due efforts will be made to conceal identity, but anonymity cannot be guaranteed.

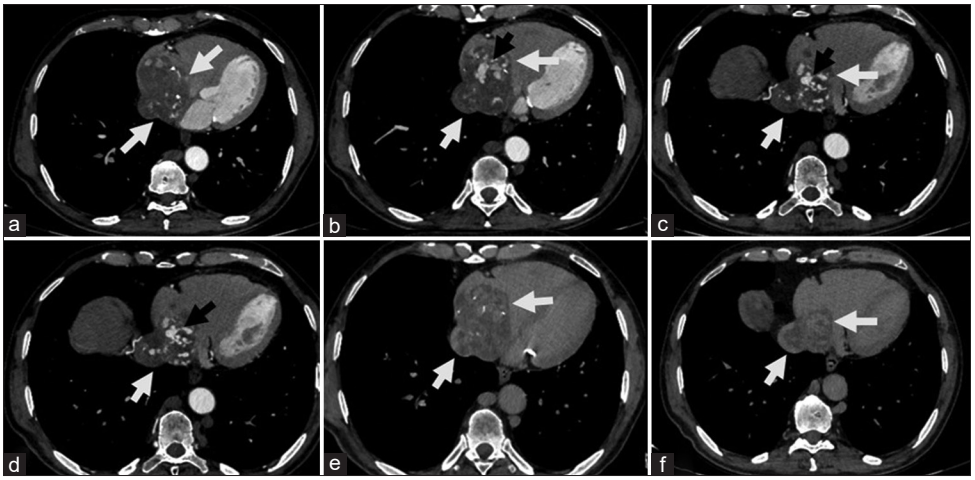

Figure 2: Arterial (a-d) and venous (e and f) phase axial computed tomography sections; hypervascular mass (white arrow) and tortuous vascular structures (black arrow) filling the right atrium

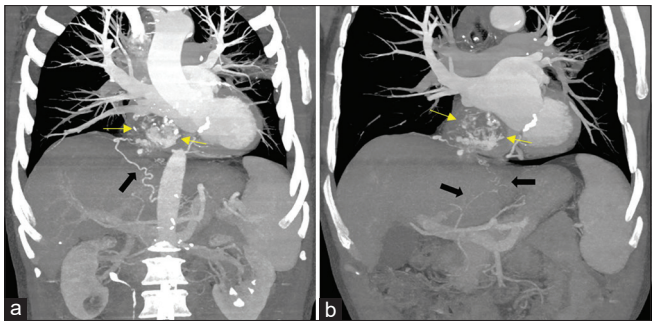

Figure 3: Coronal maximum intensity projection reformatted computed tomography angiography images; the mass that fills the right atrium (yellow arrow), the extension of the right inferior phrenic artery to the mass (a, black arrow) and left hepatic artery branch extending to the mass (b, black arrow)

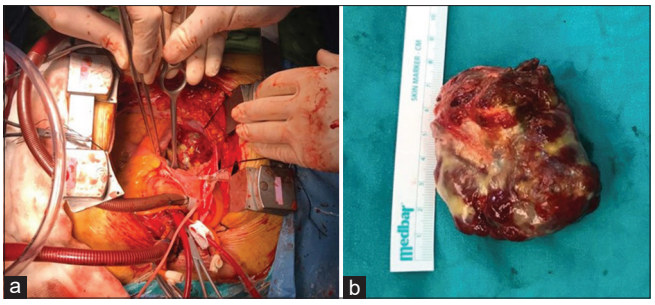

Figure 4: An intraoperative picture of the mass in the right atrium (a), the excised mass, postoperative macroscopic image (b)

Financial support and sponsorship

Nil.

Conflicts of interest

There are no conflicts of interest.

References

1. Jain D, Maleszewski JJ, Halushka MK. Benign cardiac tumors and tumorlike conditions. Ann Diagn Pathol 2010;14:215-30.
2. Wang H, Li Q, Xue M, Zhao P, Cui J. Cardiac myxoma: A rare case series of 3 patients and a literature review. J Ultrasound Med 2017;36:2361-6.
3. Umeda Y, Matsuno Y, Imaizumi M, Mori Y, Iwata H, Takiya H. Right atrial myxoma with tumor vascularity originated from the left and right coronary arteries. Int J Cardiol 2009;131:e137-9.
4. Omar HR. The value of coronary angiography in the work-up of atrial myxomas. Herz 2015;40:442-6.
5. Cianciulli TF, Cozzarin A, Soumoulou JB, Saccheri MC, Méndez RJ, Beck MA, *et al.* Twenty years of clinical experience with cardiac myxomas: Diagnosis, treatment, and follow up. J Cardiovasc Imaging 2019;27:37-47.

Case Report

Additional Tendinous Slips of Extensor Carpi Radialis Longus and Brevis of Hand: A Case Study

Abstract

Two primary muscles of the forearm of extensor group are located on the radial side of the wrist, named as the extensor carpi radialis longus (ECRL) muscle and extensor carpi radialis brevis (ECRB) muscle. At the musculotendinous junction, the ECRL and ECRB travel deep to the abductor pollicis longus, extensor pollicis brevis, and extensor pollicis longus muscles and tendons in the hand. The ECRB is covered by the ECRL as it courses distally. An additional tendon slip of the ECRL and from ECRB, respectively, was discovered during dissection of the forearm's extensor compartment and dorsum of the hand with the cadaver in the supine position. The intermedius tendinous slip from ECRL to ECRB originates from the lateral side of ECRL and gets inserted within the same tendinous sheath of the tendon of ECRB, similarly, tendinous slip from ECRB to ECRL originates from the side of ECRB, cross the intermedius slip of ECRL superficially and gets inserted on the base of second metacarpal bone with the tendon of ECRL.

Keywords: *Additional slips, extensor carpi radialis muscles, nerve entrapment syndrome*

Sonia Meend, Sunil Kumar Yadav

Department of Rachana Sharir, National Institute of Ayurveda, Jaipur, Rajasthan, India

Introduction

Two primary muscles of the forearm of extensor group are located on the radial side of the wrist, named as the extensor carpi radialis longus (ECRL) muscle and extensor carpi radialis brevis (ECRB) muscle. The ECRL originates along the lateral supra-epicondylar ridge of the humerus, inserts onto the dorsal aspect of the base of the second metacarpal bone, and is supplied by the radial nerve. In comparison, the ECRB takes origin from the lateral epicondyle of the humerus at the common extensor origin, gets inserted onto the dorsal aspect of the base of the third metacarpal bone, and is also innervated by the radial nerve. The ECRL and ECRB both are extensors of the wrist. The ECRL also serves in the abduction of the wrist. At the musculotendinous junction, the ECRL and ECRB travel deep to the abductor pollicis longus, extensor pollicis brevis, and extensor pollicis longus muscles and tendons in the hand. The ECRB is slightly shorter than the ECRL and is covered by the ECRL as it courses distally. At the wrist, the ECRL and ECRB travel through the second dorsal compartment created by the extensor retinaculum (ER).[1]

Four variant accessory radial wrist extensor muscles have been described in the literature: Extensor carpi radialis intermedius (ECRI) muscle, extensor carpi radialis tertius muscle, extensor carpi radialis accessorius muscle, and additional tendon slips of the ECRL or ECRB.[2,3] These variant accessory radial wrist extensors are believed to be present in 12%–35% of the population.[2-4] Additional tendon slips of the ECRL and ECRB have been shown to have a 20%–33% incidence rate. Young *et al*. have conducted a study over 40 cadavers out of which 27 cases (33.8%) have accessory tendon of extensor carpi radialis muscles.[2] The accessory tendons in four cases belonged to an additional muscle named ECRI, in four cases, cleft of tendon is seen and in 19 cases, an intermedius tendinous slip is seen arising from ECRL. Yoshida conducted a large study in Japan that included the dissection of 490 upper limbs and concluded around 20%–33% of the total subjects taken in the study had additional slips of ECRL or ECRB tendons splitting into two or three slips before insertion on the second, third, or even fourth metacarpals.[3]

The purpose of this report is to describe a case of additional tendon slips from ECRL and ECRB found during cadaveric

How to cite this article: Meend S, Yadav SK. Additional tendinous slips of extensor carpi radialis longus and brevis of hand: A case study. J Anat Soc India 2024;73:371-3.

Article Info

Received: 02 April 2024
Accepted: 18 November 2024
Available online: 28 December 2024

Address for correspondence:
Dr. Sonia Meend, Department of Rachana Sharir, National Institute of Ayurveda, Jaipur, Rajasthan, India.
E-mail: soniya17you@gmail.com

Access this article online

Website: https://journals.lww.com/joai

DOI: 10.4103/jasi.jasi_40_24

Quick Response Code:

dissection of a 65-year-old female body in a routine dissection in the Department of Rachana Sharir, National Institute of Ayurveda, Jaipur. This case reported did not require Institute Review Board review or approval.

Case Report

A 65-year-old female cadaver was obtained by the Department of Rachana Sharir, National Institute of Ayurveda, Jaipur, for cadaveric dissection during the winter of 2024. It is unknown if the additional tendon slip of the ECRL was known to the subject or if she experienced any symptoms associated with this accessory muscle.

An additional tendon slip of the ECRL and from ECRB, respectively, was discovered during dissection of the forearm's extensor compartment and dorsum of the hand with the cadaver in the supine position. The skin was removed from the left upper limb, and blunt dissection was used to remove the superficial fascia from the posterior forearm and dorsum of the hand. The compartments of the ER were identified. Next, the brachioradialis, ECRL, ECRB, and extensor digitorum muscles were identified and cleaned. The wrist extensor musculature was followed proximally to the common extensor tendon at the lateral epicondyle of the humerus. Further, the ECRL and ECRB were followed distally to the bases of the second and third metacarpals, respectively. The radial nerve was also identified and cleaned between the brachioradialis and brachialis muscles. While tracing the superficial branch of the radial nerve, an additional tendon slip of an ECRL was discovered [Figure 1]. This additional tendon slip originated as a muscular slip from the ECRL, traveled just superficial to the ECRL tendon, and joined the ECRB tendon. Similarly, an additional tendon slip from ECRB originated as a muscular slip was discovered. The intermedius tendinous slip from ECRL to ECRB originates from the lateral side of ECRL and gets inserted within the same tendinous sheath of the tendon of ECRB on the base of the third metacarpal bone. The intermedious tendinous slip from ECRB to ECRL originates from the side of ECRB, cross the intermedious slip of ECRL superficially, and gets inserted on the base of the second metacarpal bone with the tendon of ECRL [Figure 2].

Discussion

This case report aims to present an additional variety of ECRB and ECRL tendon slips discovered during cadaveric dissection. For medical experts, the existence of an extra tendon slip in an ECRL has many clinical and surgical ramifications. First, radial nerve entrapment in the forearm could be related to this tendon slip. The radial nerve can get compressed at any point along its path from the brachial plexus to the arm and forearm. The proximal forearm, close to the supinator muscle, is the site of entrapment that happens most frequently.[4] An additional tendon slip of an ECRL may congest the proximal forearm musculature and contribute to entrapment of the radial nerve and, therefore, should be considered in patients presenting with radial nerve pain and paresthesia.

Additional tendon slip of ECRL and ECRB can also lead to various inflammatory tendon conditions of the elbow and wrist. One of the most frequent causes of nontraumatic elbow dysfunction is lateral epicondylopathy,[5] which is characterized by a persistent symptomatic degeneration of the common extensor tendon at the lateral epicondyle of the humerus. The ECRB is the main muscle impacted in the majority of lateral epicondylopathy patients, yet no clear underlying causes have been found.[6] In the dominant limb, lateral epicondylopathy is more prevalent,[7] and in the dominant upper limb, the common extensor tendon is typically thicker.[8]

Because of the potential increase in thickness and/or workload of the radial wrist extensors with an additional tendon, an additional tendon slip of a radial wrist extensor with an attachment on or near the lateral epicondyle and

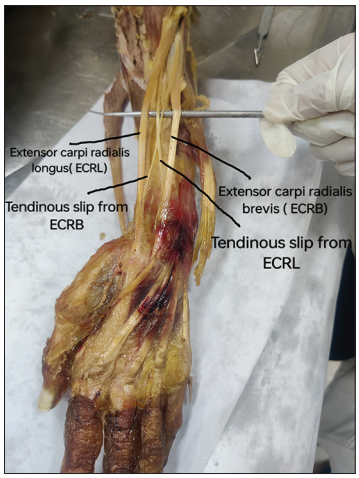

Figure 1: Tendinous slips origin from extensor carpi radialis longus and extensor carpi radialis brevis

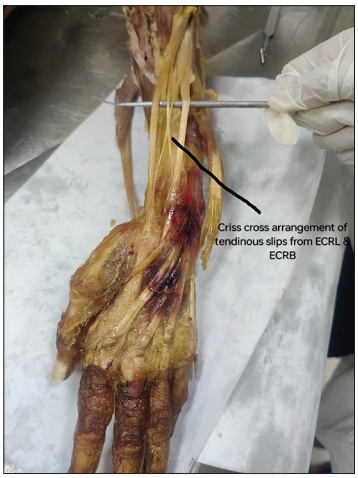

Figure 2: Crisscross arrangement of tendinous slips originating from extensor carpi radialis longus and extensor carpi radialis brevis

common extensor tendon may therefore increase the risk of lateral epicondylopathy. Intersection syndrome may also arise as a result of the extra tendon slips of an ECRB and ECRL. Tenosynovitis of the EPL tendon as it superficially crosses over to the ECRL and ECRB tendons is known as intersection syndrome. An additional tendon slip could make these tendons more susceptible to tenosynovitis or friction.

Clinicians and surgeons must be aware of the implications of additional tendon slips of an ECRL on imaging and surgical techniques. On imaging studies for mass lesions, split tears in the ECRL or ECRB, incorrect tendon identification during surgical operations, and tendon sheath effusions, variations of normal wrist extensor architecture may also be made.[9] During surgical operations, accessory tendons serve as good alternatives to surgeons. For instance, during radial wrist extensor tendon transplants for the treatment of paralytic disorders of the forearm and hand, a surgeon may use these accessory tendons.[10]

Variations in the radial wrist extensors have practical implications when diagnosing, treating, and establishing the root cause of upper limb dysfunctions. If there are an additional number of tendon slips in the dorsal compartments, tenosynovitis and tendon impingement inside the compartment may become more common.

Knowledge of muscle variants is also important for correctly interpreting imaging studies. Therefore, clinicians and surgeons must be aware of these anatomical variations to avoid misinterpretations and provide appropriate treatment.

Conclusion

The literature has reported four distinct variants of the radial wrist extensor muscles, with an incidence rate ranging from 12% to 35%. Understanding these radial wrist extensor variants is crucial for both surgeons and nonoperative clinicians because they are not uncommon and can lead to neuromuscular dysfunction such as intersection syndrome, lateral epicondylopathy, and nerve entrapment. Furthermore, studies could be conducted to examine the incidence rates of radial wrist extensor muscle variants in various geographic regions. Similarly, working on the imaging methods used to view these variations in clinical populations could also be the future scope.

Acknowledgment

We would like to thank the donors and their families for their beneficial contributions. Without their generosity, this article would not have been possible. This research received no specific grant from any funding agency in the public, commercial, or not-for-profit sectors.

Financial support and sponsorship

Nil.

Conflicts of interest

There are no conflicts of interest.

References

1. Moore KL, Dalley AF, Agur AM. Clinically Oriented Anatomy. 8th ed. USA: Wolters Kluwer; 2018.
2. Young RC, Sanudo JR, Mirapeix RM, Abrahams P *et al*. Accessory tendons of extensor muscles. Eur J Anat 1998;2:1-5.
3. Yoshida Y. Anatomical studies on the extensor carpi radialis longus and brevis muscles in Japanese. Okajimas Folia Anat Jpn 1994;71:127-35.
4. Buchanan BK, Maini K, Varacallo M. Radial Nerve Entrapment. Treasure Island, Florida: StatPearls; 2023.
5. Vaquero-Picado A, Barco R, Antuña SA. Lateral epicondylitis of the elbow. EFORT Open Rev 2016;1:391-7.
6. Wolf JM. Lateral epicondylitis. N Engl J Med 2023;388:2371-7.
7. Shiri R, Varonen H, Heliövaara M, Viikari-Juntura E. Hand dominance in upper extremity musculoskeletal disorders. J Rheumatol 2007;34:1076-82.
8. Krogh TP, Fredberg U, Ammitzbøl C, Ellingsen T. Ultrasonographic characteristics of the common extensor tendon of the elbow in asymptomatic individuals: Thickness, color doppler activity, and bony spurs. Orthop J Sports Med 2017;5. doi: 10.1177/2325967117704186.
9. Smith J, Pourcho AM, Kakar S. Sonographic appearance of the extensor carpi radialis intermedius tendon. PM R 2015;7:789-91.
10. Albright JA, Linburg RM. Common variations of the radial writs extensors. J Hand Surg Am 1978;3:134-8.

Dr. Ajai Kumar Srivastava: A Legacy in Medical Education and Anatomy

- Born in 1951 at Lucknow, Dr. Ajai Kumar Srivastava was raised by his grandparents despite his parents' presence. He completed his early education in Lucknow before entering LLRM Medical College, Meerut, where he earned his MBBS in 1973. He went on to complete his MS in Anatomy in 1977 from King George's Medical University (formerly King George's Medical College) in Lucknow, India
- Dr. Srivastava began his teaching career as a Lecturer in Anatomy at SN Medical College, Agra (1978–1980), before moving to GSVM Medical College, Kanpur (1980–1984). In 1984, he joined King George's Medical University, where he remained until his retirement in 2016. During his tenure, he progressed through the ranks to become Assistant Professor, Associate Professor, and then Full Professor of Anatomy. In 2008, he was appointed Professor and Head of the Department. He also served as Professor and Head of Anatomy at BP Koirala Institute of Medical Sciences in Nepal from 2000 to 2003
- One of his notable achievements at KGMU was the establishment of a state-of-the-art Cadaveric Lab, which became a vital resource for various specialties and conferences. Dr. Srivastava;s tenure was characterized by significant advancements in medical education, research, and institutional development, as well as upgrades to infrastructure and enhanced research opportunities
- Postretirement, he took on roles as Principal and Professor and Head of Anatomy at Hind Medical College, Mayo Institute of Medical Sciences, and Prasad Institute of Medical Sciences Lucknow. During this period, he published numerous research papers in national and international journals and participated in various conferences both in India and abroad. A life member of the Anatomical Society of India, he served as Treasurer from 2008 to 2016, successfully navigating the complex process of registering the society for Income Tax. In recognition of his exceptional academic, research, and administrative contributions, he was awarded the Founder Fellowship in 2012. He has successfully organized the National Conference of Anatomical Society of India in 2015

In 2017, he became the President of Anatomical Society of India and Presided over NATCON-65 at Raipur Chattisgarh.

- Throughout his distinguished 38-year career, Dr. Srivastava became renowned for his innovative teaching style and exceptional diagram-drawing skills, inspiring countless undergraduate and postgraduate students to become compassionate doctors. His remarkable combination of empathy, leadership, and commitment to helping others made him a trusted figure among his peers and students alike

In addition to his professional accomplishments, Dr. Srivastava had a deep love for music and sports. His melodious voice added a unique touch to every function, and he was known for his engaging performances.

- Dr. Ajai K. Srivastava's unwavering dedication to anatomy education, research, and institutional growth has left a lasting legacy at KGMU. His contributions will continue to inspire and influence the medical community for years to come.

R. K. Verma

Department of Anatomy, KGMU Lucknow, Uttar Pradesh, India

Address for correspondence: *Dr. R. K. Verma, Department of Anatomy, KGMU Lucknow, Uttar Pradesh, India. E-mail: rkkgmu@gmail.com*

Access this article online

Quick Response Code:

Website: https://journals.lww.com/joai

DOI: 10.4103/jasi.jasi_188_24

How to cite this article: Verma RK. Dr. Ajai Kumar Srivastava: A legacy in medical education and anatomy. J Anat Soc India 2024;73:374.

The Editorial Process

A manuscript will be reviewed for possible publication with the understanding that it is being submitted to Journal of the Anatomical Society of India alone at that point in time and has not been published anywhere, simultaneously submitted, or already accepted for publication elsewhere. The journal expects that authors would authorize one of them to correspond with the Journal for all matters related to the manuscript. All manuscripts received are duly acknowledged. On submission, editors review all submitted manuscripts initially for suitability for formal review. Manuscripts with insufficient originality, serious scientific or technical flaws, or lack of a significant message are rejected before proceeding for formal peer-review. Manuscripts that are unlikely to be of interest to the Journal of the Anatomical Society of India readers are also liable to be rejected at this stage itself.

Manuscripts that are found suitable for publication in Journal of the Anatomical Society of India are sent to two or more expert reviewers. During submission, the contributor is requested to provide names of two or three qualified reviewers who have had experience in the subject of the submitted manuscript, but this is not mandatory. The reviewers should not be affiliated with the same institutes as the contributor/s. However, the selection of these reviewers is at the sole discretion of the editor. The journal follows a double-blind review process, wherein the reviewers and authors are unaware of each other's identity. Every manuscript is also assigned to a member of the editorial team, who based on the comments from the reviewers takes a final decision on the manuscript. The comments and suggestions (acceptance/ rejection/ amendments in manuscript) received from reviewers are conveyed to the corresponding author. If required, the author is requested to provide a point by point response to reviewers' comments and submit a revised version of the manuscript. This process is repeated till reviewers and editors are satisfied with the manuscript.

Manuscripts accepted for publication are copy edited for grammar, punctuation, print style, and format. Page proofs are sent to the corresponding author. The corresponding author is expected to return the corrected proofs within three days. It may not be possible to incorporate corrections received after that period. The whole process of submission of the manuscript to final decision and sending and receiving proofs is completed online. To achieve faster and greater dissemination of knowledge and information, the journal publishes articles online as 'Ahead of Print' immediately on acceptance.

Clinical trial registry

Journal of the Anatomical Society of India favors registration of clinical trials and is a signatory to the Statement on publishing clinical trials in Indian biomedical journals. Journal of the Anatomical Society of India would publish clinical trials that have been registered with a clinical trial registry that allows free online access to public. Registration in the following trial registers is acceptable: http://www.ctri.in/; http://www.actr.org.au/; http://www.clinicaltrials.gov/; http://isrctn.org/; http://www.trialregister.nl/trialreg/index.asp; and http://www.umin.ac.jp/ctr. This is applicable to clinical trials that have begun enrollment of subjects in or after June 2008. Clinical trials that have commenced enrollment of subjects prior to June 2008 would be considered for publication in Journal of the Anatomical Society of India only if they have been registered retrospectively with clinical trial registry that allows unhindered online access to public without charging any fees.

Authorship Criteria

Authorship credit should be based only on substantial contributions to each of the three components mentioned below:

1. Concept and design of study or acquisition of data or analysis and interpretation of data;
2. Drafting the article or revising it critically for important intellectual content; and
3. Final approval of the version to be published.

Participation solely in the acquisition of funding or the collection of data does not justify authorship. General supervision of the research group is not sufficient for authorship. Each contributor should have participated sufficiently in the work to take public responsibility for appropriate portions of the content of the manuscript. The order of naming the contributors should be based on the relative contribution of the contributor towards the study and writing the manuscript. Once submitted the order cannot be changed without written consent of all the contributors. The journal prescribes a maximum number of authors for manuscripts depending upon the type of manuscript, its scope and number of institutions involved (vide infra). The authors should provide a justification, if the number of authors exceeds these limits.

Contribution Details

Contributors should provide a description of contributions made by each of them towards the manuscript. Description should be divided in following categories, as applicable: concept, design, definition of intellectual content, literature search, clinical studies, experimental studies, data acquisition, data analysis, statistical analysis, manuscript preparation, manuscript editing and manuscript review. Authors' contributions will be printed along with the article. One or more author should take responsibility for the integrity of the work as a whole from inception to published article and should be designated as 'guarantor'.

Conflicts of Interest/ Competing Interests

All authors of must disclose any and all conflicts of interest they may have with publication of the manuscript or an institution or product that is mentioned in the manuscript and/or is important to the outcome of the study presented. Authors should also disclose conflict of interest with products that compete with those mentioned in their manuscript.

Submission of Manuscripts

All manuscripts must be submitted on-line through the website https://review.jow.medknow.com/jasi. First time users will have to register at this site. Registration is free but mandatory. Registered authors can keep track of their articles after logging into the site using their user name and password.

- If you experience any problems, please contact the editorial office by e-mail at editor@jasi.org.in

The submitted manuscripts that are not as per the "Instructions to Authors" would be returned to the authors for technical correction, before they undergo editorial/ peer-review. Generally, the manuscript should be submitted in the form of two separate files:

[1] Title Page/First Page File/covering letter:

This file should provide

1. The type of manuscript (original article, case report, review article, Letter to editor, Images, etc.) title of the manuscript, running title, names of all authors/ contributors (with their highest academic degrees, designation and affiliations) and name(s) of department(s) and/ or institution(s) to which the work should be credited, . All information which can reveal your identity should be here. Use text/rtf/doc files. Do not zip the files.
2. The total number of pages, total number of photographs and word counts separately for abstract and for the text (excluding the references, tables and abstract), word counts for introduction + discussion in case of an original article;
3. Source(s) of support in the form of grants, equipment, drugs, or all of these;
4. Acknowledgement, if any. One or more statements should specify 1) contributions that need acknowledging but do not justify authorship, such as general support by a departmental chair; 2) acknowledgments of technical help; and 3) acknowledgments of financial and material support, which should specify the nature of the support. This should be included in the title page of the manuscript and not in the main article file.
5. If the manuscript was presented as part at a meeting, the organization, place, and exact date on which it was read. A full statement to the editor about all submissions and previous reports that might be regarded as redundant publication of the same or very similar work. Any such work should be referred to specifically, and referenced in the new paper. Copies of such material should be included with the submitted paper, to help the editor decide how to handle the matter.
6. Registration number in case of a clinical trial and where it is registered (name of the registry and its URL)
7. Conflicts of Interest of each author/ contributor. A statement of financial or other relationships that might lead to a conflict of interest, if that information is not included in the manuscript itself or in an authors' form
8. Criteria for inclusion in the authors'/ contributors' list
9. A statement that the manuscript has been read and approved by all the authors, that the requirements for authorship as stated earlier in this document have been met, and that each author believes that the manuscript represents honest work, if that information is not provided in another form (see below); and
10. The name, address, e-mail, and telephone number of the corresponding author, who is responsible for communicating with the other authors about revisions and final approval of the proofs, if that information is not included on the manuscript itself.

[2] Blinded Article file: The main text of the article, beginning from Abstract till References (including tables) should be in this file. The file must not contain any mention of the authors' names or initials or the institution at which the study was done or acknowledgements. Page headers/ running title can include the title but not the authors' names. Manuscripts not in compliance with the Journal's blinding policy will be returned to the corresponding author. Use rtf/doc files. Do not zip the files. **Limit the file size to 1 MB.** Do not incorporate images in the file. If file size is large, graphs can be submitted as images separately without incorporating them in the article file to reduce the size of the file. The pages should be numbered consecutively, beginning with the first page of the blinded article file.

[3] Images: Submit good quality color images. **Each image should be less than 2 MB in size.** Size of the image can be reduced by decreasing the actual height and width of the images (keep up to 1600 x 1200 pixels or 5-6 inches). Images can be submitted as jpeg files. Do not zip the files. Legends for the figures/images should be included at the end of the article file.

[4] The contributors' / copyright transfer form (template provided below) has to be submitted in original with the signatures of all the contributors within two weeks of submission via courier, fax or email as a scanned image. Print ready hard copies of the images (one set) or digital images should be sent to the journal office at the time of submitting revised manuscript. High resolution images (up to 5 MB each) can be sent by email.

Contributors' form / copyright transfer form can be submitted online from the authors' area on https://review.jow.medknow.com/jasi.

Preparation of Manuscripts

Manuscripts must be prepared in accordance with "Uniform requirements for Manuscripts submitted to Biomedical Journals" developed by the International Committee of Medical Journal Editors (October 2008). The uniform requirements and specific requirement of Journal of the Anatomical Society of India are summarized below. Before submitting a manuscript, contributors are requested to check for the latest instructions available. Instructions are also available from the website of the journal (www.jasi.org.in) and from the manuscript submission site https://review.jow.medknow.com/jasi.

Journal of the Anatomical Society of India accepts manuscripts written in American English.

Copies of any permission(s)

It is the responsibility of authors/ contributors to obtain permissions for reproducing any copyrighted material. A copy of the permission obtained must accompany the manuscript. Copies of any and all published articles or other manuscripts in preparation or submitted elsewhere that are related to the manuscript must also accompany the manuscript.

Types of Manuscripts

Original articles:

These include randomized controlled trials, intervention studies, studies of screening and diagnostic test, outcome studies, cost effectiveness analyses, case-control series, and surveys with high response rate. The text of original articles amounting to up to 3000 words (excluding Abstract, references and Tables) should be divided into sections with the headings Abstract, Key-words, Introduction, Material and Methods, Results, Discussion and Conclusion, References, Tables and Figure legends.

An abstract should be in a structured format under following heads: **Introduction, Material and Methods, Results,** and **Discussion and Conclusion.**

Introduction: State the purpose and summarize the rationale for the study or observation.

Material and Methods: It should include and describe the following aspects:

Ethics: When reporting studies on human beings, indicate whether the procedures followed were in accordance with the ethical standards of the responsible committee on human experimentation (institutional or regional) and with the Helsinki Declaration of 1975, as revised in 2000 (available at http://www.wma.net/e/policy/17-c_e.html). For prospective studies involving human participants, authors are expected to mention about approval of (regional/ national/ institutional or independent Ethics Committee or Review Board, obtaining informed consent from adult research participants and obtaining assent for children aged over 7 years participating in the trial. The age beyond which assent would be required could vary as per regional and/ or national guidelines. Ensure confidentiality of subjects by desisting from mentioning participants' names, initials or hospital numbers, especially in illustrative material. When reporting experiments on animals, indicate whether the institution's or a national research council's guide for, or any national law on the care and use of laboratory animals was followed. Evidence for approval by a local Ethics Committee (for both human as well as animal studies) must be supplied by the authors on demand. Animal experimental procedures should be as humane as possible and the details of anesthetics and analgesics used should be clearly stated. The ethical standards of experiments must be in accordance with the guidelines provided by the CPCSEA and World Medical Association Declaration of Helsinki on Ethical Principles for Medical Research Involving Humans for studies involving experimental animals and human beings, respectively). The journal will not consider any paper which is ethically unacceptable. A statement on ethics committee permission and ethical practices must be included in all research articles under the 'Materials and Methods' section.

Study design:

Selection and Description of Participants: Describe your selection of the observational or experimental participants (patients or laboratory animals, including controls) clearly, including eligibility and exclusion criteria and a description of the source population. *Technical information*: Identify the methods, apparatus (give the manufacturer›s name and address in parentheses), and procedures in sufficient detail to allow other workers to reproduce the results. Give references to established methods, including statistical methods (see below); provide references and brief descriptions for methods that have been published but are not well known; describe new or substantially modified methods, give reasons for using them, and evaluate their limitations. Identify precisely all drugs and chemicals used, including generic name(s), dose(s), and route(s) of administration.

Reports of randomized clinical trials should present information on all major study elements, including the protocol, assignment of interventions (methods of randomization, concealment of allocation to treatment groups), and the method of masking (blinding), based on the CONSORT Statement (http://www.consort-statement.org).

Reporting Guidelines for Specific Study Designs

Initiative	Type of Study	Source
CONSORT	Randomized controlled trials	http://www.consort-statement.org
STARD	Studies of diagnostic accuracy	http://www.consort-statement.org/stardstatement.htm
QUOROM	Systematic reviews and meta-analyses	http://www.consort- statement.org/Initiatives/MOOSE/moose.pdf statement.org/Initiatives/MOOSE/moose.pdf
STROBE	Observational studies in epidemiology	http://www.strobe-statement.org
MOOSE	Meta-analyses of observational studies in epidemiology	http://www.consort- statement.org/Initiatives/MOOSE/moose.pdf

Statistics: Whenever possible quantify findings and present them with appropriate indicators of measurement error or uncertainty (such as confidence intervals). Authors should report losses to observation (such as, dropouts from a clinical trial). When data are summarized in the Results section, specify the statistical methods used to analyze them. Avoid non-technical uses of technical terms in statistics, such as 'random' (which implies a randomizing device), 'normal', 'significant', 'correlations', and 'sample'. Define statistical terms, abbreviations, and most symbols. Specify the computer software used. Use upper italics (*P* 0.048). For all *P* values include the exact value and not less than 0.05 or 0.001. Mean differences in continuous variables, proportions in categorical variables and relative risks including odds ratios and hazard ratios should be accompanied by their confidence intervals.

Results: Present your results in a logical sequence in the text, tables, and illustrations, giving the main or most important findings first. Do not repeat in the text all the data in the tables or illustrations; emphasize or summarize only important observations. Extra- or supplementary materials and technical detail can be placed in an appendix where it will be accessible but will not interrupt the flow of the text; alternatively, it can be published only in the electronic version of the journal.

When data are summarized in the Results section, give numeric results not only as derivatives (for example, percentages) but also as the absolute numbers from which the derivatives were calculated, and specify the statistical methods used to analyze them. Restrict tables and figures to those needed to explain the argument of the paper and to assess its support. Use graphs as an alternative to tables with many entries; do not duplicate data in graphs and tables. Where scientifically appropriate, analyses of the data by variables such as age and sex should be included.

Discussion: Include summary of *key findings* (primary outcome measures, secondary outcome measures, results as they relate to a prior hypothesis); *Strengths and limitations* of the study (study question, study design, data collection, analysis and interpretation); *Interpretation and implications* in the context of the totality of evidence (is there a systematic review to refer to, if not, could one be reasonably done here and now?, what this study adds to the available evidence, effects on patient care and health policy, possible mechanisms); *Controversies* raised by this study; and *Future research directions* (for this particular research collaboration, underlying mechanisms, clinical research).

Do not repeat in detail data or other material given in the Introduction or the Results section. In particular, contributors should avoid making statements on economic benefits and costs unless their manuscript includes economic data and analyses. Avoid claiming priority and alluding to work that has not been completed. New hypotheses may be stated if needed, however they should be clearly labeled as such. About 30 references can be included. These articles generally should not have more than six authors.

Review Articles:

These are comprehensive review articles on topics related to various fields of Anatomy. The entire manuscript should not exceed 7000 words with no more than 50 references and two authors. Following types of articles can be submitted under this category:

- Newer techniques of dissection and histology
- New methodology in Medical Education
- Review of a current concept

Please note that generally review articles are by invitation only. But unsolicited review articles will be considered for publication on merit basis.

Case reports:

New, interesting and rare cases can be reported. They should be unique, describing a great diagnostic or therapeutic challenge and providing a learning point for the readers. Cases with clinical significance or implications will be given priority. These communications could be of up to 1000 words (excluding Abstract and references) and should have the following headings: Abstract (unstructured), Key-words, Introduction, Case report, Discussion and Conclusion, Reference, Tables and Legends in that order.

The manuscript could be of up to 1000 words (excluding references and abstract) and could be supported with up to 10 references. Case Reports could be authored by up to four authors.

Letter to the Editor:

These should be short and decisive observations. They should preferably be related to articles previously published in the Journal or views expressed in the journal. They should not be preliminary observations that need a later

paper for validation. The letter could have up to 500 words and 5 references. It could be generally authored by not more than four authors.

Book Review: This consists of a critical appraisal of selected books on Anatomy. Potential authors or publishers may submit books, as well as a list of suggested reviewers, to the editorial office. The author/publisher has to pay INR 10,000 per book review.

Other:

Editorial, Guest Editorial, Commentary and Opinion are solicited by the editorial board.

References

References should be *numbered* consecutively in the order in which they are first mentioned in the text (not in alphabetic order). Identify references *in text*, tables, and legends by Arabic numerals in superscript with square bracket after the punctuation *marks. References cited only* in tables or figure legends should be numbered in accordance with the sequence established by the first identification in the text of the particular table or figure. Use the style of the examples below, which are based on the formats used by the NLM *in Index Medicus*. The titles of journals *should be abbreviated* according to the style used in Index Medicus. Use complete name of the journal for non-indexed journals. Avoid using abstracts as references. Information from manuscripts submitted but not accepted should be cited in the text as "unpublished observations" with written permission from the source. Avoid citing a "personal communication" unless it provides essential information not available from a public source, in which case the name of the person and date of communication should be cited in parentheses in the text. The commonly cited types of references are shown here, for other types of references such as newspaper items please refer to ICMJE Guidelines (http://www.icmje.org or http://www.nlm.nih.gov/bsd/uniform_requirements.html).

Articles in Journals

1. Standard journal article (for up to six authors): Parija S C, Ravinder PT, Shariff M. Detection of hydatid antigen in the fluid samples from hydatid cysts by co-agglutination. Trans. R.Soc. Trop. Med. Hyg.1996; 90:255–256.
2. Standard journal article (for more than six authors): List the first six contributors followed by *et al*.

Roddy P, Goiri J, Flevaud L, Palma PP, Morote S, Lima N. *et al*., Field Evaluation of a Rapid Immunochromatographic Assay for Detection of Trypanosoma cruzi Infection by Use of Whole Blood. J. Clin. Microbiol. 2008; 46: 2022-2027.

3. Volume with supplement: Otranto D, Capelli G, Genchi C: Changing distribution patterns of canine vector borne diseases in Italy: leishmaniosis vs. dirofilariosis. Parasites & Vectors 2009; Suppl 1:S2.

Books and Other Monographs

1. Personal author(s): Parija SC. Textbook of Medical Parasitology. 3rd ed. All India Publishers and Distributors. 2008.
2. Editor(s), compiler(s) as author: Garcia LS, Filarial Nematodes In: Garcia LS (editor) Diagnostic Medical Parasitology ASM press Washington DC 2007: pp 319-356.
3. Chapter in a book: Nesheim M C. Ascariasis and human nutrition. In Ascariasis and its prevention and control, D. W. T. Crompton, M. C. Nesbemi, and Z. S. Pawlowski (eds.). Taylor and Francis,London, U.K.1989, pp. 87–100.

Electronic Sources as reference

Journal article on the Internet: Parija SC, Khairnar K. Detection of excretory *Entamoeba histolytica* DNA in the urine, and detection of *E. histolytica* DNA and lectin antigen in the liver abscess pus for the diagnosis of amoebic liver abscess. *BMC Microbiology* 2007, **7**:41. doi:10.1186/1471-2180-7-41. http://www.biomedcentral.com/1471-2180/7/41

Tables

- Tables should be self-explanatory and should not duplicate textual material.
- Tables with more than 10 columns and 25 rows are not acceptable.
- Number tables, in Arabic numerals, consecutively in the order of their first citation in the text and supply a brief title for each.
- Place explanatory matter in footnotes, not in the heading.
- Explain in footnotes all non-standard abbreviations that are used in each table.
- Obtain permission for all fully borrowed, adapted, and modified tables and provide a credit line in the footnote.
- For footnotes use the following symbols, in this sequence: *, †, ‡, §, ‖,¶ , **, ††, ‡‡
- Tables with their legends should be provided at the end of the text after the references. The tables along with their number should be cited at the relevant place in the text

Illustrations (Figures)

- Upload the images in JPEG format. The file size should be within 1024 kb in size while uploading.
- Figures should be numbered consecutively according to the order in which they have been first cited in the text.
- Labels, numbers, and symbols should be clear and of uniform size. The lettering for figures should be large enough to be legible after reduction to fit the width of a printed column.
- Symbols, arrows, or letters used in photomicrographs

should contrast with the background and should be marked neatly with transfer type or by tissue overlay and not by pen.
- Titles and detailed explanations belong in the legends for illustrations not on the illustrations themselves.
- When graphs, scatter-grams or histograms are submitted the numerical data on which they are based should also be supplied.
- The photographs and figures should be trimmed to remove all the unwanted areas.
- If photographs of individuals are used, their pictures must be accompanied by written permission to use the photograph.
- If a figure has been published elsewhere, acknowledge the original source and submit written permission from the copyright holder to reproduce the material. A credit line should appear in the legend for such figures.
- Legends for illustrations: Type or print out legends (maximum 40 words, excluding the credit line) for illustrations using double spacing, with Arabic numerals corresponding to the illustrations. When symbols, arrows, numbers, or letters are used to identify parts of the illustrations, identify and explain each one in the legend. Explain the internal scale (magnification) and identify the method of staining in photomicrographs.
- Final figures for print production: Send sharp, glossy, un-mounted, color photographic prints, with height of 4 inches and width of 6 inches at the time of submitting the revised manuscript. Print outs of digital photographs are not acceptable. If digital images are the only source of images, ensure that the image has minimum resolution of 300 dpi or 1800 x 1600 pixels in TIFF format. Send the images on a CD. Each figure should have a label pasted (avoid use of liquid gum for pasting) on its back indicating the number of the figure, the running title, top of the figure and the legends of the figure. Do not write the contributor/s' name/s. Do not write on the back of figures, scratch, or mark them by using paper clips.
- The Journal reserves the right to crop, rotate, reduce, or enlarge the photographs to an acceptable size.

Protection of Patients' Rights to Privacy

Identifying information should not be published in written descriptions, photographs, sonograms, CT scans, etc., and pedigrees unless the information is essential for scientific purposes and the patient (or parent or guardian, wherever applicable) gives informed consent for publication. Authors should remove patients' names from figures unless they have obtained informed consent from the patients. The journal abides by ICMJE guidelines:

1. Authors, not the journals nor the publisher, need to obtain the patient consent form before the publication and have the form properly archived. The consent forms are not to be uploaded with the cover letter or sent through email to editorial or publisher offices.
2. If the manuscript contains patient images that preclude anonymity, or a description that has obvious indication to the identity of the patient, a statement about obtaining informed patient consent should be indicated in the manuscript.

Sending a revised manuscript

The revised version of the manuscript should be submitted online in a manner similar to that used for submission of the manuscript for the first time. However, there is no need to submit the "First Page" or "Covering Letter" file while submitting a revised version. When submitting a revised manuscript, contributors are requested to include, the 'referees' remarks along with point to point clarification at the beginning in the revised file itself. In addition, they are expected to mark the changes as underlined or colored text in the article.

Reprints and proofs

Journal provides no free printed reprints. Authors can purchase reprints, payment for which should be done at the time of submitting the proofs.

Publication schedule

The journal publishes articles on its website immediately on acceptance and follows a 'continuous publication' schedule. Articles are compiled in issues for 'print on demand' quarterly.

Copyrights

Checklist

Covering letter

- Signed by all contributors
- Previous publication / presentations mentioned
- Source of funding mentioned
- Conflicts of interest disclosed

Authors

- Last name and given name provided along with Middle name initials (where applicable)
- Author for correspondence, with e-mail address provided
- Number of contributors restricted as per the instructions
- Identity not revealed in paper except title page (e.g. name of the institute in Methods, citing previous study as 'our study', names on figure labels, name of institute in photographs, etc.)

Presentation and format

- Double spacing
- Margins 2.5 cm from all four sides
- Page numbers included at bottom
- Title page contains all the desired information
- Running title provided (not more than 50 characters)
- Abstract page contains the full title of the manuscript
- Abstract provided (structured abstract of 250 words for original articles, unstructured abstracts of about 150 words for all other manuscripts excluding letters to the Editor)
- Key words provided (three or more)
- Introduction of 75-100 words
- Headings in title case (not ALL CAPITALS)
- The references cited in the text should be after punctuation marks, in superscript with square bracket.
- References according to the journal's instructions, punctuation marks checked
- Send the article file without 'Track Changes'

Language and grammar

- Uniformly American English
- Write the full term for each abbreviation at its first use in the title, abstract, keywords and text separately unless it is a standard unit of measure. Numerals from 1 to 10 spelt out
- Numerals at the beginning of the sentence spelt out
- Check the manuscript for spelling, grammar and punctuation errors
- If a brand name is cited, supply the manufacturer's name and address (city and state/country).
- Species names should be in italics

Tables and figures

- No repetition of data in tables and graphs and in text
- Actual numbers from which graphs drawn, provided
- Figures necessary and of good quality (colour)
- Table and figure numbers in Arabic letters (not Roman)
- Labels pasted on back of the photographs (no names written)
- Figure legends provided (not more than 40 words)
- Patients' privacy maintained (if not permission taken)
- Credit note for borrowed figures/tables provided
- Write the full term for each abbreviation used in the table as a footnote

Journal of the Anatomical Society of India on Web

https://review.jow.medknow.com/jasi

The Journal of the Anatomical Society of India now accepts articles electronically. It is easy, convenient and fast. Check following steps:

1 Registration

- Register from https://review.jow.medknow.com/jasi as a new author (Signup as author)
- Two-step self-explanatory process

2 New article submission

- Read instructions on the journal website or download the same from manuscript management site
- Prepare your files (Article file, First page file and Images, Copyright form & Other forms, if any)
- Login as an author
- Click on 'Submit new article' under 'Submissions'
- Follow the steps (guidelines provided while submitting the article)
- On successful submission you will receive an acknowledgement quoting the manuscript ID

3 Tracking the progress

- Login as an author
- The report on the main page gives status of the articles and its due date to move to next phase
- More details can be obtained by clicking on the ManuscriptID
- Comments sent by the editor and reviewer will be available from these pages

4 Submitting a revised article

- Login as an author
- On the main page click on 'Articles for Revision'
- Click on the link "Click here to revise your article" against the required manuscript ID
- Follow the steps (guidelines provided while revising the article)
- Include the reviewers' comments along with the point to point clarifications at the beginning of the revised article file.
- Do not include authors' name in the article file.
- Upload the revised article file against New Article File - Browse, choose your file and then click "Upload" OR Click "Finish"
- On completion of revision process you will be able to check the latest file uploaded from Article Cycle (In Review Articles-> Click on manuscript id -> Latest file will have a number with 'R', for example XXXX_100_15R3.docx)

Facilities

- Submission of new articles with images
- Submission of revised articles
- Checking of proofs
- Track the progress of article until published

Advantages

- Any-time, any-where access
- Faster review
- Cost saving on postage
- No need for hard-copy submission
- Ability to track the progress
- Ease of contacting the journal

Requirements for usage

- Computer and internet connection
- Web-browser (Latest versions - IE, Chrome, Safari, FireFox, Opera)
- Cookies and javascript to be enabled in web-browser

Online submission checklist

- First Page File (rtf/doc/docx file) with title page, covering letter, acknowledgement, etc.
- Article File (rtf/doc/docx file) - text of the article, beginning from Title, Abstract till References (including tables). File size limit 4 MB. Do not include images in this file.
- Images (jpg/jpeg/png/gif/tif/tiff): Submit good quality colour images. Each image should be less than 10 MB) in size
- Upload copyright form in .doc / .docx / .pdf / .jpg / .png / .gif format, duly signed by all authors, during the time mentioned in the instructions.

Help

- Check Frequently Asked Questions (FAQs) on the site
- In case of any difficulty contact the editor

Journal of
The Anatomical Society of India

Salient Features:

- Publishes research articles related to all aspects of Anatomy and Allied medical/surgical sciences.
- Pre-Publication Peer Review and Post-Publication Peer Review
- Online Manuscript Submission System
- Selection of articles on the basis of MRS system
- Eminent academicians across the globe as the Editorial board members
- Electronic Table of Contents alerts
- Available in both online and print form.

The journal is registered with the following abstracting partners:
Baidu Scholar, CNKI (China National Knowledge Infrastructure), EBSCO Publishing's Electronic Databases, Ex Libris – Primo Central, Google Scholar, Hinari, Infotrieve, Netherlands ISSN center, ProQuest, TdNet, Wanfang Data

The journal is indexed with, or included in, the following:
SCOPUS, Science Citation Index Expanded, IndMed, MedInd, Scimago Journal Ranking, Emerging Sources Citation Index.

Impact Factor® as reported in the 2022 Journal Citation Reports® (Clarivate Analytics, 2023): 0.4

Editorial Office:
Dr. Vishram Singh, Editor-in-Chief, JASI
B5/3 Hahnemann Enclave, Plot No. 40, Sector 6,
Dwarka Phase – 2, New Delhi - 110 075, India.
Email: editorjasi@gmail.com
(O) | Website: www.asiindia.in

The journal is owned and run by The Anatomical Society of India